Master Thesis

Mobility Management and eICIC in LTE Femtocells

by

Pantha Ghosal

Faculty of Engineering and IT

University of Technology, Sydney

August, 2017

Supervisor : A/Prof. Dr. Kumbesan Sandrasegaran

Declaration

To the best of my knowledge and belief this work was prepared without aid from any other sources except where indicated. Any reference to material previously published by any other person has been duly acknowledged. This work contains no material which has been submitted or accepted for the award of any other degree in any institution.

Signature .....

Date .....

Acknowledgement

It would not have been possible to complete this thesis without the kind support and guidance from the great people around me, to only some of whom it is possible to mention here.

Above all, I would like to mention my father Engr. Nirmal Chandra Ghosal, whose vision and dream about his son have taken me into the field of higher study and research. Without the kind support and great patience of my loving wife Purnata Snigdha, it would be very tough to complete this thesis. Moreover, my mother Mamata, sister Sharmistha, my daughter Proggya Promita, all the friends and family members have given me their unequivocal support throughout, as always, for which my mere expression of thanks does not suffice.

I would like to express my sincere gratitude to my principal supervisor Associate Professor. Kumbesan Sandrasegaran, this thesis would not have been possible without his help, support ant patience. Dr. Sandrasegaran, has been invaluable both in Telecommunication and personal level, for which I am extremely grateful.

Abstract

LTE-Long Term Evolution was proposed in Release 8 by Third Generation Partnership Project (3GPP) with a new Radio Access Network (RAN) and an Evolved Packet Core (EPC) Network to provide a smooth migration to 4G network. The number of mobile subscribers and data usage have increased exponentially since the roll-out of LTE because of new higher capacity LTE air-interface. This has created new challenges for the network operators to provide a satisfactory quality of service to the mobile users especially in indoor scenarios.

One solution to provide better indoor user experience in a cost effective manner is use of femtocells which were introduced in 3GPP LTE, Release 8. Femtocells are short ranged indoor small cells, which share the same spectrum with macrocell and could have a limited user access. Higher data rate, improved indoor coverage, QoS and longer battery life could be achieved with the deployment of femtocells. Nonetheless, the plug-and-play capability and lower cost of these small cells pose huge interference problems in uplink and downlink when installed in dense urban areas and in an unplanned way.

Interference management and handover are two important factors to be considered while implementing LTE network with femtocells. The use of hard handover in 3GPP LTE and LTE-A systems coupled with the absence of a direct signaling interface between macrocell and femtocell may cause call drops and delay in mobility management. The objective of this research is to address the challenges posed by handover performance and interference mitigation in LTE system with femtocells.

In this work, a speed based handover algorithm is proposed,

simulated in LTE-SIM and optimized by introducing Almost Blank Sub-Frames (ABSF) and Cell Range Expansion (CRE) interference coordination schemes. Simulation results show that, better user experience can be achieved in terms of delay, fairness, reduced number of call-drops while maximizing the throughput.

Contents

List of Figures

List of Tables

List of Acronyms

3GPP	3rd Generation Partnership Project
4G	Fourth Generation
ABSF	Almost Blank Subframes
BLER	Block Error Rate
BW	Bandwidth
CC	Component Carrier
CDF	Cumulative Distribution Function
CDMA	Code Division Multiple Access
CQI	Channel Quality Indicator
CRE	Cell Range Expansion
CRS	Cell Specific Reference signal
DwPTS	Downlink Pilot Channel
eNB	evolved NodeB
EPS	Evolved Packet System
ExPF	Exponential Proportional Fairness
FAP	Femtocell Access Points
FDD	Frequency-Division Duplex
FFR	Fractional Frequency Reuse
FUE	Femtocell User
HARQ	Hybrid Automatic Repeat request
HeNB	Home eNodeB

HOL	Head of Line
HSPA	High-Speed Packet Access
ICI	Inter Cell Interference
ICIC	Inter Cell Interference Coordination
ISI	Inter-Symbol Interference
LTE	Long Term Evolution
MCS	Modulation and Coding Scheme
MLWDF	Maximum Largest Weighted Delay First
MME	Mobility Management Entity
MUE	Macrocell User
NCL	Neighbouring Cell List
NRT	Non-Real-Time service
OFDM	Orthogonal Frequency Division Multiplexing
OFDMA	Orthogonal Frequency Division Multiple Access
PAPR	Peak-to-Average Power Ratio
PDCCH	Physical Downlink Control Channel
PDSCH	Physical Downlink Shared Channel
PF	Proportional Fair
PUSCH	Physical Uplink Shared Channel
QAM	Quadrature Amplitude Modulation
QoS	Quality of Service
QPSK	Quadrature Phase Shift Keying

RB	Resource Block
RE	Resource Element
RNC	Radio Network Controller
RSRP	Reference Signal Received Power
RSS	Received Signal Strength
RT	Real-Time Service
SAE	System Architecture Evolution
SC-FDMA	Single Carrier Frequency Division Multiple Access
SFR	Soft Frequency Reuse
SFFR	Soft Fractional Frequency Reuse
S-GW	Serving GateWay
SINR	Signal to Interference and Noise Ratio
SON	Self-Organizing Networks
TB	Transport Blocks
TDD	Time-Division Duplex
TTI	Transmission Time Interval
TX	Transmitter
UpTS	Uplink Pilot Time Slot
UTRAN	UMTS Terrestrial Radio Access Network
WCDMA	Wide-band Code Division Multiple Access

Chapter 1

Introduction

Mobile networks have evolved considerably over the last 20 years and this has resulted in mobile phones becoming indispensable in our daily lives. The number of mobile subscribers and usage of mobile data has increased at an unprecedented pace. Second Generation (2G) Global System for Mobile Communication (GSM) was designed to carry voice traffic with limited data capability. Enhanced Data rates for GSM Evolution (EDGE)[1] was a part of International Telecommunication Union's (ITU) Third Generation (3G) definition and backward-compatible extension of GSM. EDGE allowed improved data transmission rates and considered as pre-3G radio technology. Data usage started to proliferate with the launch of Third Generation (3G) mobile system such as the Universal Mobile Telecommunications System (UMTS). Increased availability of 3G communication technologies, inception of smart mobile devices and applications and flat rate for unlimited data download were the key factors of mobile traffic explosion[4]. This resulted in congestion in 2G and 3G networks. To improve end-user throughput, cell capacity and to reduce user plane latency, 3GPP aimed to keep mobile communication systems competitive over time-scales of 10 years and beyond. Figure 1.1 is the resulting LTE architecture that evolved from UMTS. Evolved Packet Core(EPC) and evolved UMTS Terrestrial Radio Access Network(eUTRAN) were defined

in 3GPP Release 8 and enhanced in further 3GPP Releases. There

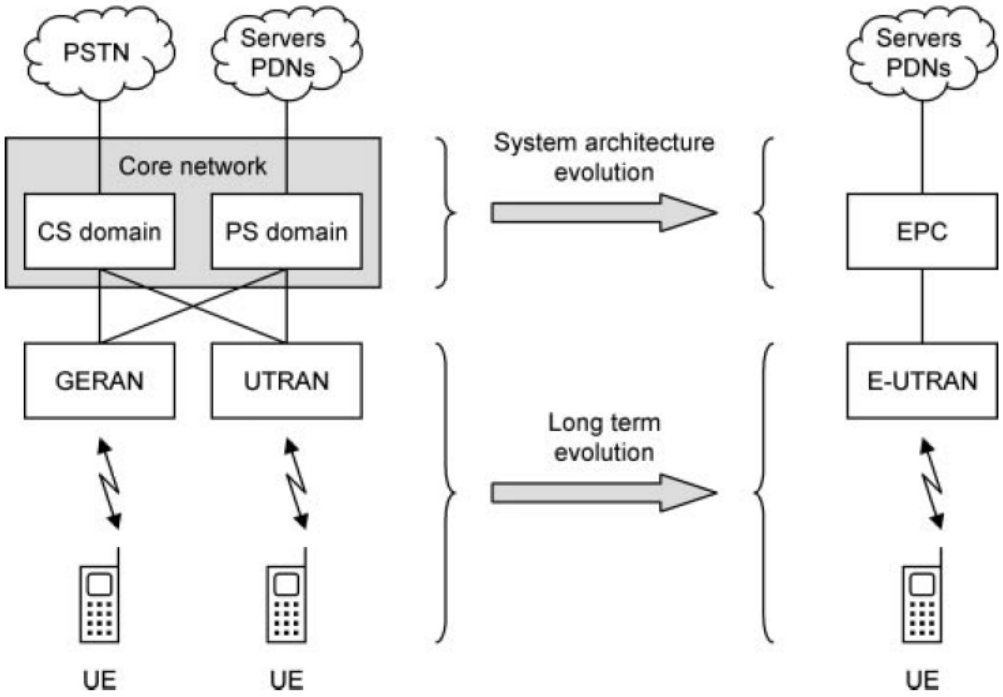

Figure 1.1: Evolution of LTE Network Architecture for GSM and UMTS [4]

is no Circuit-Switched(CS) domain, EPC is designed to support IP data traffic and voice traffic as Voice over IP(VoIP) over same packet switched(PS) network. The evolved UMTS Terrestrial Radio Access Network(eUTRAN) is the replacement of UTRAN which maintains EPC's communication to user equipment(UE)[2].

The evolution of LTE from earlier 3GPP systems is shown in Figure 1.2. TeliaSonera launched the first LTE network in Oslo and Stockholm in December, 2009 [8]. The main attributes [9] that differentiate Release 8 from previous releases are stated below:

* Peak data rate of 100 Mbps in the downlink and 50 Mbps in the uplink.

* Improved spectral efficiency and supports co-existence with legacy standards (e.g. GSM/(EDGE), UMTS and CDMA2000.

* Operates both in Frequency Division Duplex (FDD) and Time Division Duplex (TDD) modes.

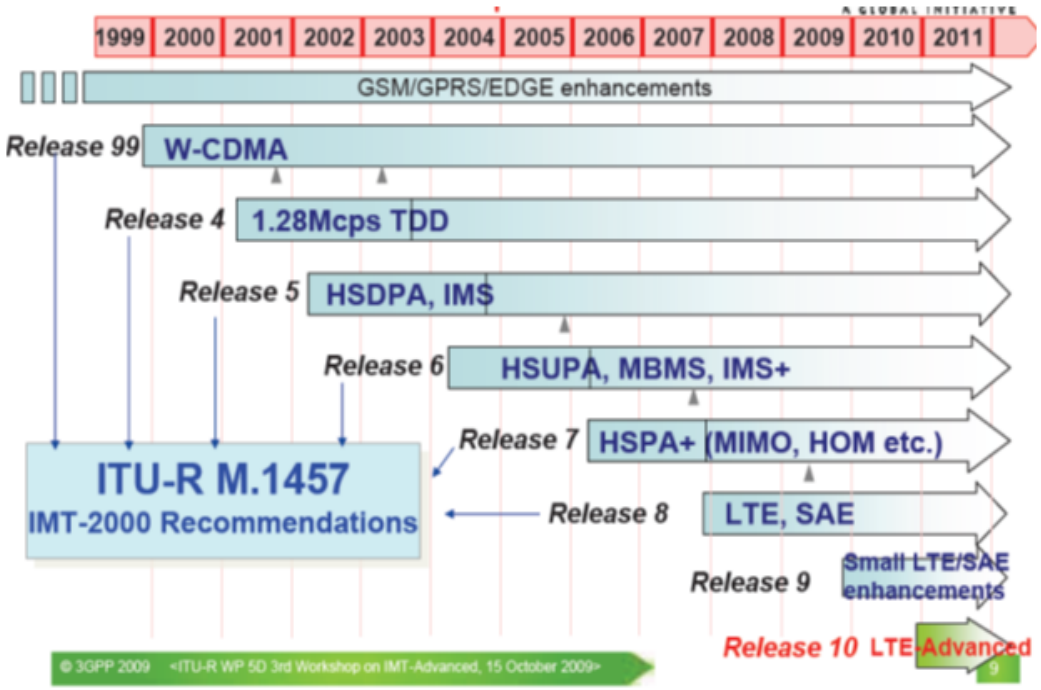

Figure 1.2: Evolution of 3GPP standards[10]

* Packet-switched interface eliminates cost and complexity related to earlier circuit-switched legacy networks.

* Orthogonal Frequency Division Multiple Access (OFDMA) for downlink and Single Career-Frequency Division Multiple Access (SC-FDMA) for uplink to conserve battery life.

* Increased spectrum flexibility that supports six channel bandwidths from 1.4 MHz to 20 MHz.

* Support for spatial multiplexing (MIMO), up to four layers on the downlink.

* Faster physical layer control mechanism that supports lower latencies for handover and connection set-up time compared to previous mobile communication technologies.

For LTE systems, 3GPP has set requirements shown in Table 1.1 which should be met by evolved UTRAN [11].

Table 1.1: LTE Requirement [11]

	Parameter	**Requirement**	**Conditions**
Downlink	Peak transmission rate	>100 Mbps	2x2 spatial multiplexing
	Peak spectral efficiency	>5 bps/Hz	LTE in 20MHz FDD
	Average cell spectral efficeincy	>1.6-2.1 bps/Hz/cell	
	Cell edge spectral efficeincy	>.04-.06 bps/Hz/cell	2x2 spatial multiplexing
	Broadcast spectral efficiency	>1bps/Hz	
Uplink	Peak transmission rate	>50 Mbps	Single antenna transmission
	Peak spectral efficiency	>2.5 bps/Hz	LTE in 20MHz FDD
	Average cell spectral efficiency	>.66-1.0 bps/Hz/cell	
	Cell edge spectral efficiency	>.02-.03 bps/Hz/cell	Single antenna transmission
System	Round trip time	<10ms	
	Connection setup time	<100ms	From idle to active
	Operating Bandwidth	1.4-20 MHz	

1.1 System Description

The architecture of 4G networks is described in this section.

1.1.1 LTE Network Architecture

LTE has a flat architecture consisting of evolved NodeB (eNB), Serving Gateway (S-GW), Packet Data Network(PDN) Gateway (P-GW) and Mobility Management Entity (MME) [12] as illustrated in Figure 1.3. System Level Architecture(SAE) comprises core network and Long Term Evolution(LTE) includes eUTRAN, air interface and end-user. EPC and eUTRAN are collectively refereed as Evolved Packet System (EPS) [4].

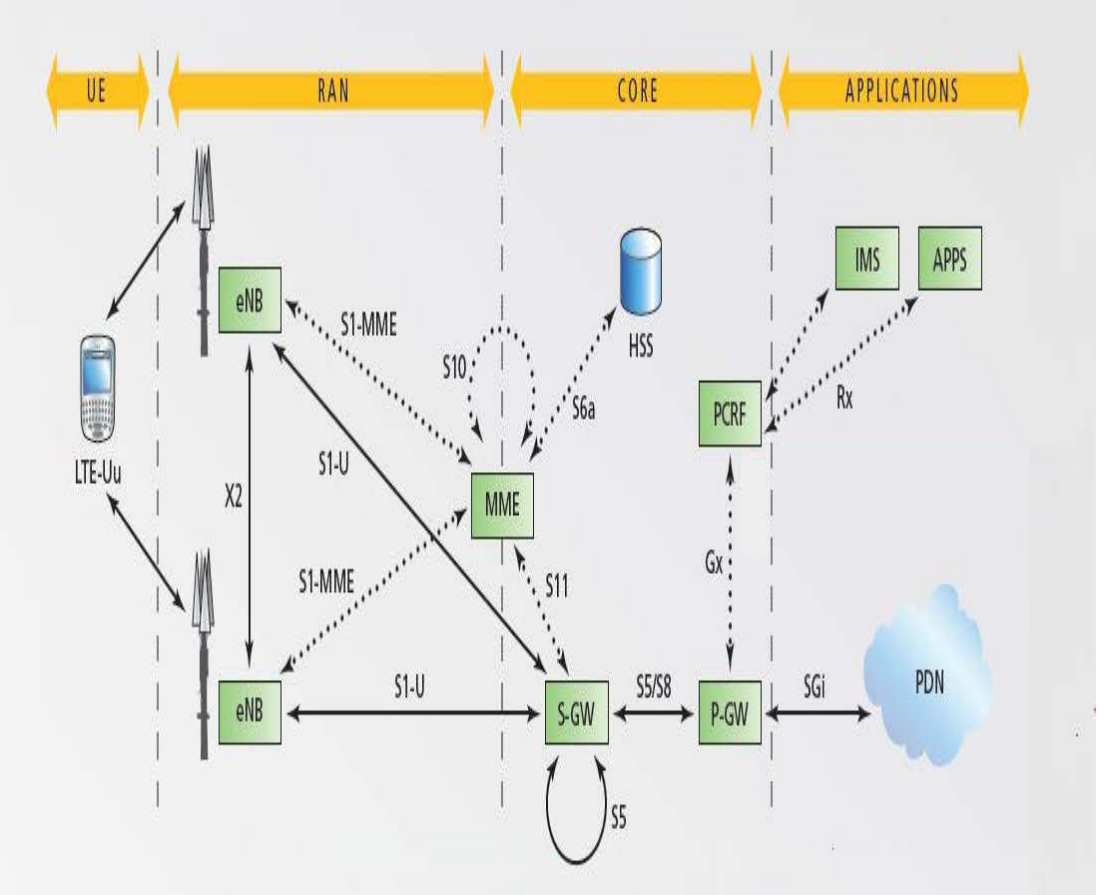

Figure 1.3: LTE architecture [7]

The eUTRAN consists only one node, known as evolved-NodeB

(eNodeB/eNB) that interfaces to UE. The functionalities of a Radio Network Control (RNC) in 3G networks are performed by eNBs in LTE [13]. The RNC processing load is distributed among several eNBS that leads to latency reduction. Radio Resource Management (RRM), header compression, ciphering and reliable delivery of packets and admission control are functions performed by an eNB [12], [14].

X2 and S1 are the two main interfaces in LTE network architecture. X2 interface maintains the interconnection between neighbouring eNBs and is mainly used for signalling and packet forwarding during handover. On the other hand, S1 interface connects eNBs to the EPC components- Mobility Managemenet Entity(MME), Serving Gateway(S-GW) and Packet Data Network(PDN) Gateway(P-GW) [4]. All network interfaces are based on IP protocol.

MME is the control plane entity that manages network access and user mobility. The main functions of MME are: a) idle-mode UE reachability including tracking and paging b) roaming, authentication, authorization, P-GW/S-GW selection, c) bearer activation and deactivation procedures, security negotiation and so on. S-GW servers as a local mobility anchor for UE and is user a plane gateway to the eUTRAN which performs IP routing and forwarding functions and maintains data paths between eNB and P-GW. The P-GW is user plane gateway and performs interfacing with external Packet Data Networks (PDNs) (such as the Internet). Additionally, it performs several IP functions such as address allocation, policy enforcement, packet filtering and routing [5].

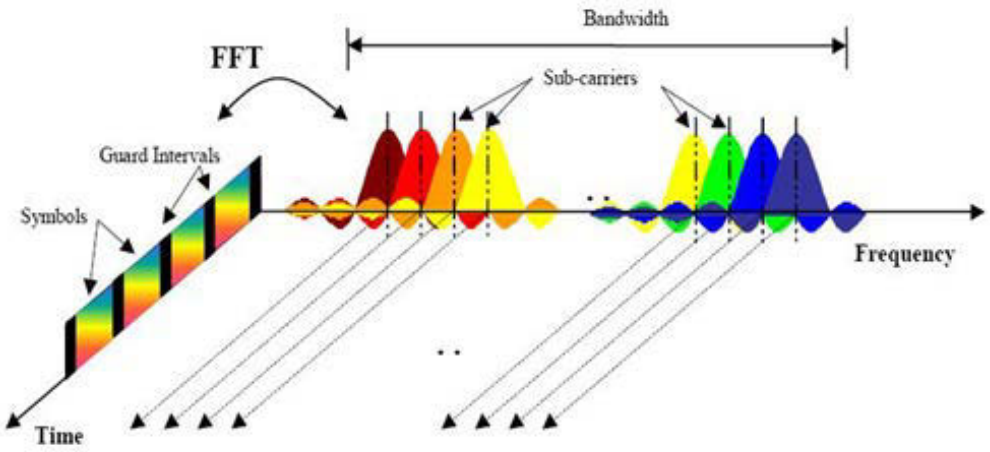

Figure 1.4: Illustration of the OFDM transmission technique[19]

1.1.2 Orthogonal Frequency Division Multiplexing

Orthogonal Frequency Division Multiplexing (OFDM) splits available spectrum into multiple sub-carriers which are mutually orthogonal as shown in Figure 1.4 [19]. The downlink transmission scheme for E-UTRA FDD and TDD modes are based on Orthogonal Frequency Division Multiple Access. Benefits of OFDM are as follows:

1. Guard period (cyclic prefix- 1.1.3.1) at the transmitters removes Inter Symbol Interference (ISI) of multi-carrier transmission since the guard period is longer than the channel impulse response [16].

2. Access to OFDMA allows schedulers to dynamically allocate radio resources in time and frequency domain based on specific resource allocation policy, giving a high degree of freedom to the schedulers.

3. Smooth evolution from previous radio access technologies to LTE is possible due to its spectrum flexibility [20].

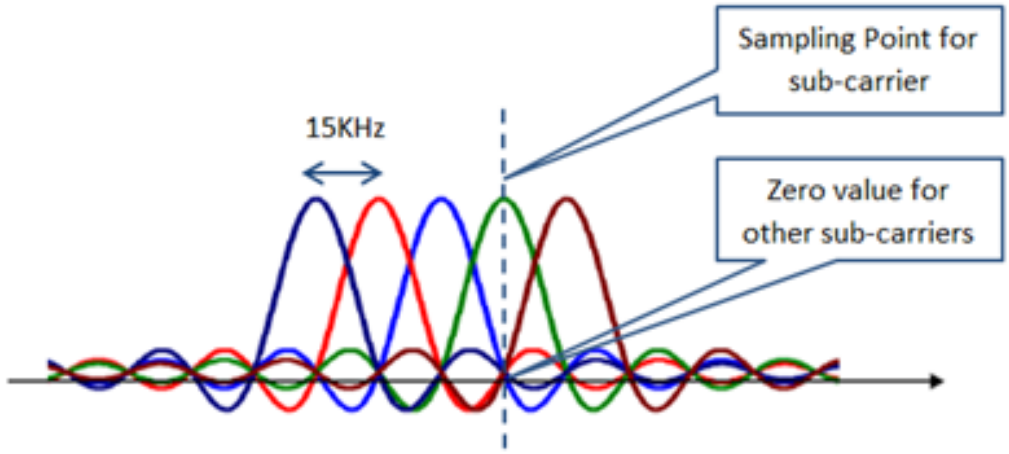

Figure 1.5: Adjacent sub-carriers with OFDMA[16]

1.1.2.1 Orthogonal Frequency Division Multiple Access

In LTE OFDMA, narrowband sub carriers have spacing of 15 KHz and are mutually orthogonal to each other. Figure 1.5 shows at a sampling point of a sub-carrier, in frequency domain all other sub-carriers have zero value to maintain the orthogonality between each other[16]. OFMDA is the multi-user version of OFDM [17].

1.1.2.2 Single-Carrier Frequency Division Multiple Access

Single Carrier-Frequency Division Multiple Access (SC-FDMA)is regarded as Discrete Fourier Transform(DFT) of OFDMA. In SC-FDMA, data symbols are transformed to frequency domain from time domain by DFT and it utilizes single carrier modulation. The Peak-to-Average Power Ratio (PAPR)in SC-FDMA is comparatively lower than OFDMA [18]. The high PAPR in OFDMA signals leads to complex and costly power amplifier design. Low PAPR of SC-FDMA enables to design efficient amplifier in a cost effective way for UEs [19].

1.1.3 LTE Frame Structure

LTE supports both Time Division Duplex (TDD) and Frequency Division Duplex (FDD) and two different types of frame structures for FDD and TDD are defined in E-UTRA.Radio resources are distributed in time-frequency manner which is shown in Figure 1.6.

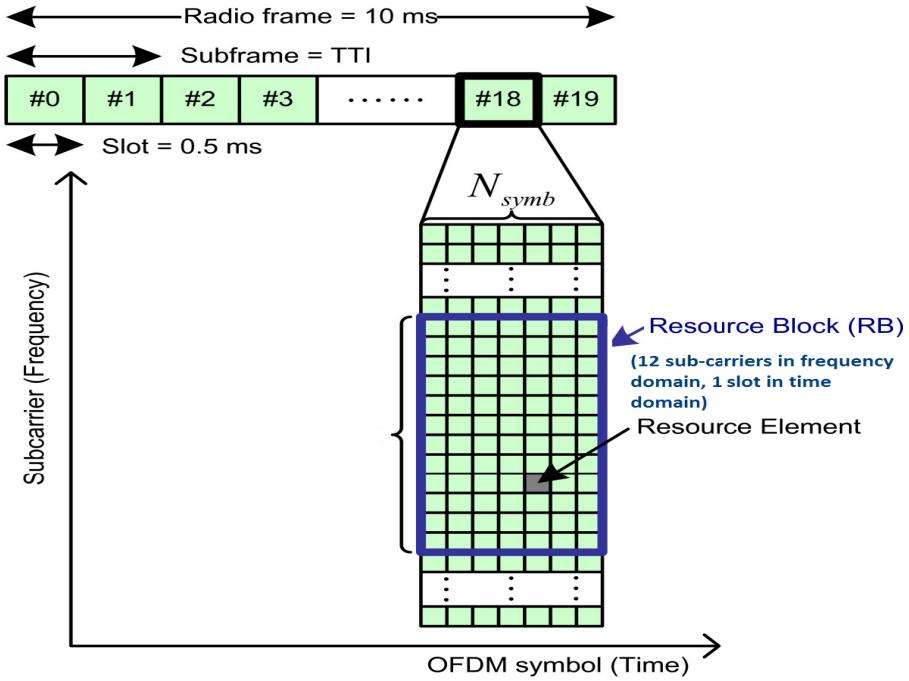

Figure 1.6: Downlink resource grid [32]

1.1.3.1 FDD Frame Structure

As shown in FDD frame structure Figure 1.7, each radio frame has 10 sub-frames of duration 1ms. Each sub-frame is divided into two 0.5ms slots [27]. Each slot comprises of six or seven symbols. The shorter time span at the beginning of each symbol is added to counter Inter Symbol Interference (ISI) and is called Cyclic Prefix (CP) [28]. When there are seven OFDM symbols in each slot, its called normal CP and extended CP when the number of symbols is six. In the frequency domain sub-carrier spacing is 15Khz. One sub-carrier in frequency domain and one symbol in time domain

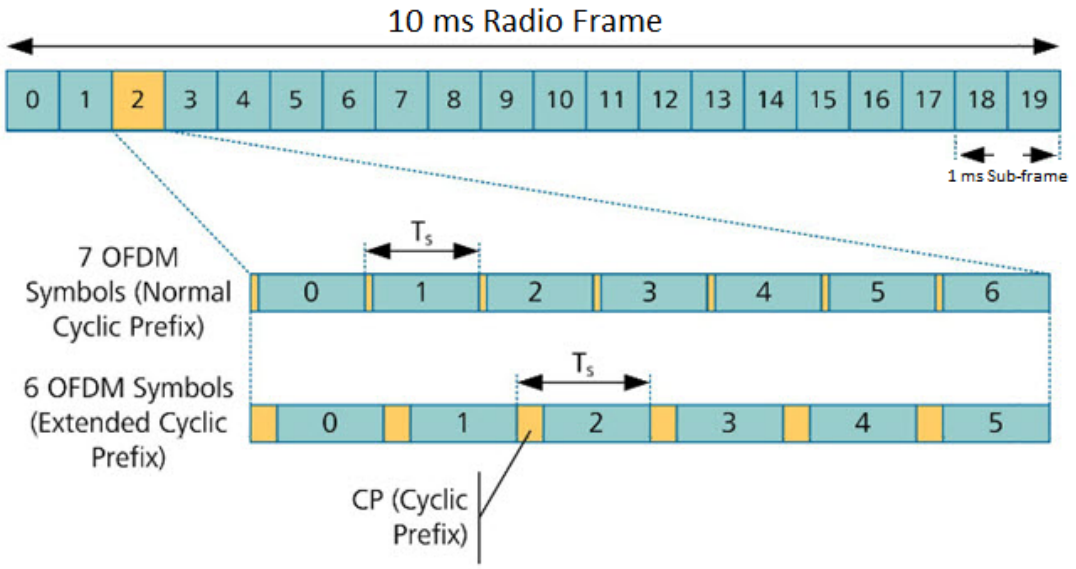

Figure 1.7: FDD Radio Frame [35]

forms a Resource Element (RE). Twelve consecutive sub carriers of 180KHz (15 kHz each) and 7 OFDM symbols (for normal CP) or six OFDM(for extended CP) symbols is called a Resource Block (RB). Two consecutive RBs within a slot form a Physical Resource Block (PRB). PRB is the smallest resource allocation unit assigned to an UE [32] in LTE. The time duration of a PRB is called Transmission Time Interval (TTI) [22] which is 1ms.

Figure 1.8 represents a detailed view of a resource grid for 20 MHz system bandwidth. From the resource grid, it can be seen that central 6 resource blocks are mainly used for control and synchronisation channels, such as, Physical Broadcast Channel (PBCH), Physical Downlink Control Channel (PDCCH), Physical Control Format Indicator Channel (PCFICH), Physical Downlink Shared Channel (PDSCH) and Primary Synchronization Signal (P-SS). A brief description of these control channels are given below [26]

Downlink Physical Broadcast Channel (PBCH) : PBCH is mapped to the six centred resource blocks as shown in Figure 1.8. It carries only Master Information Block (MIB) and decoding of MIB by UE provides the information such as System

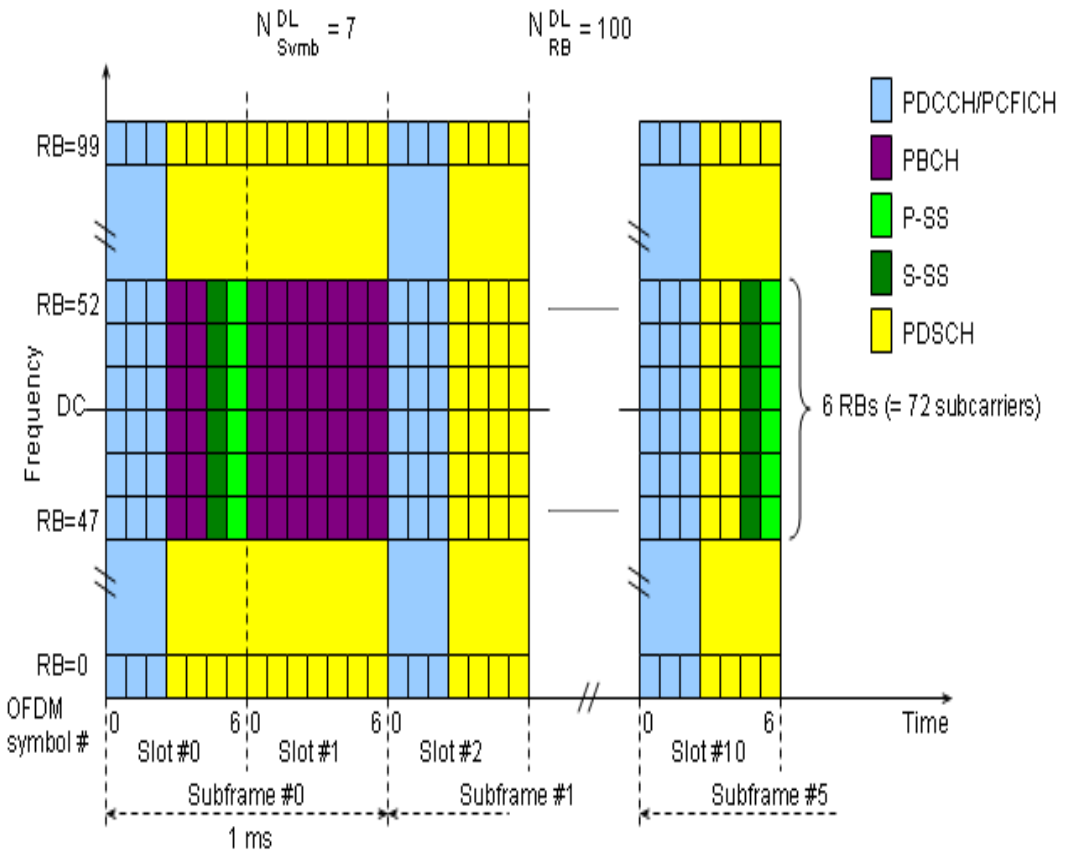

Figure 1.8: FDD Radio Frame [26]

Frame Number (SFN), DL bandwidth, number of TX antennas and reference signal transmit power [29].

Physical Downlink Control Channel (PDCCH) : PDCCH represents downlink control signals only and is mapped usually on the first three OFDM symbols in each downlink sub-frame. It carriers scheduling, power control and ACK/NACK information [30].

Physical Control Format Indicator Channel (PCFICH) : PCFICH is transmitted on the first symbol of a sub-frame and denotes the number of OFDM symbols at the beginning of a sub-frame containing PDCCH. It has the modulation type of $QPSK$ [31].

Primary Synchronization Signal (PSS) : PSSs are mapped

around the six centred RBs. PSSs are used for downlink frame synchronisation and determination of Physical Cell ID [29].

Physical Downlink Shared Channel (PDSCH) : PDSCH carries DL payload and Random Access Response Messages (RARM). PDSCH uses Adaptive Modulation and Coding(AMC) with Quadrature Phase Shift Keying (QPSK), 16 Quadrature Amplitude Modulation (QAM) and 64 QAM [29].

1.1.3.2 TDD Frame Structure

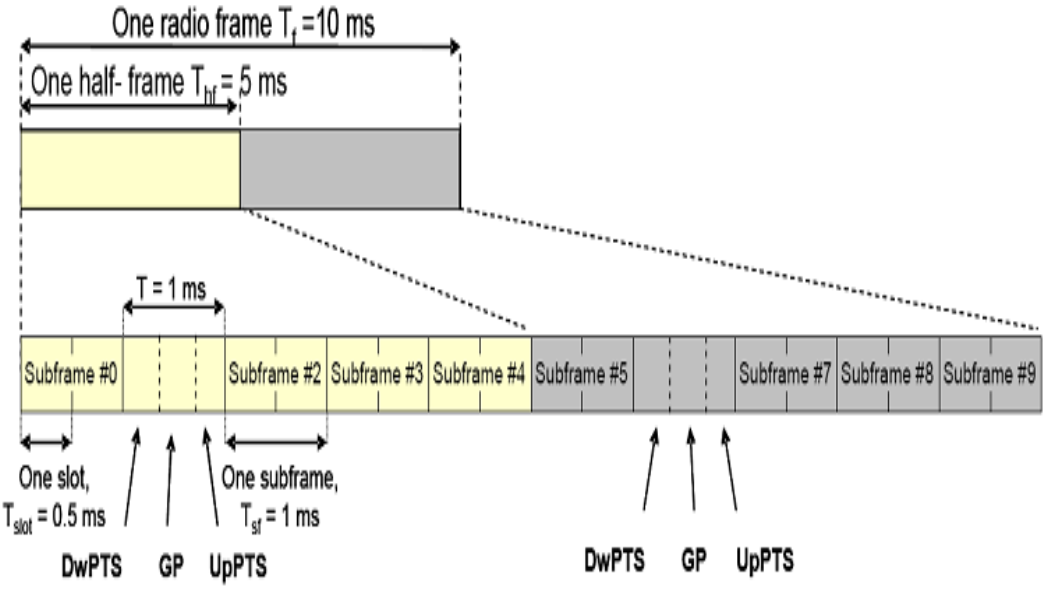

Figure 1.9: LTE TDD Frame Structure [19]

The 10 ms downlink radio frame is divided into two half frames each with the length of 5ms. Half-frames are divided into 1ms long five sub-frames which is shown in Figure 1.9. These sub-frames may be divided into three special sub-frames- Downlink Pilot Timeslot (DwPTS), Guard Period (GP), and Uplink Pilot Timeslot (UpPTS) taking the total length of 1ms where, DwPTS and UpPTS facilitates downlink and uplink synchronisation respectively [34].

1.1.4 Bandwidth

LTE can operate on a number of carrier frequencies and this allows LTE to operate in different geographical areas. As depicted in

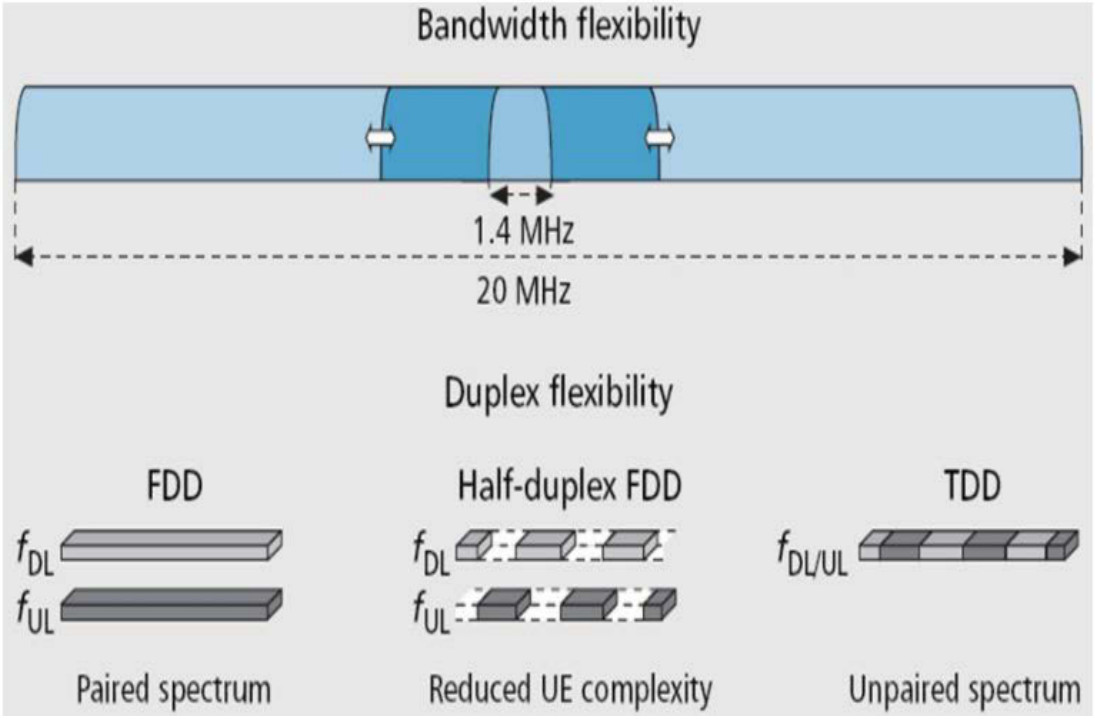

Figure 1.10: LTE spectrum flexibility. Half duplex FDD is seen from a terminal perspective [36]

Figure 1.10, the overall system bandwidth of LTE ranges from 1.4 MHz up to 20 MHz and Table 1.2 shows the corresponding number of radio blocks for each bandwidth (RB)[36].

Table 1.2: Number of resource blocks for different LTE bandwidths (FDD and TDD)

Channel Bandwidth (MHz)	1.4	3	5	10	15	20
Number of Resource Blocks	6	15	25	50	75	100

1.2 LTE Femtocell Network Architecture

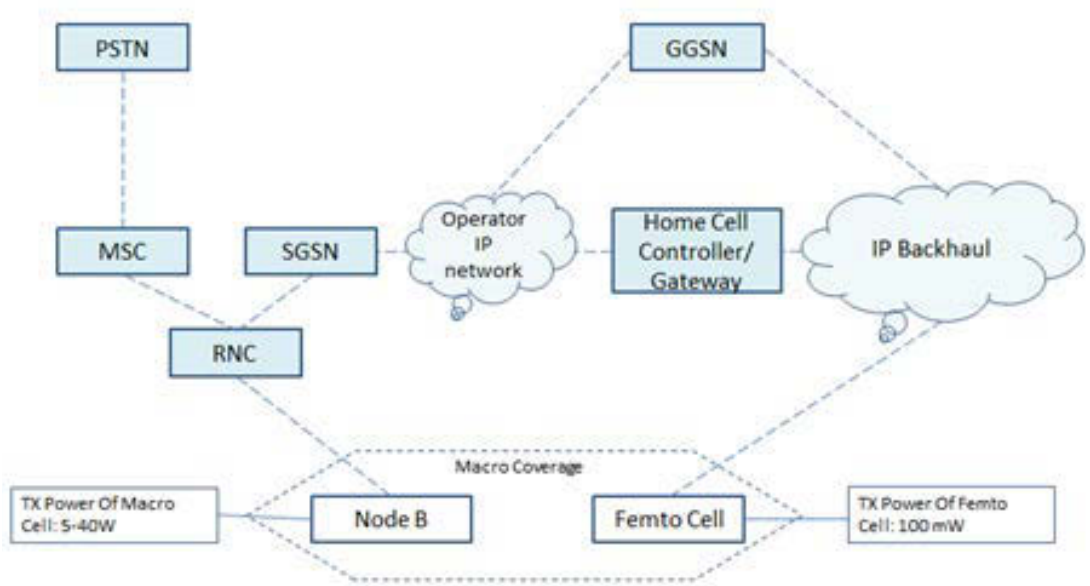

Figure 1.11: Femtocell network diagram [36]

In the current wireless communication systems, the primary challenge is to improve the indoor coverage, capacity enhancement and provide mobile services with high data rates in a cost effective manner [37]. Network coverage and capacity can be improved when a transmitter and receiver of a mobile network are positioned closed to each other. However, this results in installing more base stations throughout the coverage area, which is not economically feasible. Miniature home base stations, popular by the name of femtocells [9], can solve this capacity and coverage related problem, are considered as promising option for the mobile operators. The inclusion of femtocell in 3GPP commenced in Release 8 and continued in later releases. Figure 1.11 shows femtocell network architecture. Femtocells or Femto Access Points (FAPs) are small in size, portable, provide limited coverage (10-30m) and consume lower power (10-100mw) compared to Macrocell eNB (MeNB). FAPs operate in operator's licensed spectrum and are connected to the core network

Table 1.3: Traditional Cellular versus Femtocell comparison [9]

Attribute	**Cellular**	**Femtocellular**
Infrastructure cost	10,000−100,000	100−200
Infrastructure finance	Operator	End user
Backhaul	Expensive E1/T1 lines	DSL
Planning	Operator	End user (no central planning)
Deployment	Operator	End user (Plug and Play)
Quality of Service (QoS)	Operator controlled	Best effort
Control	Operator via O&M	Operator via internet
Mobility	Good/Excellent	Best effort
Data throughput	Limited	Excellent

through broadband communication link [38]. FAPs can improve the indoor received signal strength where the MeNB signal is poor. High speed data rate, QoS and longer battery life (since UE do not need to communicate with distant MeNB at high transmit power) is possible for femtocell users(FUEs) served in a femtocell area. A comparison between macrocell and femtocell is given in Table 1.3 [9].

1.2.1 Access Modes in Femtocells

Femtocells can support a limited number of users. In general, femtocells are designed to operate in one of three different access modes described below [40]-

Open Access Mode : Provides access to all users and are suitable for public places like university, shopping mall, airport terminals. This type of access mode is prone to huge congestion at the busy hours and lower spectrum utilization at weekends and off-peak hours.

Closed Access Mode : Except some specific users, access is restricted in this mode for all. The owner of the femtocell has

the authority to decide which UE can access the femtocell. The group of subscribers allowed to access the femtocells are defined as Closed Subscriber Group (CSG) in 3GPP.

Hybrid Access Mode : This access mode allows only a particular number of non-femtocell users to access FAP. Hybrid access mode takes the benefit from both the open and closed access modes.

Closed access mode is mostly preferred for its strong security feature. However, in this research work based on the obtained performance evaluation results in closed access mode, a modification on hybrid access mode is simulated for the improvement of system throughput and mitigation of interference in macro-femto network.

1.3 Problem Statements and Research Objectives

Femtocells are expected to improve indoor coverage and capacity at cell edge with a higher spectrum utilization. However, integration of femtocells in predominant macrocellular network and handover in macro-femto scenarios are the most challenging issues in mobile communication [40]. Dense and unplanned deployment, access control and short cell radii make the mobility management more complicated. Dense deployment and short cell radii of femtocells increase the number of target cells which leads to increasing handover probability, possible handover failure and high interference. Moreover, the difference in received signal strengths between femtocells and eNB and restricted access to FAP, that degrades SINR of both macro and femto-tier users at the cell edge. In this research work, a number of handover algorithms have been studied and the aim of this thesis was to develop a new adaptive speed based handover algorithm which is capable of satisfying the following conditions:

1. It will improve the system performance by minimizing cross-tier interference.
2. It will enable the system to maximize system throughput.
3. It will improve the SINR for both macro and femto tier users and improve spectral efficiency and fairness.

1.4 List of Publications

The majority of the contribution in the thesis material has been presented peer reviewed journals and conferences.

Journals

1. Ghosal, P, Barua, S, Subramanian, R, Xing, S, Sandrasegaran, K, A Novel Approach for Mobility Management in LTE Femtocells, International Journal of Wireless and Mobile Networks(IJWMN), vol. 6, no. 5, pp. 45-58, October 2014.http://airccse.org/journal/jwmn/6514ijwmn04.pdf.

2. Xing, S, Ghosal, P, Barua, S, Subramanian, R, Sandrasegaran, K, System Level Simulation for Two Tier Macro-Femto Cellular Networks, International Journal of Wireless and Mobile Networks (IJWMN), November 2014.http://airccse.org/journal/jwmn/6614ijwmn01.pdf.

3. Kim, A H, Barua, S, Ghosal, P, Sandrasegaran, K, Macro with Pico Cells (HetNets) System Behavior With Well-known Scheduling Algorithms, International Journal of Wireless and Mobile Networks (IJWMN), vol. 6, no. 5, pp. 109-122, October 2014. http://airccse.org/journal/jwmn/6514ijwmn09.pdf.

Conference

1. Xing, S., Ghosal, P., Sandrasegaran, K., Daeinabi, A. (2014, November). System level simulation for femtocellular networks. In Telecommunication Networks and Applications Conference (ATNAC), 2014 Australasian (pp. 164-169). IEEE.

Chapter 2

Mobility Management and Handover

Femtocell Access Points(FAPs) create a two tier (macro tier and femto tier) mobile network architecture when deployed in same licensed spectrum with macro-cellular network [39]. Femtocells improve indoor network capacity, coverage and quality. However, dense and unplanned deployment of femtocells may increase the interference in both macro and femto-tiers, leading to challenges in interference and mobility management. This chapter discusses the main types of interference in two-tier network architecture and key interference management and handover algorithms in the literature.

2.1 Interference in Femtocells

In two-tier network architecture, a user which is served by a FAP is called a Femtocell User (FUE) whereas a user served in macro-tier is known as Macroll UE(MUE). Co-channel deployment of femtocells in same frequency bands as macrocell may lead to high uplink and downlink interference in both tiers [42]. The area of the femtocell coverage in which users do not experience any communication due to this high interference is called a **dead zone**. Based on the in-

terference in two-tier architecture, interference management can be divided into two main types which are illustrated in Figure 2.1.

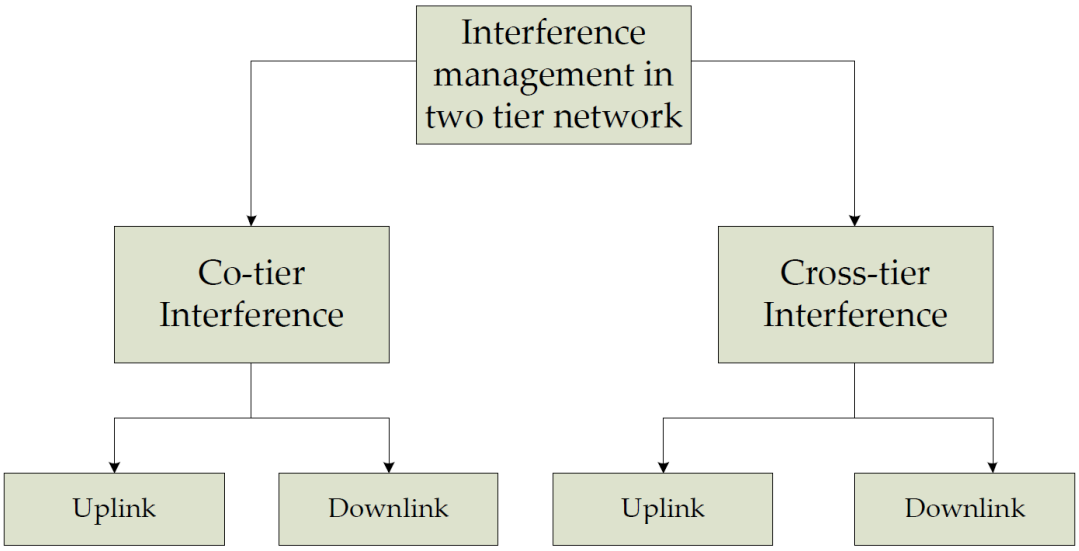

Figure 2.1: Interference management schemes in OFDMA based femtocell network [39]

2.1.1 Co-tier Interference

Interference between network elements in the same tier is referred to the **co-tier interference** [39]. The deployment of FAPs increase the chances of power leaks through windows or doors. If the Signal to Interference plus Noise Ratio (SINR) is below a threshold due to this co-tier interference, this would create a dead zone. Downlink co-tier interference at a femtocell caused by another femtocell is shown by the dotted line in Figure 2.2. A FUE acts as an uplink interferer to neighbouring FAPs when it tries to communicate with its serving FAP with high transmit power.

2.1.2 Cross-tier Interference

When femtocells operate in a shared macrocell spectrum it may cause severe co-channel interference with increasing number of

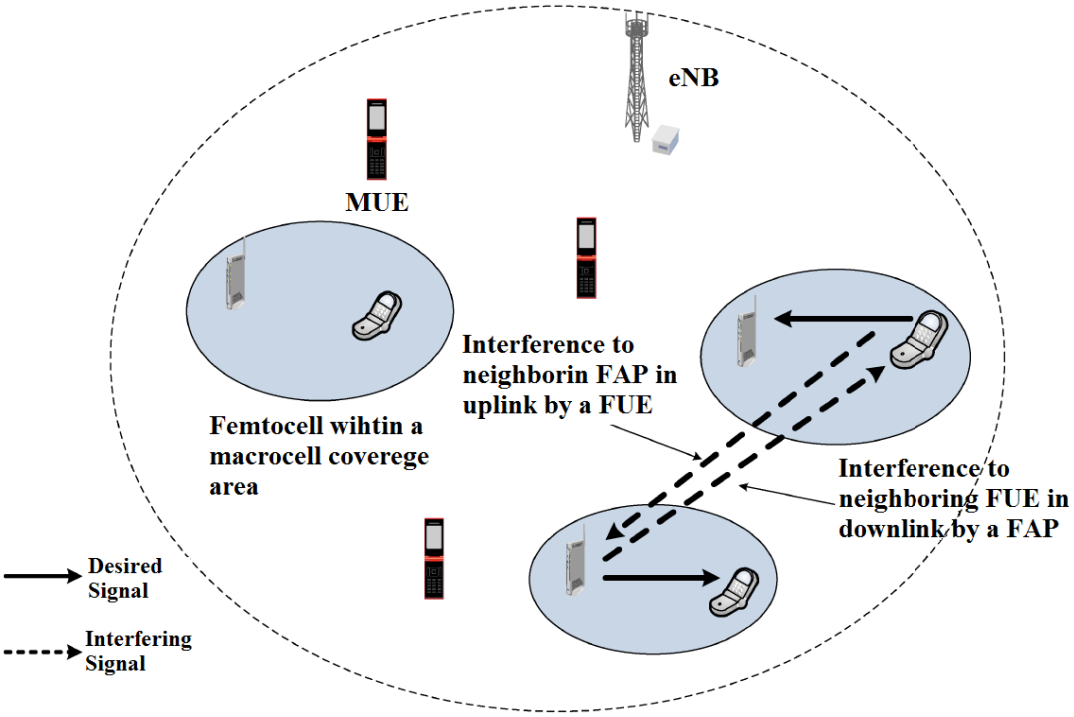

Figure 2.2: Co-tier interference scenarios in femtocell network [39]

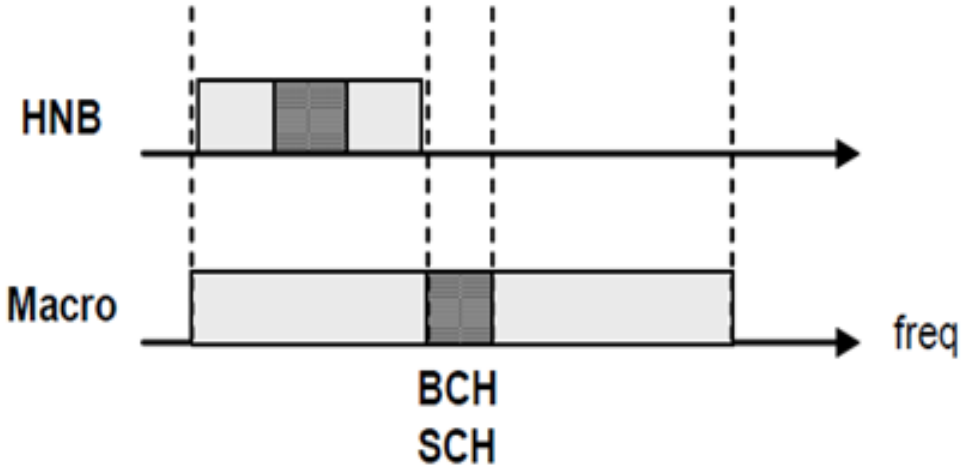

Figure 2.3: System frequency bandwidth spectrum [43]

FUEs. On the other hand, dedicated spectrum for femtocells could prevent co-channel interference but comes with higher spectrum cost and poor resource utilisation and spectrum scarcity. Therefore, analysing the trade-off between the resource utilization and co-channel interference is important. In LTE partial co-channel

configuration [104] which is shown in Figure 2.3, the spectrum of femtocell does not overlap with the central six resource blocks [27] of the macrocell downlink spectrum in which important control information is transmitted. Thus, MUEs will be able to communicate with eNBs through Downlink Physical Broadcast Channel (PBCH) and synchronisation signals. Figure 2.4 shows an example of downlink cross-tier interference caused by FAP to the nearby MUE.

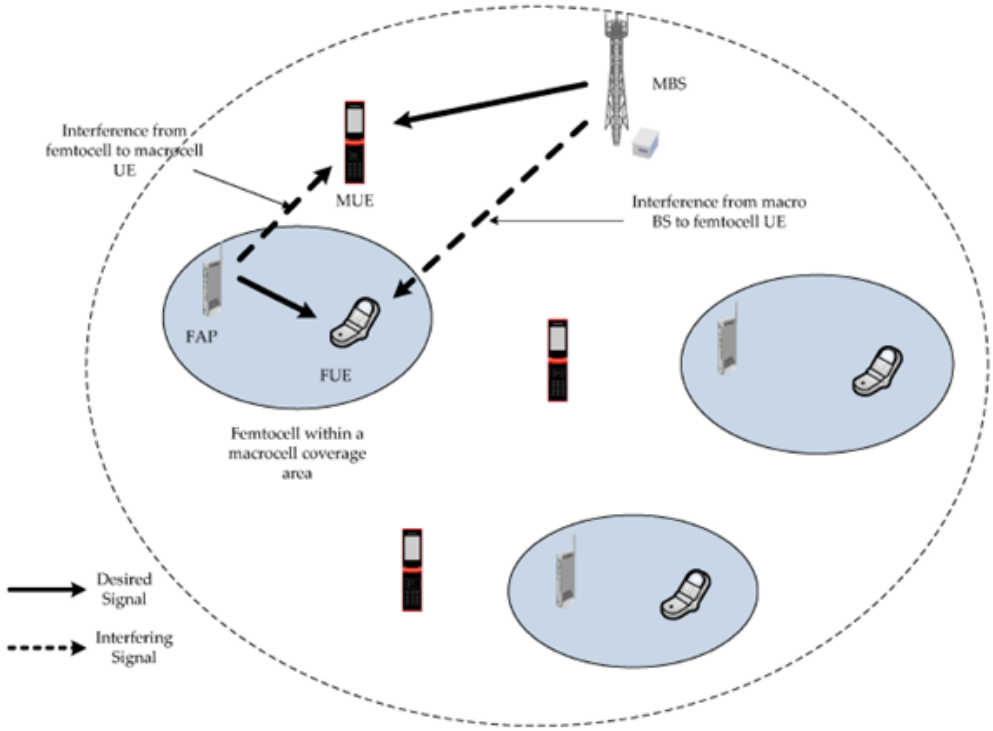

Figure 2.4: Cross-tier interference scenario [39]

In case of closed access mode, the area around the femtocell becomes a restricted zone for MUE since it doesn't have access to FAP. There will be high uplink interference in cases where, femtocells are located at cell edge and MUE is located outside FAP coverage area [44]. On the other hand, the serving area of a femtocell will shrink if a nearby eNB transmits signals with higher transmit power to reach distant MUE.

2.2 Interference Management Techniques

Downlink interference management technique is dependent on factors such as spectrum sharing, allocation of sub channels, exchange of information among nodes, and formation of groups of FAPs. Interference management techniques to solve co-tier and cross-tier interference in both uplink and downlink are categorized into three types: a) interference cancellation b) interference avoidance/coordination and c) distributed interference management as shown in Figure 2.5.

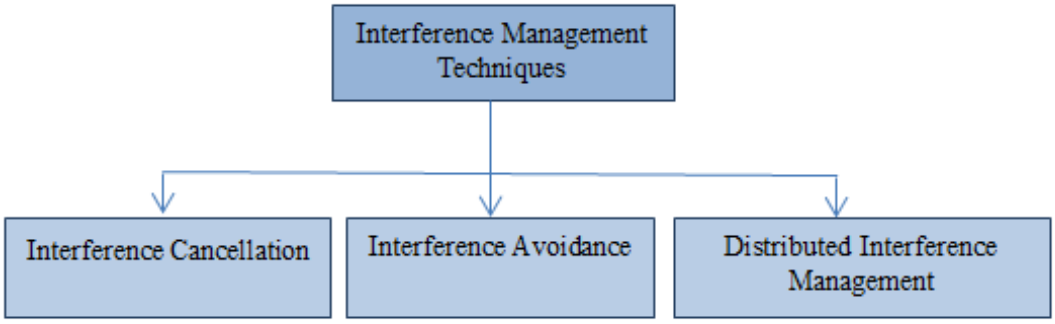

Figure 2.5: Different interference management techniques in femtocells [39]

In interference cancellation schemes, the interference is cancelled at the receiver using the received signal. According to Andrews [48] cancellation is performed by first decoding the received signal and then cancellation of interference utilizing the decoded information along with the channel estimation. Successive Interference Cancellation (SIC) and Parallel Interference Cancellation (PIC) [48]-[53] are two methods used in interference cancellation.

Another mechanism to reduce cross-tier interference is spectrum splitting in which the allocated bandwidth is divided into two separate portions for femto and macro tiers. In this case, only co-tier interference will exist but spectrum splitting will lead to spectrum inefficiency as well as a higher cost due to scarcity of available spec-

trum [75].

A third mechanism for interference management is centralized management of femtocells. This is complex because information to FAPs is sent through backhaul DSL link. A large number of FAPs within a macrocell coverage area may cause huge congestion in backhaul and incur delay[39]. So, instead of providing large information through backhaul, distributed control schemes (distributed interference management/ interference coordination schemes) have become popular [85].

2.2.1 Interference Coordination by Time-Domain Sub-Frame Alignment

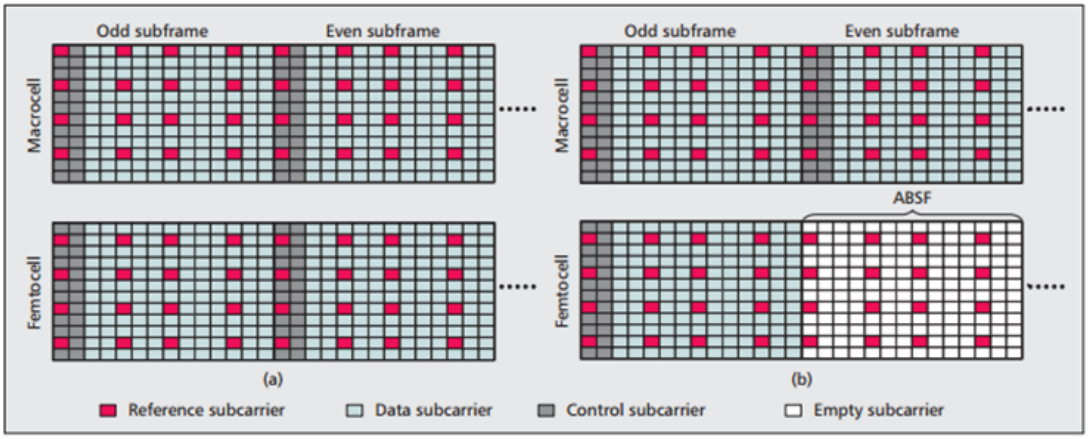

Figure 2.6: Enhanced ICIC by scheduling Almost Blank Sub-Frames [62]

To mitigate the intercell interference in presence of femtocells, extended Intercell Interference Coordination (eICIC) was introduced in 3GPP, Release 10. eICIC introduced the concept of Almost Blank Sub-Frames(ABSF) where no control or data signals except Cell Specific Reference Signals(CRS) are scheduled in sub-frames. When a MUE is located outside of FAP and shares the same spectrum with FUE, it creates both uplink and downlink interferences, these interfering MUEs are referred as Victim MUEs(VMUE). When the

sub-frames of eNB and FAP are aligned as in Figure 2.6(a), both of their data and control channels overlap. Femtocells are called aggressor [42] since they create downlink interference to VMUEs. To avoid downlink cross-tier interference, femtocells schedule ABSFs as shown in Figure 2.6(b). However, interference due to reference signals still exists in this technique.

2.2.2 Femto-aware Spectrum Arrangement Scheme

In [59], authors proposed femto-aware spectrum arrangement to avoid cross-tier co-channel interference. The available spectrum is divided into macrocell spectrum and shared macro-femto spectrum where the macrocell spectrum is exclusively used by MUEs. This

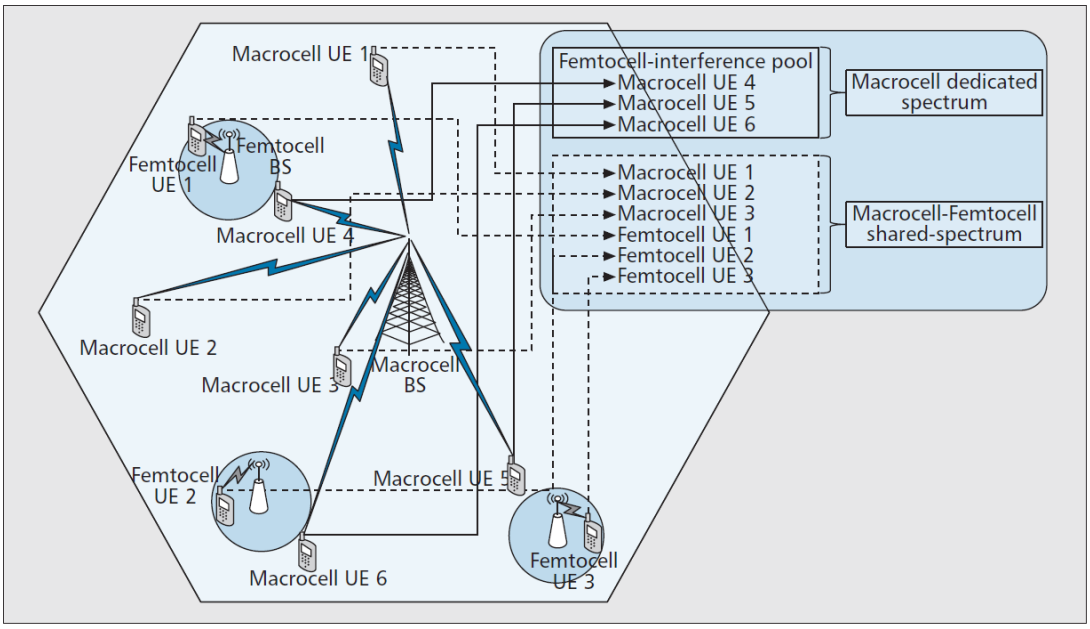

Figure 2.7: Femto aware spectrum arrangement scheme [59]

partitioning is implemented by mobile operators and the eNBs are aware of the spectrum allocation. Here, eNB creates an interference pool consisting MUEs which create uplink interference to the nearby FAP operating in shared spectrum at cell edge. Upon receiving the

channel quality information from the interfering MUE, eNB assigns that MUE to interference pool and allocates in dedicated macrocell spectrum to avoid uplink and downlink cross-tier interferences. Figure 2.7 illustrates the scenario where macrocell users UE4, UE5, and UE6 are using the shared spectrum and pose a threat to the nearby FAPs. To avoid this interference, these MUEs are assigned to the interference pool by the eNB where they are allocated to dedicated macrocell spectrum. UE1, UE2, UE3 are using the shared spectrum but since these are not near to FAP serving area, they are free to operate in the same shared spectrum. However, in this scheme, the co-tier interference, which can be problematic in dense deployment is not considered and it may not be efficient with the increasing number of macrocell UE in the shared spectrum.

2.2.3 Fractional Frequency Reuse

In wireless communication, frequency reuse refers to the reuse of the same carrier frequency or set of frequencies at neighbouring cells as shown in Figure 2.8(a) to improve the network performance and spectral efficiency. The rate at which frequency can be reused in the network is known as reuse factor. In hard frequency reuse, allocated bandwidth is divided into a number of non-overlapping sub-band groups according to the reuse factor. Each group is assigned to cells having the same frequency reuse pattern. In Soft Frequency Reuse (SFR), overall bandwidth is used by all the eNBs with a reuse factor of one but there is a power restriction on each sub-carrier [84] as illustrated in Figure 2.8(b) in cluster of 7 cells.

Strict Fractional Frequency Reuse (SFFR) is a compromise between the above mentioned reuse techniques, where the allocated spectrum is divided into two overlapping groups. Users near to the eNB (in terms of path loss) are assigned into inner part (centre zone) with lower transmit power and reuse factor of one. On the

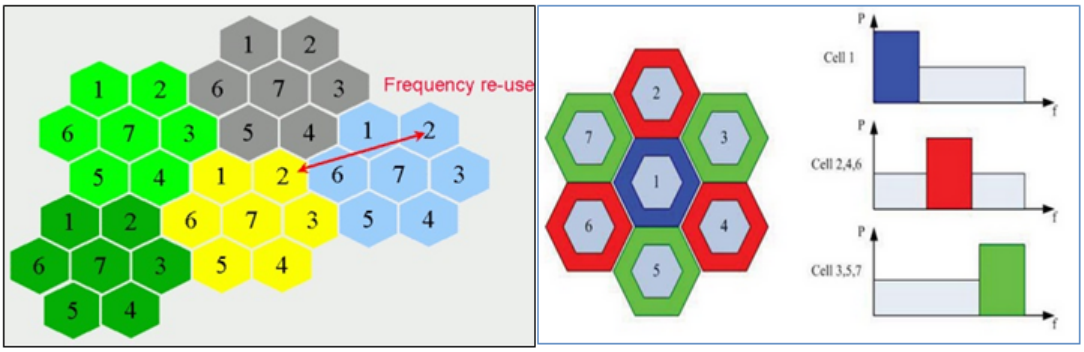

Figure 2.8: a) Cell-frequency-reuse [77], b) frequency planning and power allocation for SFR Scheme [77]

other hand, rest of the users called cell edge users are allocated rest of the bandwidth (edge zone) with higher transmit power and reuse factor greater than one [84] which is depicted Figure 2.9. Frequency reuse schemes can mitigate the co-channel or inter-cell interference at the cell edge since the allocated frequency sub-bands are different in neighbouring cells. In the edge zone, only a fraction of the

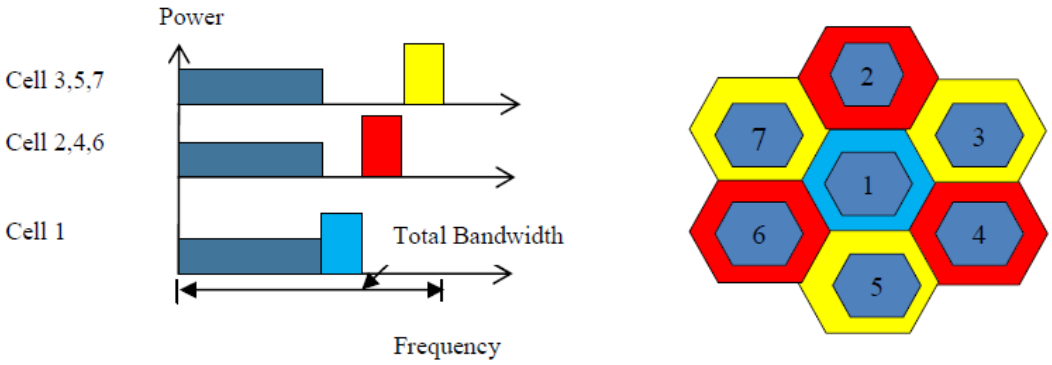

Figure 2.9: Strict Fractional Frequency Reuse (SFFR)[84]

available band is allocated. This reduced spectrum allocation at the cell edge may affect network throughput and capacity of that region. Moreover, throughput and capacity may not increase with increasing number of users in the cell edge area.

2.3 Handover Algorithms for Femtocells

In the two tier macro-femto scenario, there are three possible handover scenarios [106] as shown in Figure 2.10. When an UE is moving into a femtocell coverage from a macrocell coverage area, an inbound handover (Inbound HO) takes place. In an outbound handover(Outbound HO), the UE switches to macrocell coverage from the femtocell coverage. When the FUE is moving from one FAP coverage area to another FAP coverage area, it is called an Inter-FAP handover. In the outbound handover, handover decision parameters include the measurement of $SINR$, QoS, $ReceivedSignalStrengthIndicator(RSSI)$ of the neighbouring cells of UE's neighbour cell list. On the other hand, in an Inbound HO or Inter-FAP handover, apart from RSS and RSQ , access control, interference, user speed, available bandwidth and position have to be taken into consideration. Moreover, unlike macrocell,

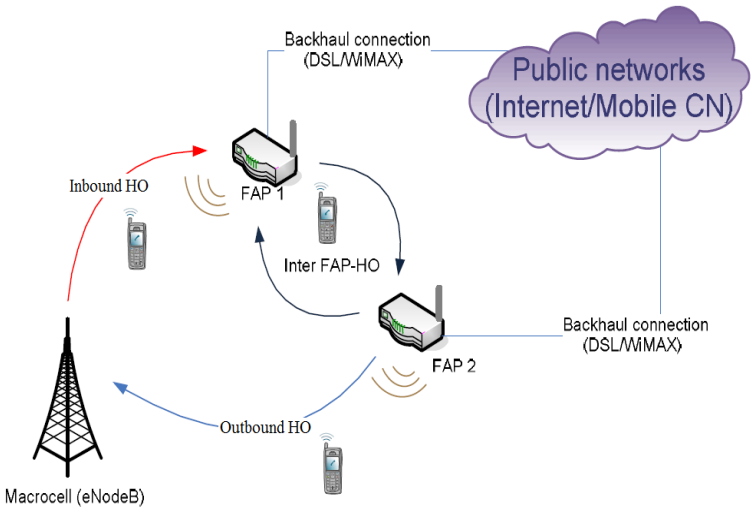

Figure 2.10: Handover scenarios in presence of Femtocells [106]

femtocell network does not have a X2 interface between FAPs. The use of DSL backhaul link between FAP and eNB incurs delay and makes the handover decision slower than in a macro-cellular net-

work. Moreover, rapid fluctuation in RSS from serving and target cells or frequent user movement between serving and target cell near a femtocell-eNB boundary may cause multiple subsequent handovers between serving and target cells. This successive handovers are known as ping-pong in handover [105]. Frequent releasing and reserving of radio resources because of ping-pong, could decrease the QoS, network performance and results in frequent call drops. In this section, a number of proposed handover algorithms are discussed to improve network performance and reduce the ping-pong effect. Handover to/from/between FAPs [64] can be based on- a) Received Signal Strength (RSS/RSRP), b) user speed, c) cost-function based, d) interference experienced at user end or serving cell, and e) energy emission.

2.3.1 Received Signal Strength Based Algorithms

The handover decision algorithms is based on the $ReceivedSignalStrength(RSS)$ as shown in Figure 2.11. To minimize the ping-pong effect, the RSS based algorithms considers a $HandoverHysteresisMargin(HMM)$ to compare the RSS of the source and target cell.

2.3.1.1 Received Signal Strength Based Algorithms

When an UE enters the coverage area of femtocells, it most likely experiences a large difference in received powers between macrocell and femtocells [i.e., eNB(46dBm) and FAP(20dBm)]. The proposed algorithm in [66] compensates the RSS difference in a single macrocell-femtocell scenario by developing an exponential window function.

When user is moving in straight line from eNB to FAP at a

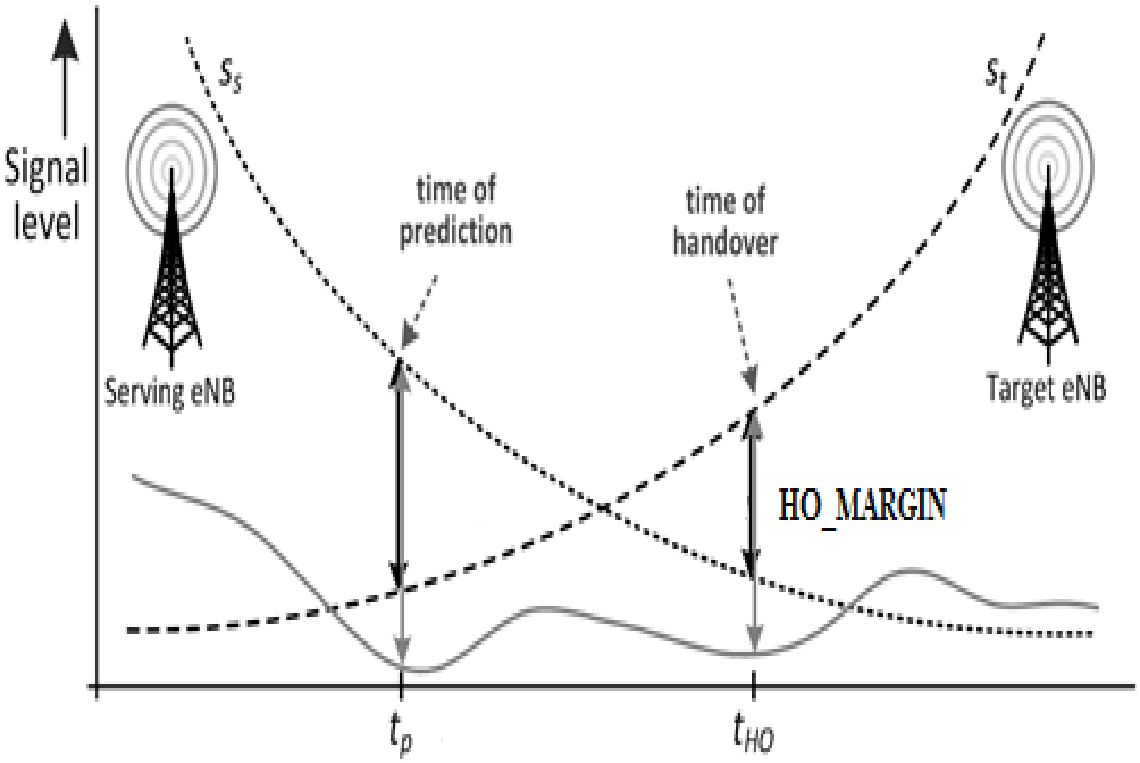

Figure 2.11: Received signal strength based HO [65]

constant speed with unity antenna gains and at time instant k the RSS from eNB and FAP are represented by $s_m[k]$, $s_f[k]$ respectively. Transmit power and path loss from eNB and FAP are denoted as $P_{m,tx}$ $P_{f,tx}$ $PL_m[k]$ $PL_f[k]$ respectively, $s_m[k]$, $s_f[k]$ can be given as follows:

$$s_m[k] = P_{m,tx} - PL_m[k] - u_m[k] \tag{2.1}$$

$$s_f[k] = P_{f,tx} - PL_f[k] - v_m[k] \tag{2.2}$$

where, $u_m[k]$ and $v_m[k]$ are the lognormal shadowing. Exponential window function $[k] = 1/d_1 \exp(kd_s/d_1)$ in Equation 2.3 and 2.4 is applied to prevent abrupt variation in RSS, where, d_s is distance between two adjacent measurement locations and d_1 is the window length.

$$\bar{s}_m[k] = w[k] * s_m[k] \tag{2.3}$$

$$\bar{s}_f[k] = w[k] * s_f[k] \tag{2.4}$$

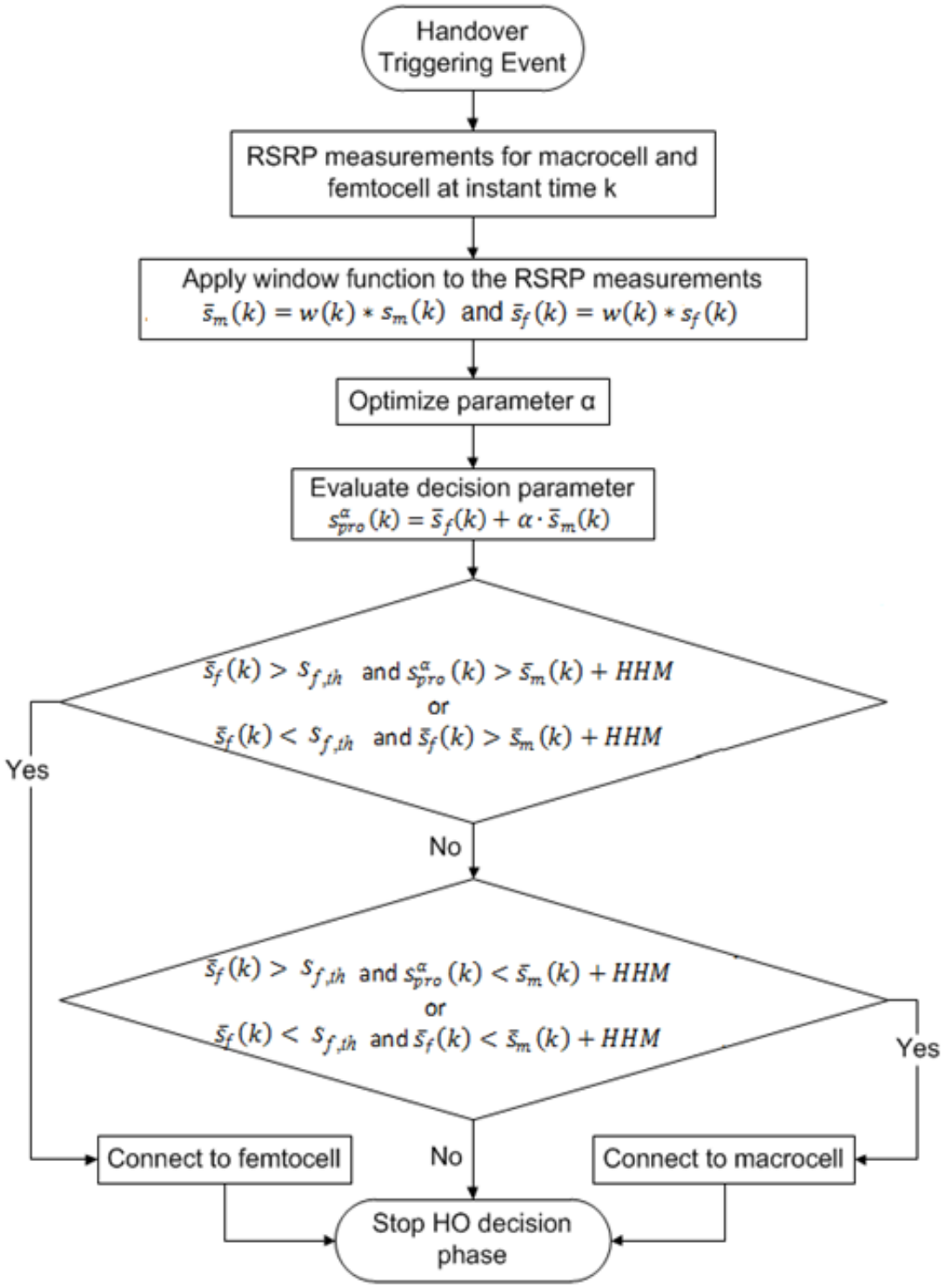

Figure 2.12: HO algorithm based on RSS [66]

here, $w[k]$ denotes the exponential window function and $\bar{s}_m[k]$, $\bar{s}_f[k]$ represent the filtered RSS of the macrocell and the femtocell at time k respectively. These filtered signals are then combined into a

RSS-based decision parameter based on the following equation [66]:

$$s^{\alpha}_{pro}[k] \;=\; \bar{s}_f[k] + \alpha \bar{s}_m[k] \tag{2.5}$$

where, $\alpha \,\epsilon\, [0,\, 1]$ is the combination factor to compensate the large difference between transmit power of eNB and FAP. The algorithm proposed in [66] is depicted in Figure 2.12. For inbound mobility, handover to the femtocell is possible,

$$if, \quad \bar{s}_f[k] > s_{f,th} \quad \text{and } s^{\alpha}_{pro}[k] > \bar{s}_m[k] + HMM \tag{2.6}$$

$$or \quad \bar{s}_f[k] < s_{f,th} \quad \text{and } \bar{s}_f[k] > \bar{s}_m[k] + HMM \tag{2.7}$$

On the other hand, for connecting to macrocell from femtocell is performed,

$$if, \quad \bar{s}_f[k] < s_{f,th} \quad \text{and } \bar{s}_f[k] + HMM < \bar{s}_m[k] \tag{2.8}$$

$$or \quad \bar{s}_f[k] > s_{f,th} \quad \text{and } s^{\alpha}_{pro}[k] < \bar{s}_m[k] + HMM \tag{2.9}$$

here, $s_{f,th}$ is the threshold RSS from target femtocell$(-72dBm)$[66] and HMM is the adaptive hysteresis margin. The advantages of this algorithm is that, it considers the difference in transmit powers between eNB and FAP and includes optimization parameter α to compensate RSS from FAP and eNB. Nevertheless, UE speed, bandwidth availability, user subscription and interference were not considered in this single cell macro-femto model.

2.3.1.2 Received Signal Strength and Path Loss Based HO Algorithm

Authors in [68] proposed a handover decision algorithm that considers path loss along with RSS for inbound mobility into femtocells. Similar to the proposals in [66],[67], this path-loss based algorithm considers exponential window function $w(k)$ on the RSS measurements. Handover to femtocell from macrocell is possible if a) the filtered RSS measurement of the femtocell exceeds a minimum threshold($-72dBm$), denoted by $RSS_{th,f}$, b) the filtered RSS signal of the femtocell exceeds the filtered macrocell RSS plus the HHM, and c) the observed path-loss between user and FAP is less than the path-loss between UE and the macrocell. The HO algorithm flowchart is illustrated in Figure 2.13.

The main feature of this algorithm is that it considers path-loss between UE and the target cell. However, the algorithm considers single macro-femto model which may not be realistic because in dense urban scenarios, this path-loss based model may be prone to fast variation which will in turn influence ping-pong effect during handover.

2.3.1.3 Speed Based Handover Algorithm

The main decision criterion for this type of algorithm is user speed. In [69], authors proposed handover algorithm considering two decision parameters: user speed and traffic type. Based on speed, either proactive or reactive handover decisions are performed. Proactive handover is one in which a handover takes place before RSS of the serving cell reaches a pre network defined hysteresis margin. To minimize handover delay and packet loss for real time traffic is the purpose of pro-active handover. In reactive handover, handover execution is initiated when minimum RSS is reached. The purpose of reactive handover is to reduce ping-pong effect(2.3). Figure 2.14

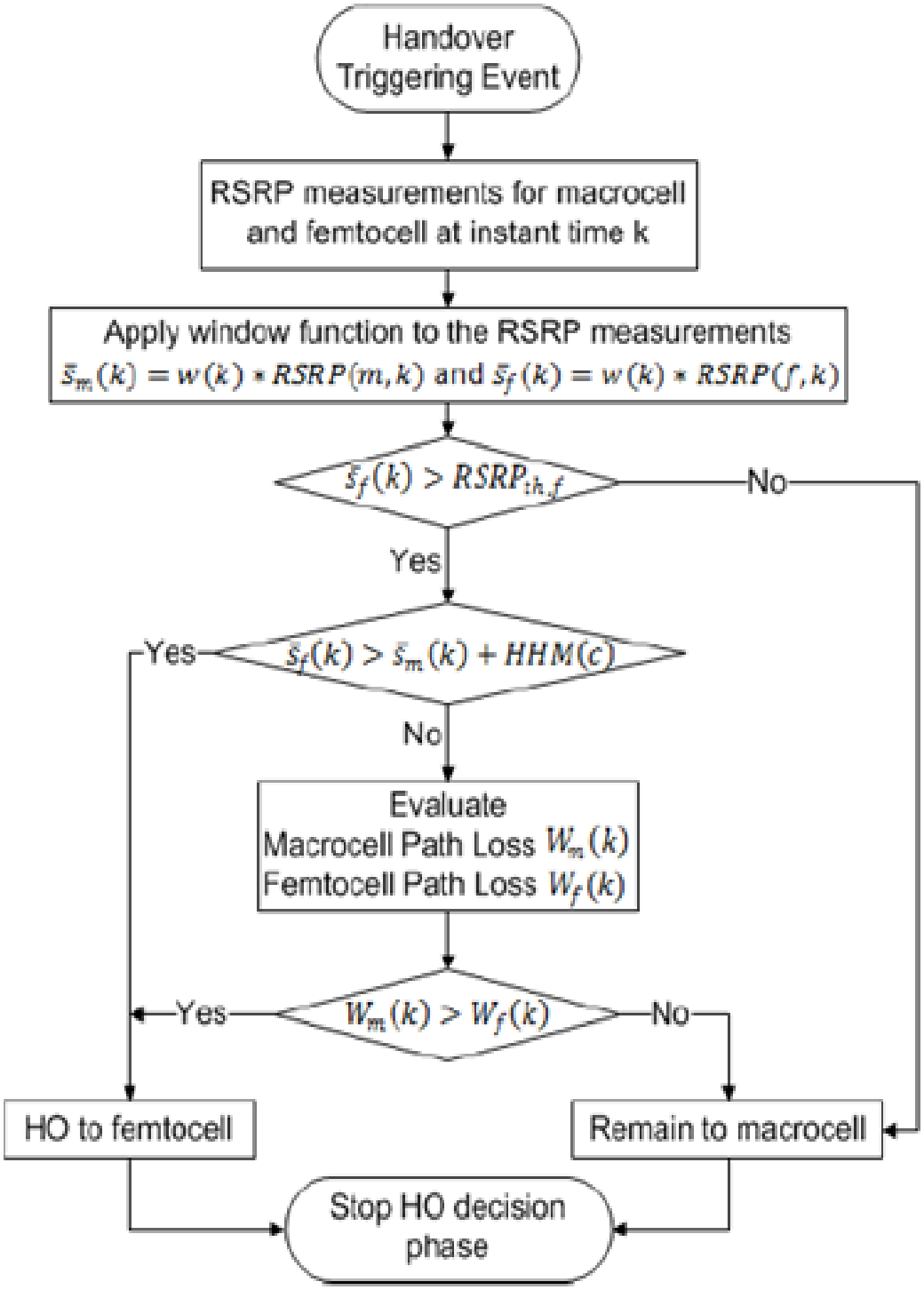

Figure 2.13: HO algorithm based on RSS and path-loss [68]

illustrates the operation of multiple macrocell-femtocell scenarios.

In the Figure 2.14, when the UE speed is higher than 10kmph, there will be no handover from macrocell to femtocell. When UE

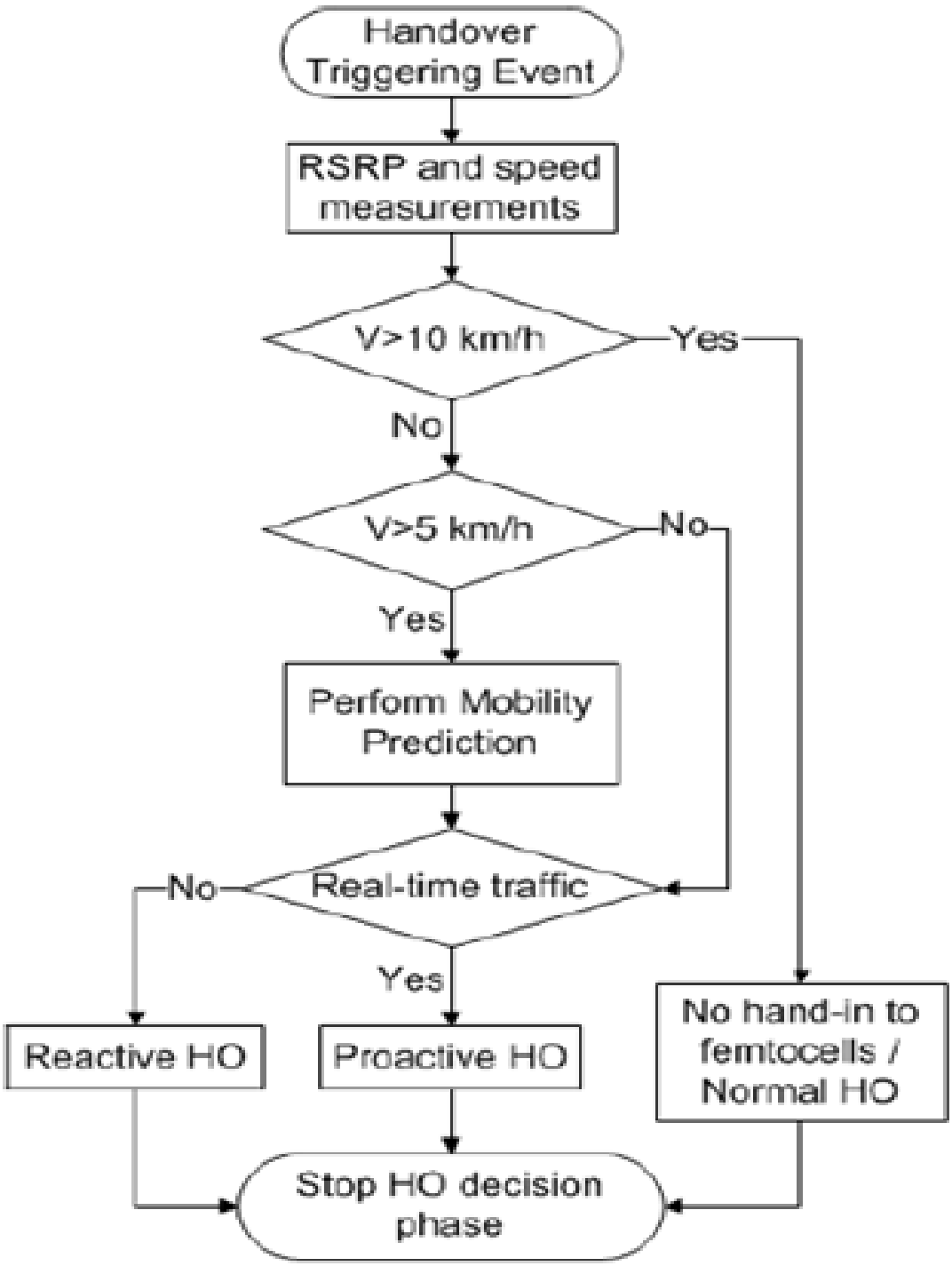

Figure 2.14: Speed based HO algorithm [69]

has the speed between 5 to 10kmph then this algorithm performs prediction model using Markov-Chain [70] to predict the direction of the user using current position and speed. If the UE moves towards

the femtocell, then the proposed model performs either proactive handover if the traffic is real-time or reactive handover if the traffic is non-real time. Same approach is followed for the users below 5 kmph without mobility prediction. This proposed algorithm is expected to reduce the handover probability for the users with medium speed (5kmph$\leq$ speed$\leq$ 10kmph) [Speed levels are explained in Appendix A.1] and provide better QoS for the real-time traffic users.

2.3.1.4 Interference-aware Handover Algorithms

While cell selection/reselection in idle mode or handover in active more, UE performs continuous measurement of the RSS on pilot channels of the neighbouring cells to choose the best serving cell. To simplify and make the selection process faster, serving macrocell periodically broadcasts list of cells (Neighbouring Cell List) and pilot channels to UE. UE periodically sends back the measurement report to serving macrocell to decide probable cell selection/reselection or handover. But authors in [72] proposes a double threshold algorithm where decision phase is performed at FAP end. The interference-aware handover algorithms mainly consider the level of interference experienced at UE or serving cell from the surrounding neighbouring cells. The proposed algorithm in [72] considers the $RSRP$ and $RSRQ$ measurements of macro and femtocell while initiating HO decision. As illustrated in Figure 2.15 when an MUE moves from macrocell coverage to femtocell coverage, it continuously monitors the $RSRP$ and $RSRQ$ of the neighbouring cells. Handover to femtocell is possible if at least one of the following conditions apply:

1.$RSRP_m < RSRP_{th,1}$ and $RSRQ_f > RSRQ_m$ or,
2.$RSRP_f \geq RSRP_{th,2}$ for time interval T and
$RSRQ_f > RSRQ_m$)

Both conditions have to satisfy the bandwidth availability in femtocell with the UE requirements. Failure to satisfy these conditions results in UE staying in macrocell coverage. The strong feature of the

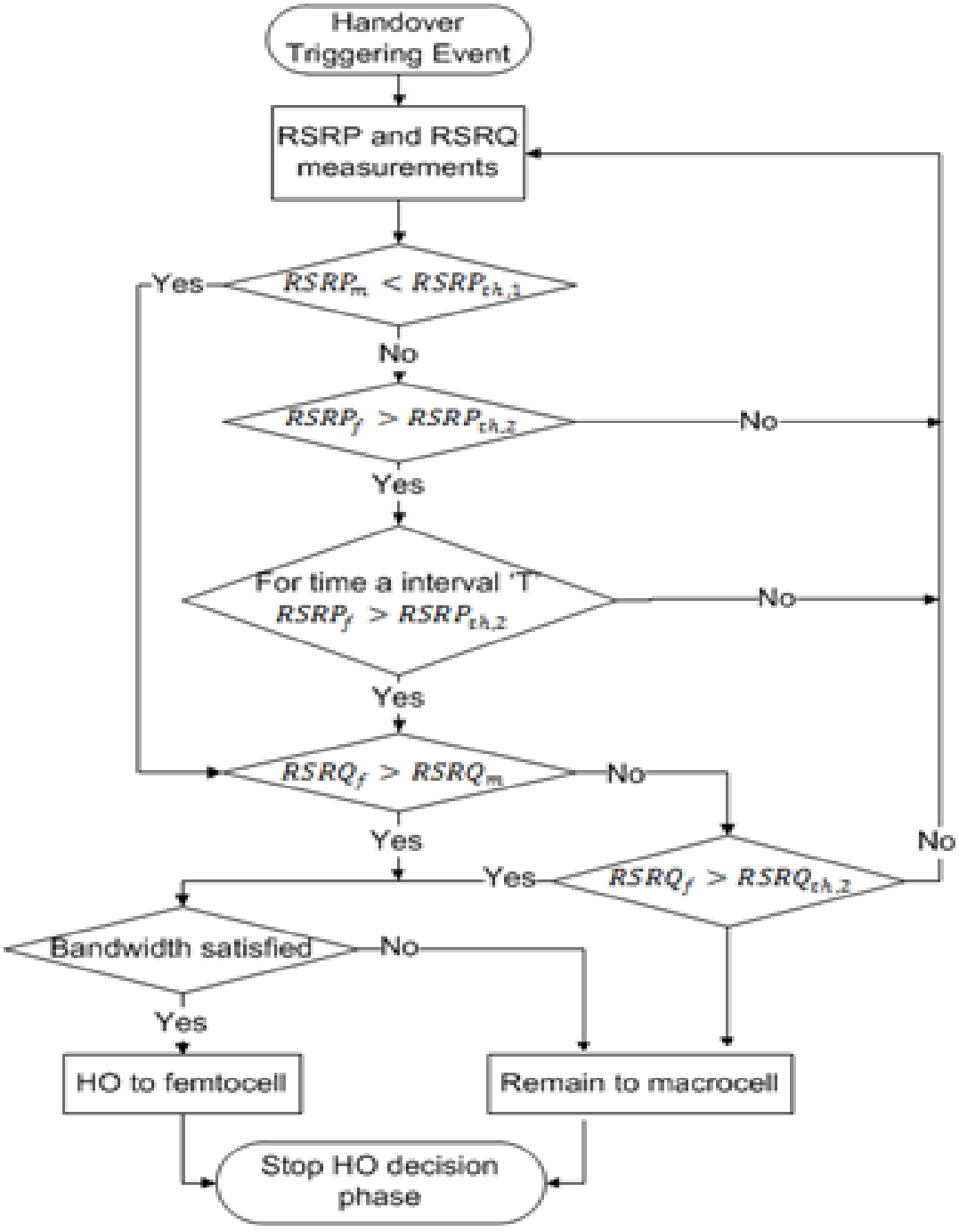

Figure 2.15: Interference aware HO algorithm[64]

proposed algorithm is that it considers double threshold in $RSRP$ measurements which reduces the number of unnecessary handover in presence of FAPs. Additionally, the user will experience better QoS since the $SINR$ performance is expected to be enhanced for taking RSQ measurement reports in consideration. However, at the time of deep channel fading the RSQ comparison may rise the probability of handover failure.

2.3.1.5 Interference-aware Intracell Handover Algorithm

Authors in [69], proposed Intracell HO (IHO) that can cope with cross-tier interference in co-channel deployments. In the proposed IHO algorithm, serving cell and target cell are the same cell, i.e., when an UE (non-subscriber to CSG) suffers interference in presence of femtocell in its serving channel, it is assigned to a new sub-channel in same serving macrocell or assign less interfered sub-channel to all interfering femtocells. When a non-subscriber macrocell user experiences interference in serving sub-channel k (experienced $SINR$ less than a given threshold$SINR^{IHO}$), the serving M_m cell requests for the measurement report from the UE. The measurement report sent by the non-subscriber UE has the RSS of the serving macrocell in sub-channel $k(RSS^k_{m,y})$ and $RSS(RSS^k_{j,y})$ of the neighbouring cells (from neighbouring cell list $N_m = \epsilon N_0, ..., N_j, ..., N_{j-1}$). The serving macrocell compares the reported RSS values and launch IHO upon satisfying equation 2.10.

$$RSS^k_{m,y} < RSS^k_{j,y} + \Delta Q_{IHO} \quad \forall j \in N_m \tag{2.10}$$

When a femtocell satisfies equation 2.10, it is considered as an interferer to the non-subscriber macrocell user UE^{ns}_y and serving macrocell will launch IHO. Here, hysteresis margin is denoted by ΔQ_{IHO} and the number of interfering femtocells is r is denoted by $\Theta_k = A_0, ..., A_{10}, ..., A_{r-1}$. In the proposed algorithm an IHO is

performed by the serving macrocell if, 1) at least one sub-channel is free where the UE can be reallocated, 2) the free sub-channel has suffered less interference than the current serving sub-channel. When there are more than available sub channels, UE will be handed over to the sub-channel h that suffers the least interference (selected by serving macrocell upon the periodic CQI report) and if there is no sub-channel available fulfilling the above requirements, no IHO will be performed in macrocell but in all interfering femtocells,Θ_k. To minimize signalling overhead it is best practice to perform IHO in macrocell that all interfering femtocells. When there is no free sub-channels in interfering femtocells, forbidding approach is performed where the subscribed femtocell user (FUE) UE_x^s , is disconnected from sub-channel k for a period of time ΔT_{IHO} . This approach results in reduced throughput for the femtocells. Thus distributed power control is proposed by the authors, where instead of disconnecting the FUE , the interfering femtocell reduces the transmitting power in sub-channel k for a period of time ΔT_{IHO} . Figure 2.16 depicts a flowchart version of the proposed algorithm.

The strong feature of this algorithm is that it takes the received interference power from neighbouring cells in consideration. On the other hand, handing over of the femtocell users to other channels may erratically raise the interference in adjacent femtocells or users and decrease the throughput.

2.4 Summary

This chapter initially studied the causes of cross and co-tier interferences in presence of femtocells in a macrocell scenario. Thereafter, several interference management schemes such as femto-aware spectrum arrangement, FFR, ABSF, are discussed in detailed in Section 2.2. Moreover, increasing interference in the network at the time of handover with the presence of femtocells are conferred in Section

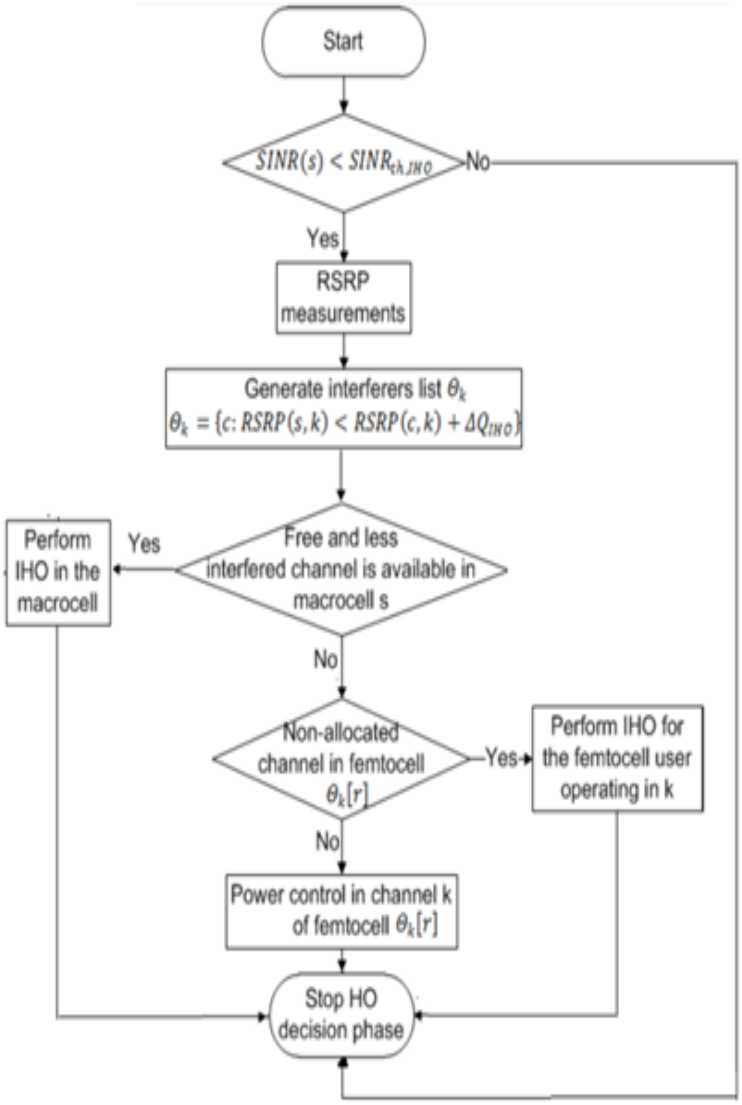

Figure 2.16: HO algorithm based on Intracell HO

2.3. A number of well-known handover techniques such as max RSRP based, user speed, experience interference(by UE) based are studied to adapt an algorithm for this research work. A number of modifications were made to the speed based handover algorithm [69] to optimize handover failures, interference and improve network throughput which are discussed in later chapters.

Chapter 3

enhanced Inter-cell Interference Coordination (eICIC)-ABSF

This chapter studies on various handover algorithms and challenges of interference management in presence of FAPs. The main purpose of this comparative study is to propose a new handover strategy that minimizes the interference and maximizes system throughput. For this research, the experiments and simulations are performed in LTE-Sim which is an event-driven simulator written in C++ [88]. The four main modules of LTE-Sim are: a) the Simulator, b) the NetworkManager, c) the FlowsManager and d) the FrameManager. The classes and functions of the modules are explained in Appendix A.1.

3.1 Femtocell Scenario

In LTE-Sim, femtocell scenario, FAPs and eNBs are identified by unique IDs and it's position is defined by a cartesian coordinate system [88]. UE information such as CQI feedbacks, uplink channel quality, and uplink scheduling request are managed by ID and position tracking. In order to form a femtocell scenario, the information of number of buildings, locations of the buildings with FAP, build-

ing type, location of FUE, etc., were defined in femtocell scenario header file ($SingleCellWithFemto.h$) of $LTE - Sim$. Figure 3.1 illustrates femtocell environment with different building patterns in a macrocell scenario.

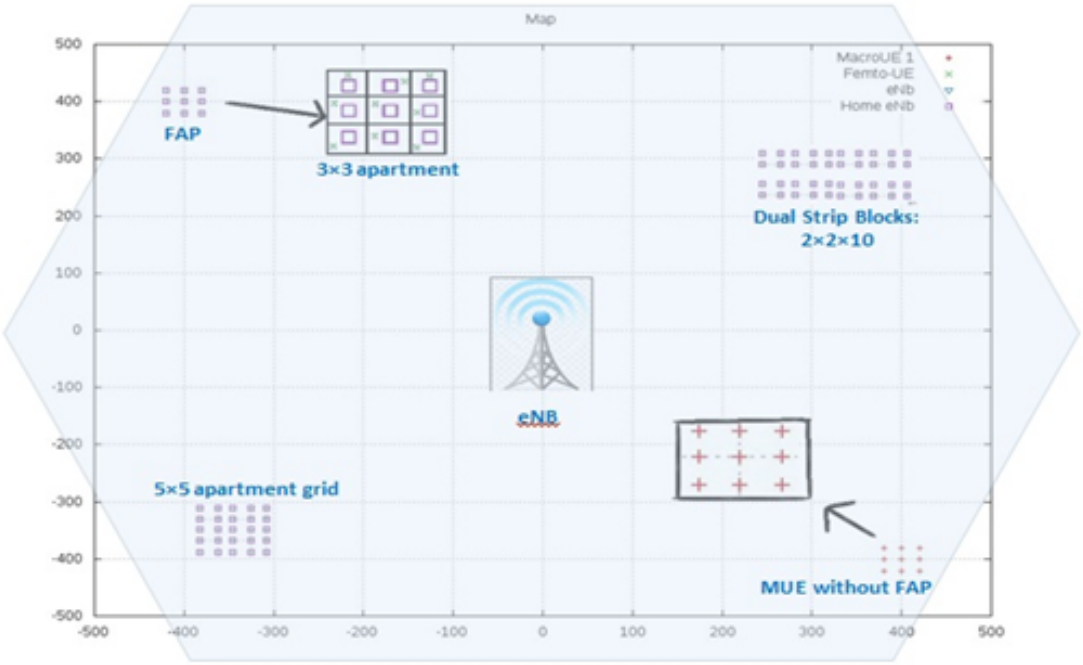

Figure 3.1: Femtocell scenario with building configurations a) 3×3 apartment grid b) 5×5 apartment grid c) dual 2×10 strip Blocks

This apartment grids shown in Figure 3.1 can be can be modified according to the traffic environment. In this research work, 3×3 apartment grid was considered. In this research, we have considered apartment has a length and width of 10 meters each, to form a squared area of $100m^2$. Grid of apartments inside the building could be defined by configuring the grid settings (i.e. building types) in the header file ($SingleCellWithFemto.h$). Building walls are formed in $NetworkManager.cpp$ where, function $NetworkManager :: CreateBuildingForFemtocells()$ gets the building ID, defined in $SingleCellWithFemto.h$ and creates the building according to the building type as presented in Figure 3.1. Modified class diagram of femtocell scenario is depicted in Figure 3.2.

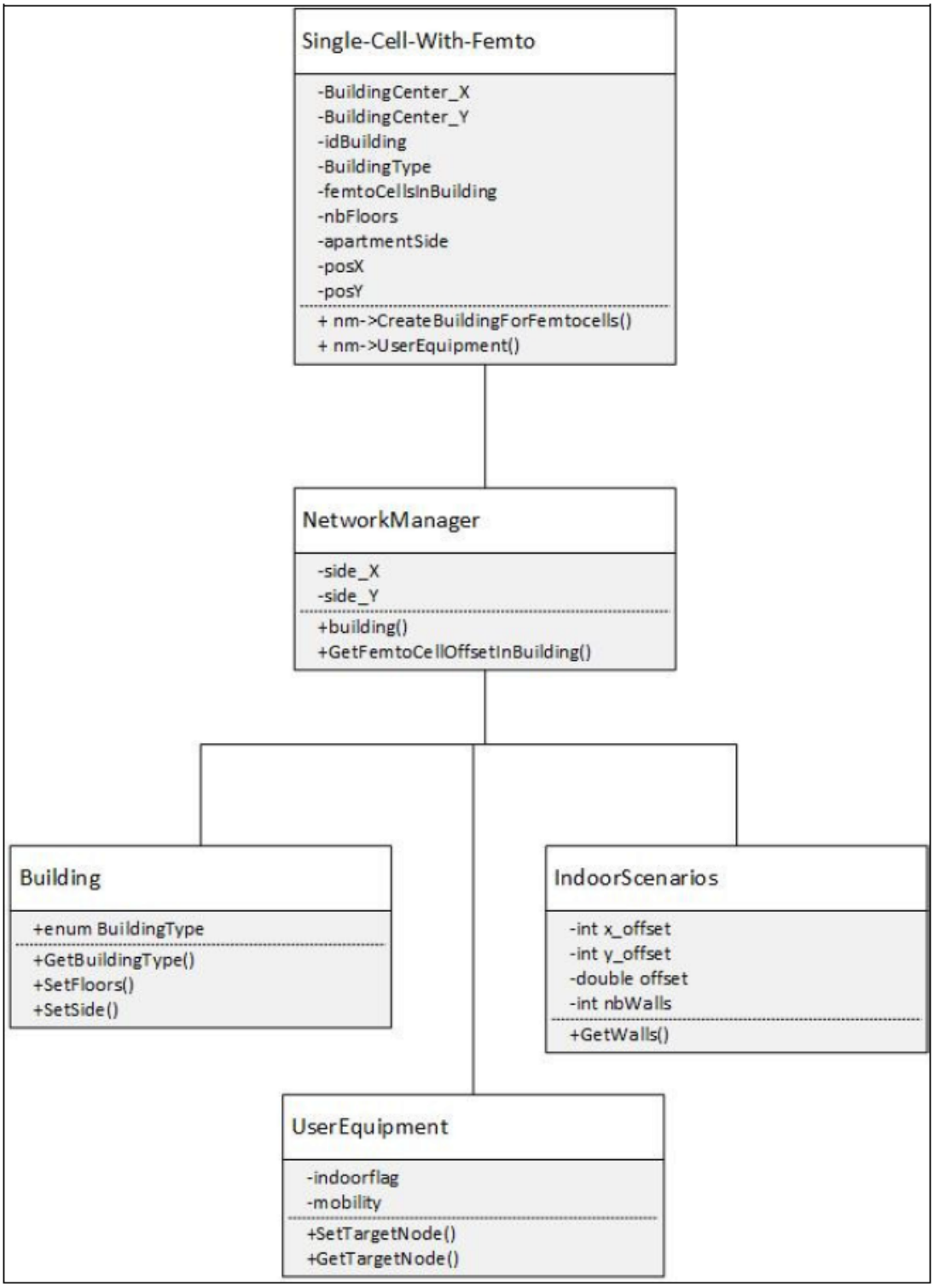

Figure 3.2: Modified class diagram of femtocell scenario in LTE-Sim.

3.1.1 Proposed Speed Based Algorithm

Femtocells are connected to network through backhaul broadband connection. Due to the absence of X2 interface, the handover de-

cision and execution phase take more time than the conventional macro-cellular handover. Moreover, FAPs have less computational capability. But handover decision algorithms based on energy efficiency [73] or cost function [71] have computational burden due to complex algorithms to low powered FAPs and it may add delay to the handover decision procedure. Keep these factors in mind and incorporate eICIC techniques (such as, Cell Range Expansion(CRE) and Almost Blank Sub-Frames) a new speed based handover algorithm was primarily modelled for this research, which is shown in Figure 3.3.

This speed based handover algorithm mainly includes a) access control b) received signal strength and c) traffic type as decision criterion. This speed based algorithm is inspired by speed based handover algorithm proposed in [69]. Unlike the model in [69], Markov-Chain prediction model was not considered in this research work, considering MME knows the speed and location of user [102].

After checking the $RSRP$ measurement report from UE, eNB checks whether the user is in the list of closed access user group or not. If the UE is a listed FUE moving in a speed between 5-10kmph and its $SINR$ is below $-3dB$ for 50ms, the reactive handover in Section (2.3.1.3) is for non-Real Time(NRT) user and pro-active handover in Section (2.3.1.3) is [69] for real-timer user. Listed user moving higher than 10kmph will not be handed over to FAP. On the other hand, there will be no handover to the FAP, for the users not listed in closed access user group. These MUEs will be considered VMUEs if their CQI is below 3 for 50ms. To mitigate cross-tier interference and improve the performance of VMUEs, eNB initiates ABSF in the FAP. ABSF stops when the VMUEs experience CQI greater than 4. The performance of the packet schedulers (PF, M-LWDF and EXP/PF) considering all the users are experiencing real-time traffic (Video flow) modelled with infinite buffer application.

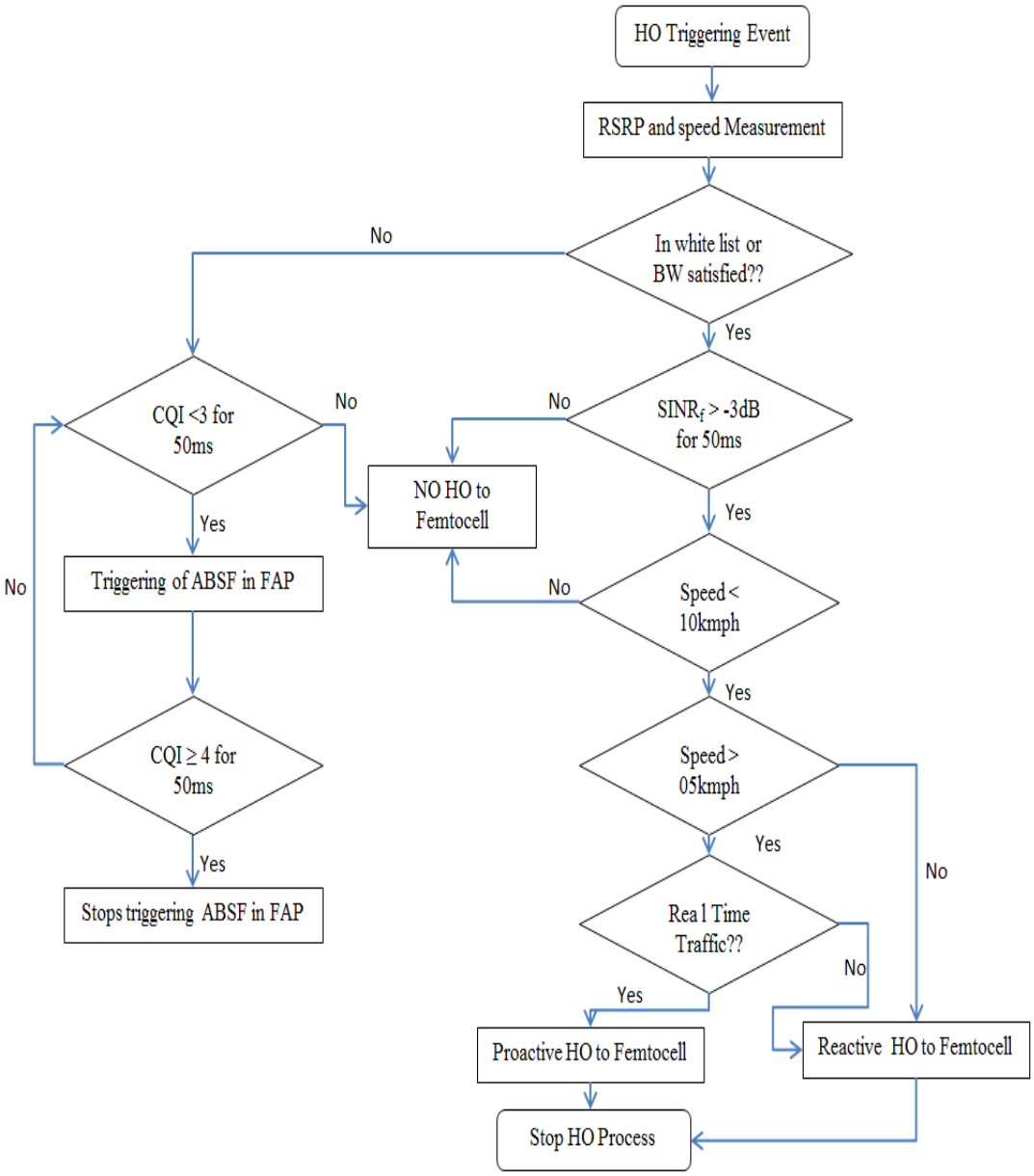

Figure 3.3: Proposed speed based handover model

3.1.2 Link Performance Model

Transport Block (TB): TB is the amount of data transmitted in 1ms sub-frame. The number of bits sent or TB size depends on number of PRB and Modulation and Coding Scheme (MCS) assigned to a user.

Block Error Rate (BLER): BLER is the indication of ratio of erroneous transport blocks (an erroneous transport block is one

where cyclic redundancy check is wrong) to the total number of transport blocks sent [82] during Radio Link Monitoring (RLM). TB with 10% of BLER is accepted in LTE [81].

Channel Quality Indicator (CQI): CQI is measurement report performed by UE on downlink channel. CQI is reported in every TTI by the active UE. CQI is used by eNB to determine MCS and perform packet scheduling [81]. There are fifteen different MCS values which correspond to fifteen CQI values in LTE. For a specific CQI value, transport block size can be obtained from table 7.1.7.1-1 and 7.1.7.2.1-1 of 3GPP 36.213 documents [81] which is summarized in Table 3.1.

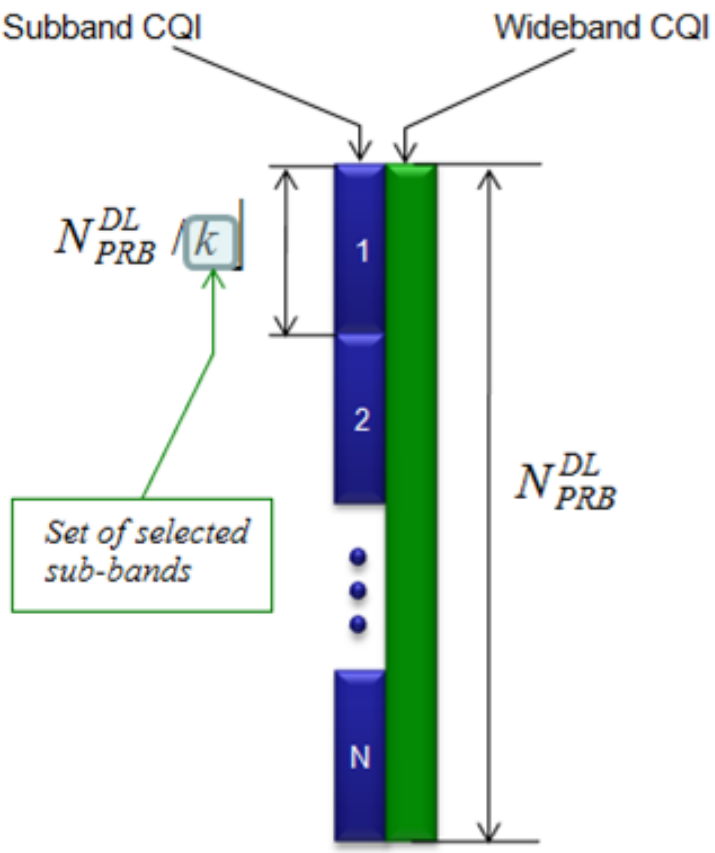

Figure 3.4: Wideband CQI and CQI of selected sub-bands [83]

In LTE, there are periodic and aperiodic CQI reporting. In

CQI	Modulation	MCS	Bits/Symbol	REs/PRB	N-PRB	TBS	Efficiency
1	QPSK	0	2	138	20	536	0.1523
2	QPSK	0	2	138	20	536	0.3770
3	QPSK	2	2	138	20	872	0.8770
4	QPSK	5	2	138	20	1736	1.4766
5	QPSK	7	2	138	20	2417	1.9141
6	QPSK	9	2	138	20	3112	2.4063
7	16QAM	12	4	138	20	4008	2.7305
8	16QAM	14	4	138	20	5160	3.3223
9	16QAM	16	4	138	20	6200	3.9023
10	64QAM	20	6	138	20	7992	4.5234
11	64QAM	23	6	138	20	9912	5.1152
12	64QAM	25	6	138	20	11448	5.5547
13	64QAM	27	6	138	20	12576	6.2266
14	64QAM	28	6	138	20	14688	6.9141
15	64QAM	28	6	138	20	14688	7.4063

Table 3.1: MCS and TB size [80]

periodic reporting, CQI is transmitted periodically (in each TTI) from UE to eNB. UE sends periodic CQI report in PUCCH when no UL data is sent. In instance, when UE sends uplink data, CQI report is sent in PUSCH since UE cannot transmit both PUSCH and PUCCH at the same time [81].

The granularity of this frequent periodic CQI reporting is relatively rough. To obtain large and more detailed CQI report in a single reporting instance aperiodic reporting is used (transmitted over PUSCH). Aperiodic CQI report can be measured in three levels: wideband, UE selected sub-band, and higher layer configured sub-band [81]. The wideband CQI report is the effective $SINR$ observed by the UE on the entire downlink system bandwidth as shown in Figure 3.4. In selected sub-band reporting, UE measures CQI only in a set of preferred sub-bands (the best k sub-bands), assuming communication with eNB is only maintained over those selected k sub-bands. UE then reports one CQI value for the wideband and one differential CQI value for the set [81].

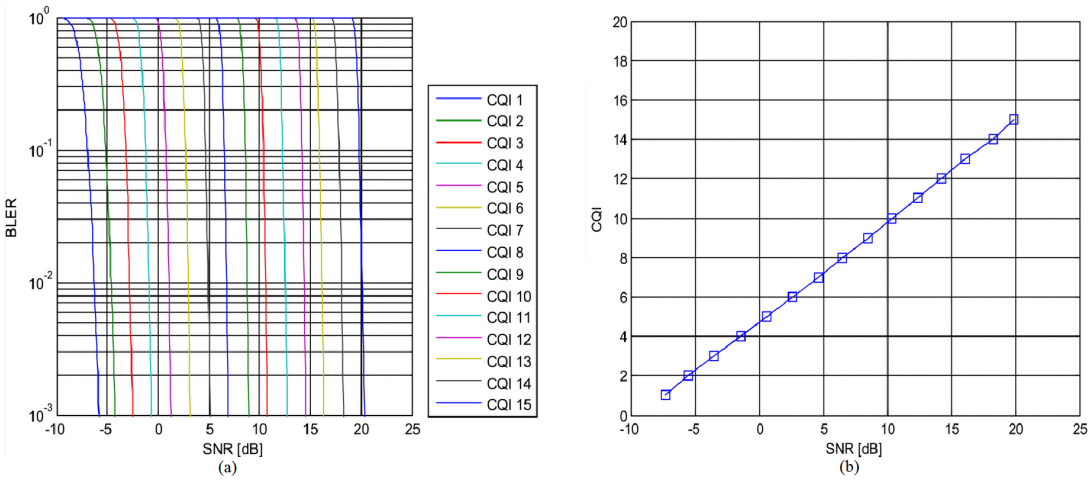

Figure 3.5: a) SNR-BLER curves obtained for 1.4 MHz, b) SINR-CQI mapping

Effective $SINR$ of TB can be obtained from Exponential Effective Signal to Interference and Noise Ratio Mapping (EESM). It is then mapped to the BLER from Additive White Gaussian Noise (AWGN) link-level performance curves as shown in Figure 3.5(a).

Each AWGN-BLER curve corresponds to a specific CQI level. From this AWGN SINR-BLER map, UE selects the $SINR$ value corresponds to a 10% BLER in each curve .UE then utilizes the selected SINR with the corresponding CQI value to map SINR-CQI plot as shown in Figure 3.5(b).

3.1.3 Preliminary Simulation Results (Indoor Throughput Improvement)

Performance gain of the users located at the cell edge (466m northwest from the eNB) as show in Figure 3.1 can be achieved by deploying FAPs. Users inside the building(3×3 apartment grid) had poor network coverage because of path-loss and wall attenuation. Simulation results in Figure 3.6 shows the improvement in VoIP and Video throughput of indoor subscribers with the presence of FAPs. Simulation parameters are summarized in Table 3.2.

Table 3.2: Simulation Parameters

Parameter	**Value**
Operating BW	5 MHZ
eNB transmit power	43dBm
FAP transmit power	20dBm
Macrocell radious	500m
Building type	3×3
Apartment size	$100m^2$
Number of VMUE	5
Number of MUE	5
Users FUE	3 per FAP
Scheduler	PF
Bias value	2dB
Application	Video
ABSF Pattern	1/8, 2/8, 3/8(FDD)
Flow time	100sec

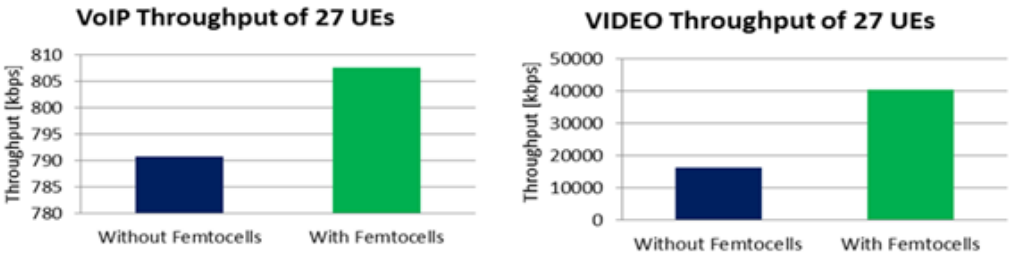

Figure 3.6: a) VoIP throughput comparision b) Video throughput comparison of 27 UEs

3.1.4 Simulation Scenario with Inter-cell Interference and ABSF

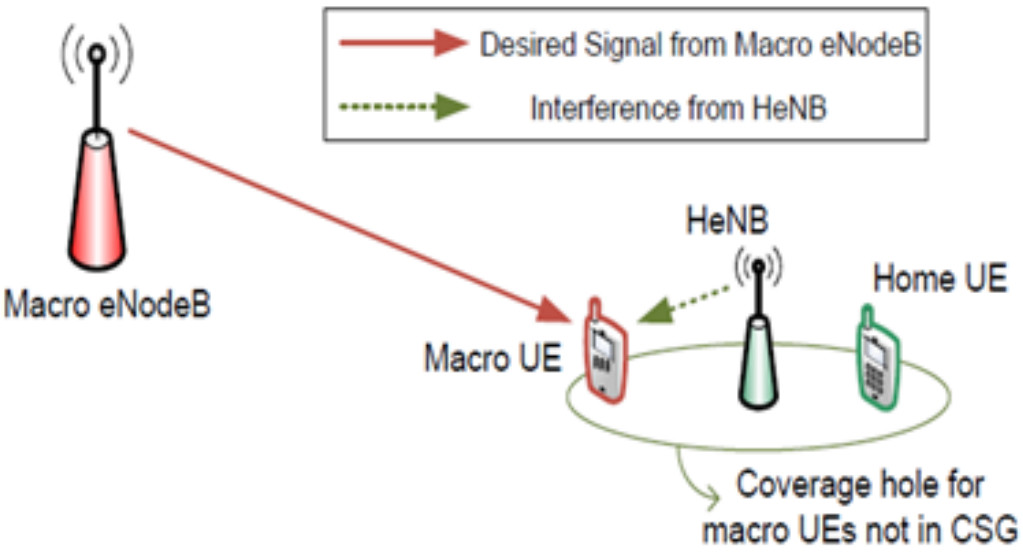

Figure 3.7: Inter-cell interference in presence of femtocell[99]

As shown in Figure 3.7, when an UE served by the eNB reaches near FAP coverage area, it faces strong downlink interference from that FAP. Due to the high DL interference, that MUE is subject to low SINR and unable to send control or data channels in the shared PRBs, which results in reduced throughput and call drop. This affected macrocell user is known as Victim Macrocell User (VMUE). Figure 3.8 shows the simulation scenario where five macrocell users are located at cell edge on both sides of the eNB. Macrocell users(VMUEs) on lower right corner of eNB are near to

FAP coverage area and experiencing poor SINR due to high DL interference. The scenario as shown in Figure 3.1 considers 3×3 apart-

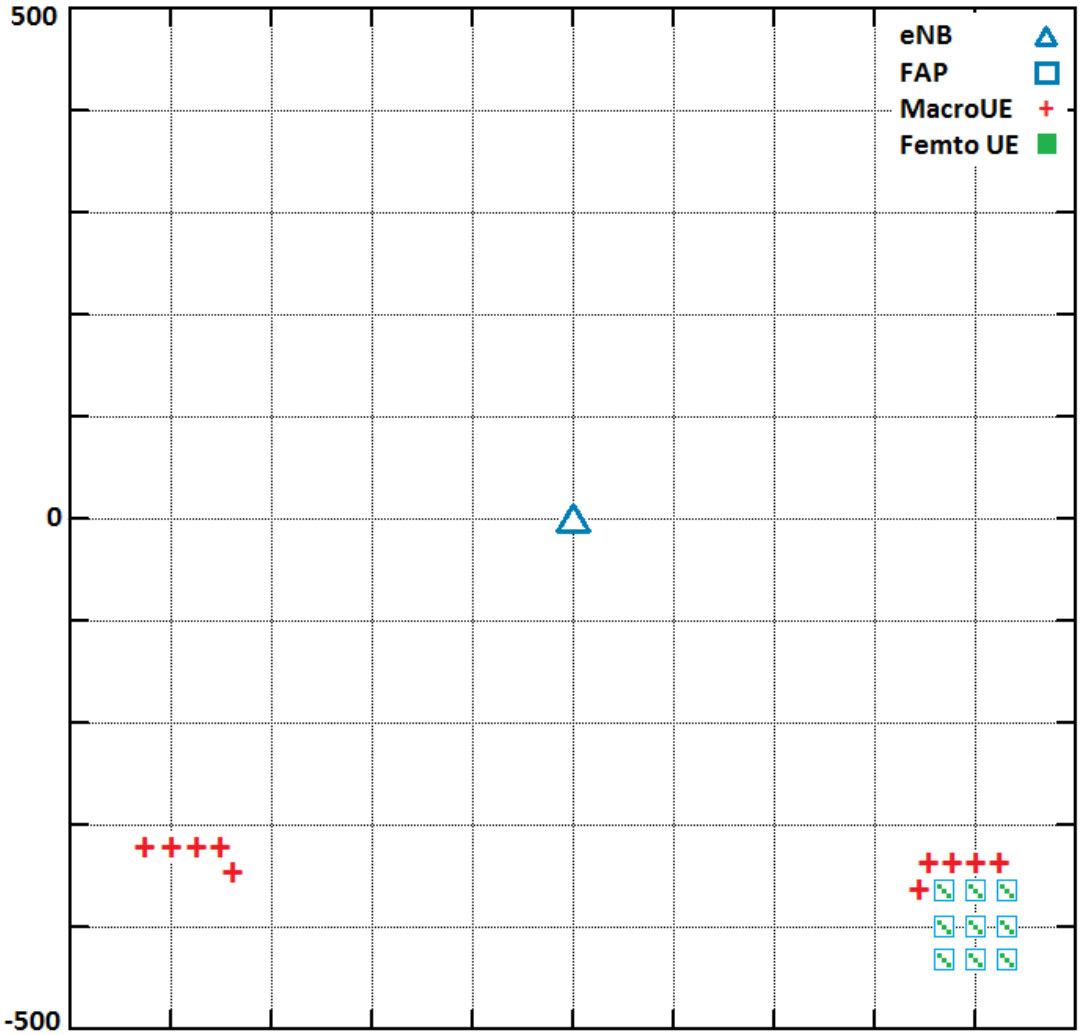

Figure 3.8: Single macrocell-femtocell scenario with 5 MUE and 5 VMUE

ment grid (nine FAPs in nine apartments) with three static FUEs per FAP. Aggressor FAP is generating ABSF (FDD 1/8 pattern) to mitigate downlink interference to the VMUEs. It was assumed that all the users are distributed uniformly and running video application with constant rate R kbps, where R is selected according to the required input load(video traffic). Cost-231 Hata model was considered for urban path loss environment and both the shadow fading and path loss were considered fixed for each TTI. LTE packet scheduler allocates PRBs to the UEs based on different scheduling

criteria, such as, channel condition, fairness among different MUEs, traffic type, Head Of line(HOL) packet delay and queue status in the buffer. Different scheduling algorithms prioritize users depending on different above mentioned criteria and once a user with a highest metric is selected, number of bits/PRB depends on assigned MCS selected on the basis of CQI feedback from UE [93]. The scheduling decisions are based on a different scheduling algorithms (PF, EXP-PF, M-LWDF) but in this section PF downlink scheduler was considered.

Proportional Fair algorithm, which is a channel aware/QoS unaware scheduling strategy, assigns PRBs based on the channel quality experienced by the UE plus the past average data rate of the user [94]. PF selects user with the highest metric M and provides trade-off between system throughput and fairness.

$$M_{i,k} = \arg\max \frac{R_i(t)}{\bar{R}_i(t)} \tag{3.1}$$

$$\bar{R} = (1 - \frac{1}{t_c}) * \bar{R}(t-1) + \frac{1}{t_c} * R_i(t-1) \tag{3.2}$$

where, $M_{i,k}$ is scheduling metric computed for i^{th} user at k^{th} subchannel, $R_i(t)$ is the instantaneous achievable data rate and $\bar{R}_i(t)$is the average data rate of user i at time t, t_c is the window size.

M-LWDF [95] supports multiple Real Time(RT) data users with different QoS requirements and considers head of line packet delay to calculate priority metric.

$$M = \arg\max \alpha_i W_i(t) \frac{R_i(t)}{\bar{R}_i(t)} \tag{3.3}$$

$$\alpha_i = -\frac{log\delta_i}{\tau_i} \tag{3.4}$$

where, $W_i(t)$ is HOL packet delay of i^{th} user at time t, τ_i is delay threshold and δ_i denotes maximum probability of i^{th} user to exceed

HOL delay threshold.

EXP/PF considers both the characteristics of PF and EXP rules [96]. PF maximizes system throughput whereas EXP considers an exponential function of end-to-end delay of RT services. EXP/PF supports RT services with different QoS requirements and non-RT services with AMC and TDM system . Depending on the service type, scheduling metric M can be expressed as-

$$M = \arg\max \begin{cases} \exp\left(\frac{a_i W_i - a\overline{W(t)}}{1+\sqrt{a\overline{W(t)}}} \frac{R_i(t)}{\overline{aW(t)}}\right) if & i \in RT \\ \frac{w(t)}{P(t)} \frac{R_i(t)}{\overline{R}_i(t)} & if \quad i \in NRT \end{cases} \tag{3.5}$$

$$a\overline{w(t)} = \frac{1}{N_{RT}} \sum_{i \in RT} a_i W_i(t) \tag{3.6}$$

$$w(t) = \begin{cases} w(t-1) - \epsilon & if \quad W_{max} > \tau_{max} \\ w(t-1) + \frac{s}{k} & if \quad W_{max} < \tau_{max} \end{cases}$$

here, $P(t)$ is the average number of waiting packets for all RT services at time t, ε and k are constants, and $\bar{W}_i[t]$ represents the average HOL packet delay W_{max} and τ_{max} are the maximum HOL packet delay out of RT service users and maximum delay constraint of all RT service users, respectively. Now, to incorporate ABSF with different type of schedulers, scheduling metric M was designed in this research work considering the blanking pattern (blanking rate $\leq$ 3/8 (for FDD) and $\leq$ 2/10 (for TDD) [86] and reported CQI of the VMUE. The scaled scheduling metric can be expressed as follows-

$$M'_{i,k} = \beta M_{i,k} \tag{3.7}$$

here, β is the scaling factor which is zero for VMUE during non-ABSF mode, and in ABSF mode set to 10 to provide highest priority metric to the VMUEs. To make the metric computation unaffected

for the normal MUEs the scaling factor β is 1 in both ABSF and non-ABSF modes.

3.1.5 VMUE Tracking

In Figure 3.7, it is considered that, macrocell users at the cell edge experience low SINR due to high interference from the neighbouring FAPs. VMUE sends $RSRP$ measurement report to the eNB, which contains a list of neighbouring cells (including interfering FAP). The $RSRP$ of these listed neighbouring cells is the interference level experienced by the VMUE. The measured $RSRP$ (ranging from -44 to -140 dBm [79]) in the measurement report is sorted in descending order so that the FAP with highest interference come first and eNB triggers aggressor FAPs with appropriate ABSF pattern. The drop in $SINR$ level of macrocell users because of these interfering FAPs is taken into account to track down their victim state. A MUE is considered as a VMUE if the SINR falls below $-3db$ threshold(i.e. CQI feedback 3). The degradation in SINR could be instantaneous, so, considering a MUE as victim at that instant could be misleading. For that reason, tracking period was kept 50ms in this research. As proposed in [87], the tracking of VMUE starts when the wideband CQI report is 3. The reported CQI value is then filtered by equation 3.8.

$$CQI_f = \alpha.CQI[n] + (1-\alpha).CQI_f[n-1] \tag{3.8}$$

where $CQI_f[n]$, $CQI_f[n-1]$ are the filtered CQI values at time instants n and, $n-1$ respectively, $CQI[n]$ is the reported CQI at time instant n, and the scaling factor α is the blanking i.e., ABSF per pattern period. So, after a tracking period if the filtered CQI becomes equal or less than 3, the MUE is marked as victim. Tracking stops when the filtered CQI report of the VMUE becomes 4.

3.2 Simulation Results with Almost Blank Sub-frames

3.2.1 Throughput

After implementing ABSF in $LTE-Sim$, Figure 3.9 demonstrates that with the presence of ABSF, throughput of the VMUEs has increased drastically. Figure 3.10 shows, even with increasing number of VMUE, the ABSF has clear performance improvement in terms of throughput. It can be seen from Figure **??** that, macrocell reaches its maximum aggregated throughput when the number of victim users is six and there is no ABSF initiated. Macrocell throughput degrades with the increase of DL interference between FAP users and neighbouring victim macrocell users. It can be said intuitively, in this simulation environment when victim macrocell user reaches 6, SINR starts degrading so as the Throughput.

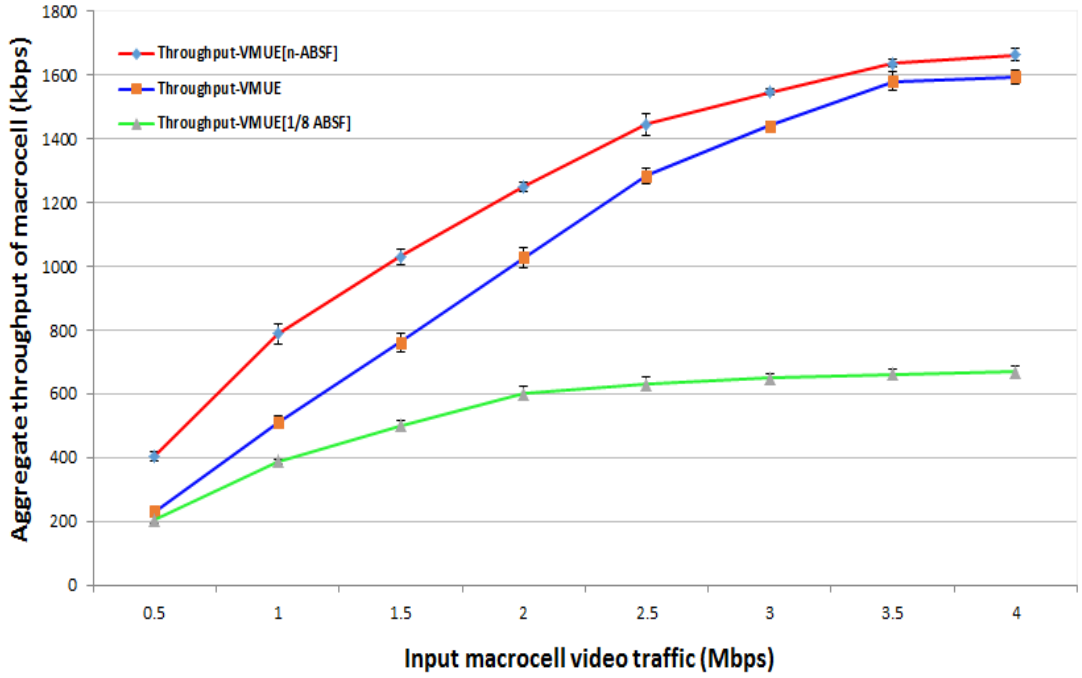

Figure 3.9: Throughput comparison with and without ABSF

Further simulation with ABSF patterns (2/8 and 3/8) are shown

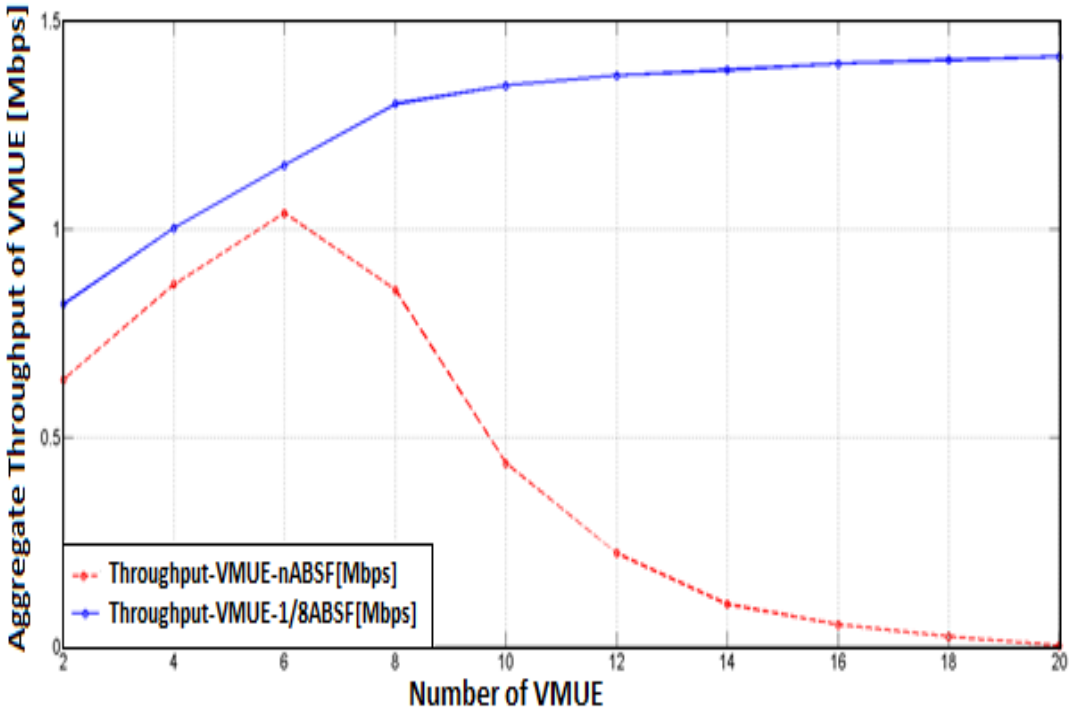

Figure 3.10: Macrocell aggregate throughput comparison with increasing number of VMUE

in Figure 3.11. From this figure it can be seen that, with the increasing number of blanked sub-frames in aggressor femtocells, the aggregate throughput of the macrocell increases. This improved throughput is because of the improved performance of the victim macrocell users. Similarly, with ABSF 3/8 pattern macrocell throughput reaches its maximum comparing to the non-ABSF mode.

In ABSF, muting of the sub-frames reduces the effective bandwidth allocated for the femtocell users. To provide DL interference free bandwidth to VMUEs, almost 12.5-37% of bandwidth is blanked for the triggered FAP(aggressor FAP). So, ABSF comes with a significant degradation of throughput for FUEs with increasing ABSF patterns. It can be seen from Figure 3.12 that for a fixed number of VMUE (in this scenario number of VMUE was kept five) with increasing number of ABSF patterns the throughput decreases substantially and the pattern shows the aggregated throughput of the femtocells has decreased to almost 12.5%, 25% and 37% for 1/8, 2/8, 3/8 FDD ABSF modes to the non-ABSF mode respectively.

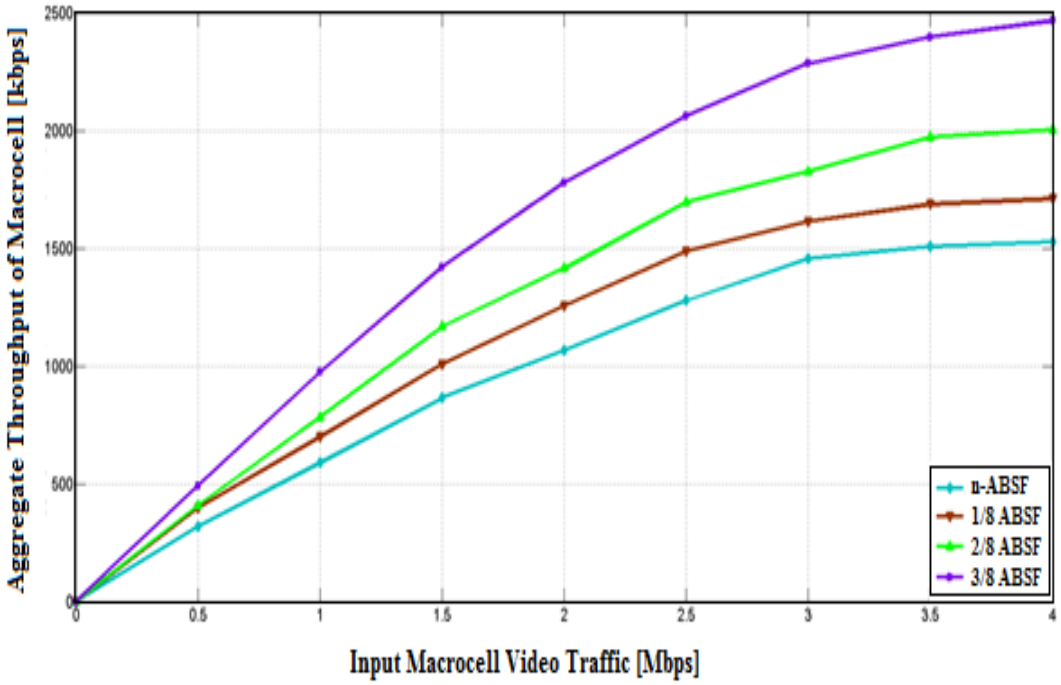

Figure 3.11: Aggregated macrocell throughput with different ABSF patterns

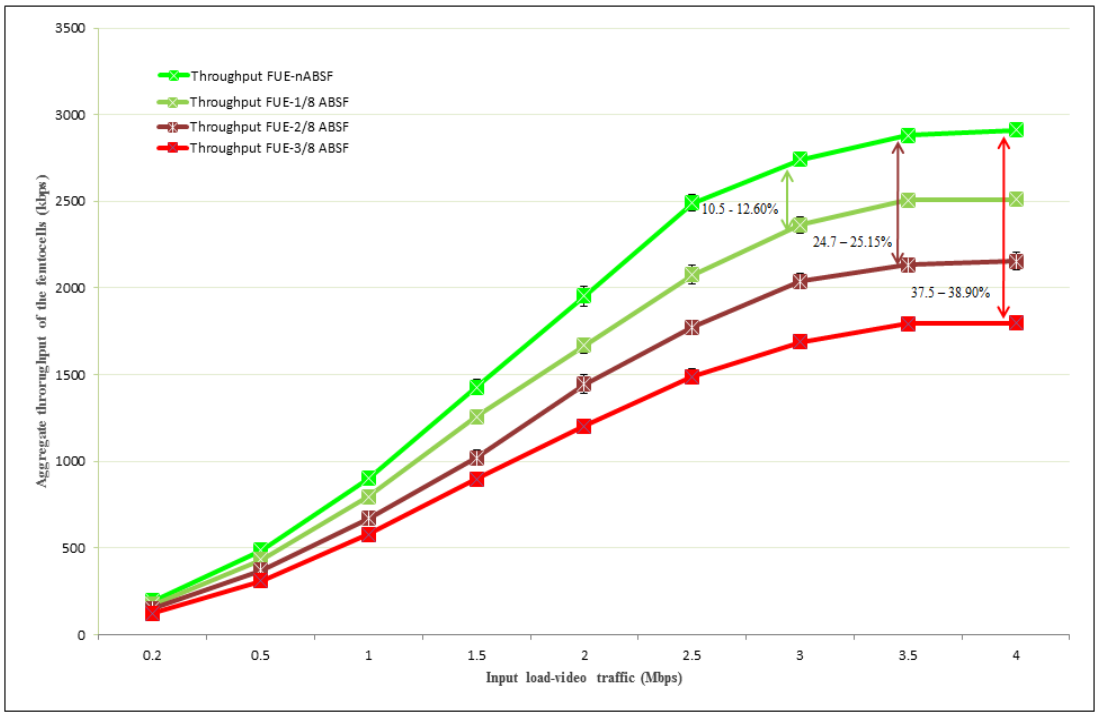

Figure 3.12: Aggregated throughput comparison of FAPs using different ABSF modes

3.2.2 Network Spectral Efficiency

Spectral efficiency refers to the net bit rate(excluding error-correcting codes) transmitted over a given bandwidth((bit/s)/Hz). From Figure 3.13, it can be intuitively explained that, spectral efficiency is directly linked with the blanking rate. As the intra-cell interference increases, the ABSF blanking rate also increases. This results in lower spectral efficiency. Spectral efficiency is the lowest in case of 3/8 ABSF mode. On the other hand, spectral efficiency is maximum when there is no ABSF triggered, it reaches maximum with increasing number of users till service load reaches its threshold and has a down-trend afterwards.

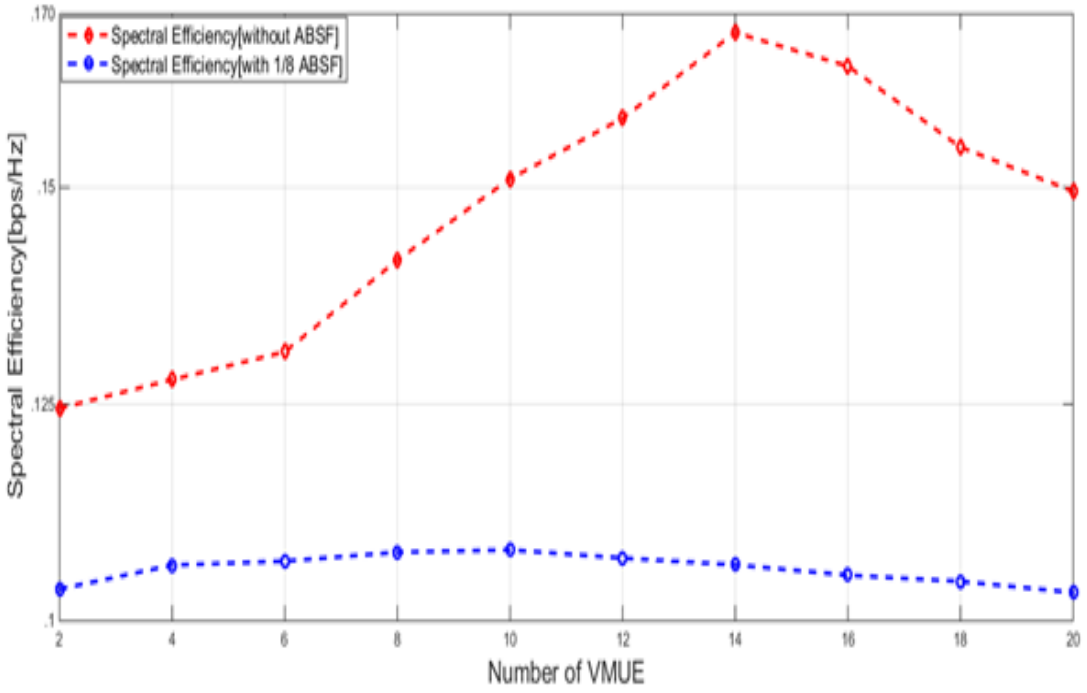

Figure 3.13: Network spectral efficiency comparison with different ABSF patterns

3.2.3 Packet Loss Ratio(PLR)

From Figure 3.14, it can be seen that PLR decreases with increasing ABSF pattern (1/8-3/8) and ABSF 3/8 mode has the lowest PLR.

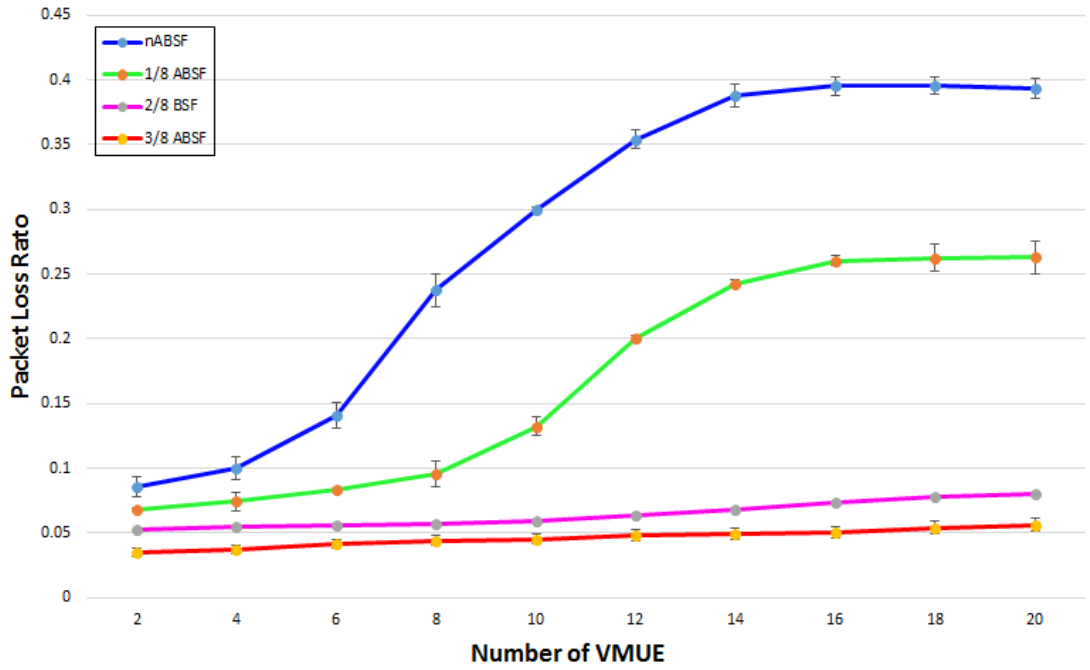

Figure 3.14: PLR comparison with different ABSF patterns.

The increasing number of blanked sub-frames as well as reduced interference due to ABSF results in decreasing packet loss.

3.2.4 Fairness Index(FI)

Fairness measure is one of the key performance indicators that determines whether users or applications with bad channel condition is getting fare share of system resources or not. Jains Fairness (equation 3.9) method is used to calculate the fairness among users in this research[103].

$$J(x_1, x_2, ..., x_m) = \frac{(\sum_{j=1}^{m} x_j)^2}{m(\sum_{j=1}^{m} x_j)^2} \tag{3.9}$$

here, x_m is the data rate of m^{th} user. Jain's fairness index ranges from 0 to 1. Index is 1 when resources are distributed equally among all the users. Increasing ABSF pattern means higher resource utilization for macrocell users, which is shown in Figure 3.15. ABSF

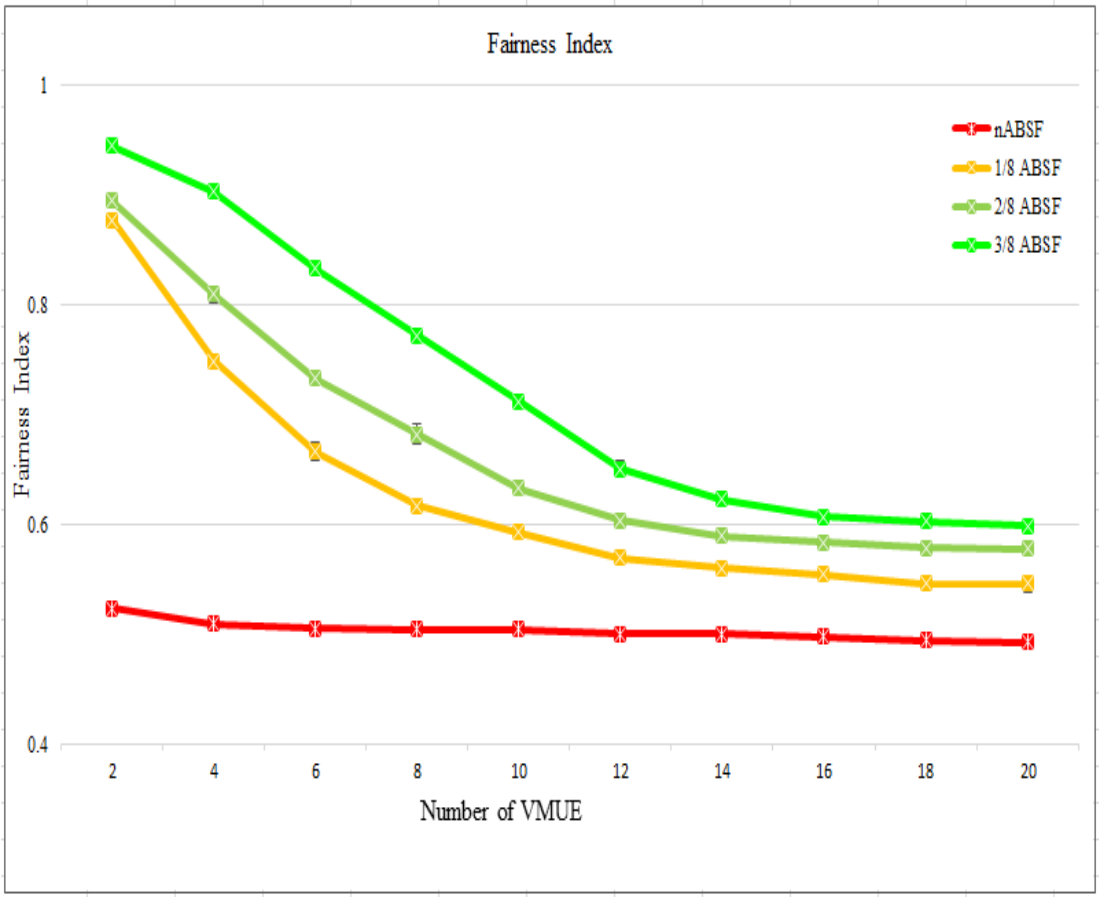

Figure 3.15: Fairness Index comparison with different ABSF Patterns

3/8 mode has the highest index and 1/8 has the lowest index compared to the non-ABSF mode.

3.2.5 Performance Comparison with Different Scheduling Algorithms

It can be seen that higher modes of ABSF improves the throughput of the VMUEs and decreases throughput of FUEs and increases congestion in femtocell coverage area. 1/8 ABSF improves the VMUE performance as well as in 1/8 pattern throughput reduction in FAP is the lowest (as shown in the simulation results above). So, future simulations in this research maintained 1/8 ABSF as a reference. EXP/PF and MLWDF show better performance than channel aware/ *QoS* unaware scheduling algorithm PF. Figure 3.16 to Figure 3.19 shows the performance of different schedulers with ABSF 1/8 pattern.

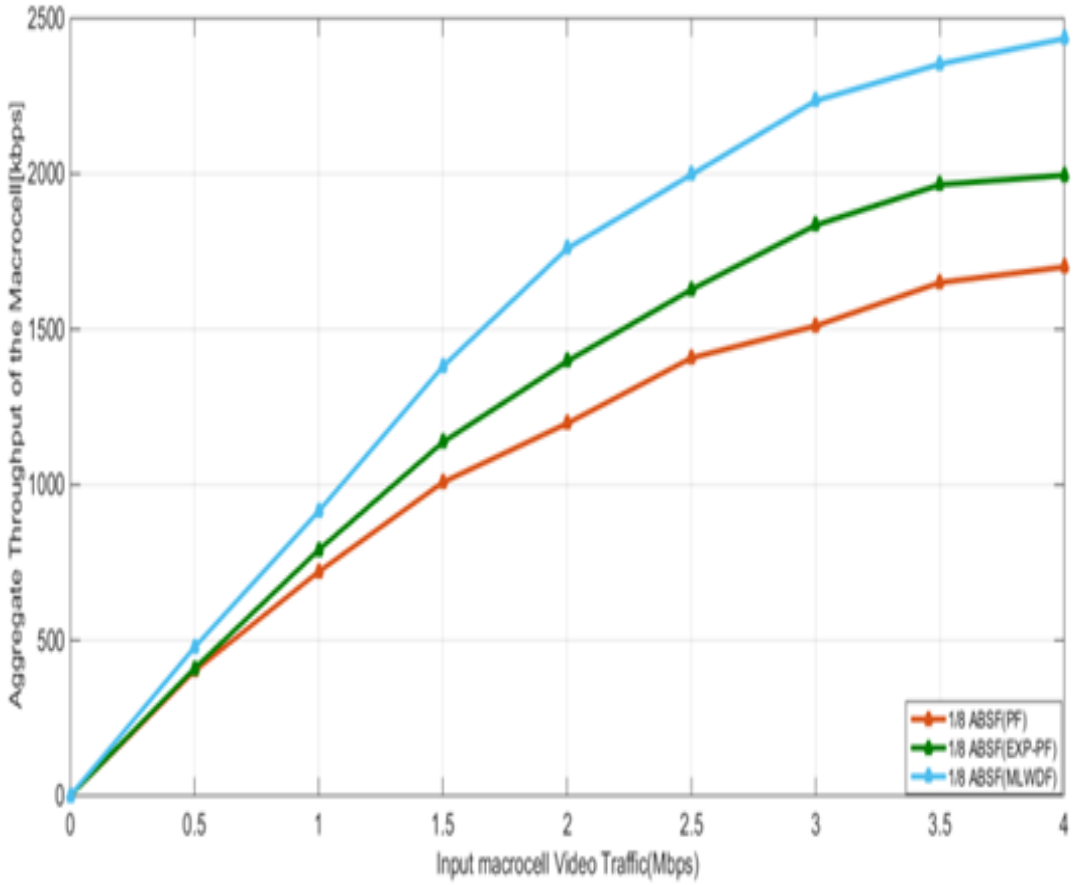

Figure 3.16: Throughput comparison with different scheduler

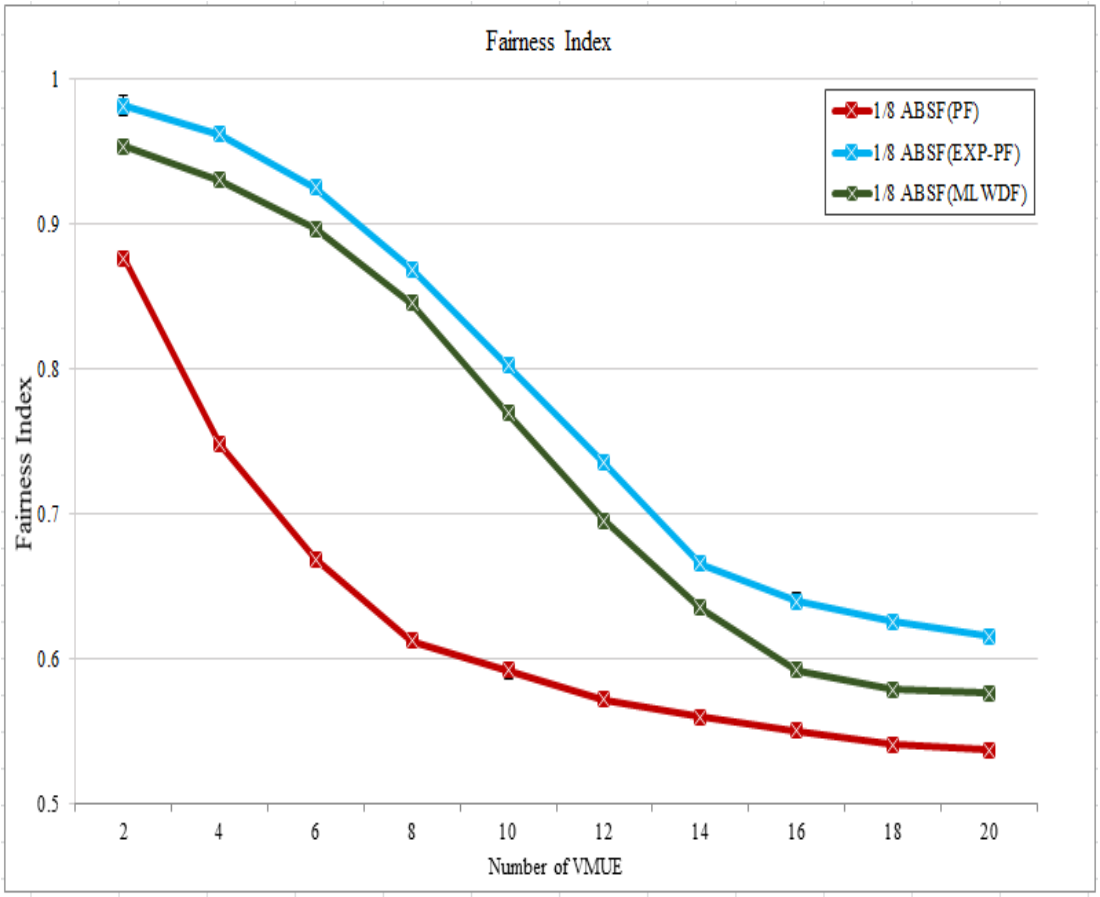

Figure 3.17: Fairness Index comparison with different schedulers

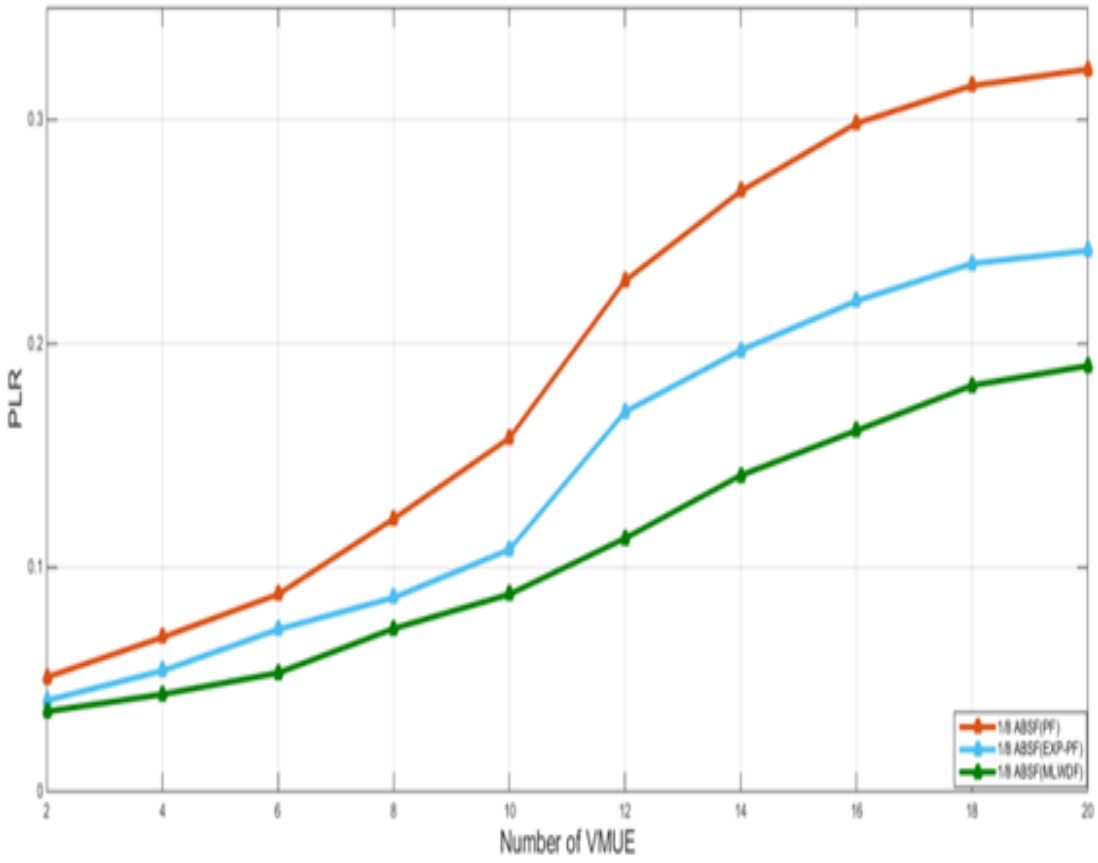

Figure 3.18: Packet loss ratio comparison with different schedulers

3.3 Summary

This chapter gives a detailed description of the simulator platform used in this research work. The modification in speed based handover algorithm used in this research is discussed in Section 3.1.1. A comparative study on well known scheduling algorithms, PF, ML-WDF and EXP/PF is also conversed in this chapter. Interference management(ABSF) through tracking of victim macrocell users and adaptation of several modifications in PF is discussed in Section 3.1.5. With the proposed algorithm, a significant improvement in network performance could be obtained, which was shown in the simulation results. The results obtained are in line with the results in literature and discussed in Appendix .A.3.

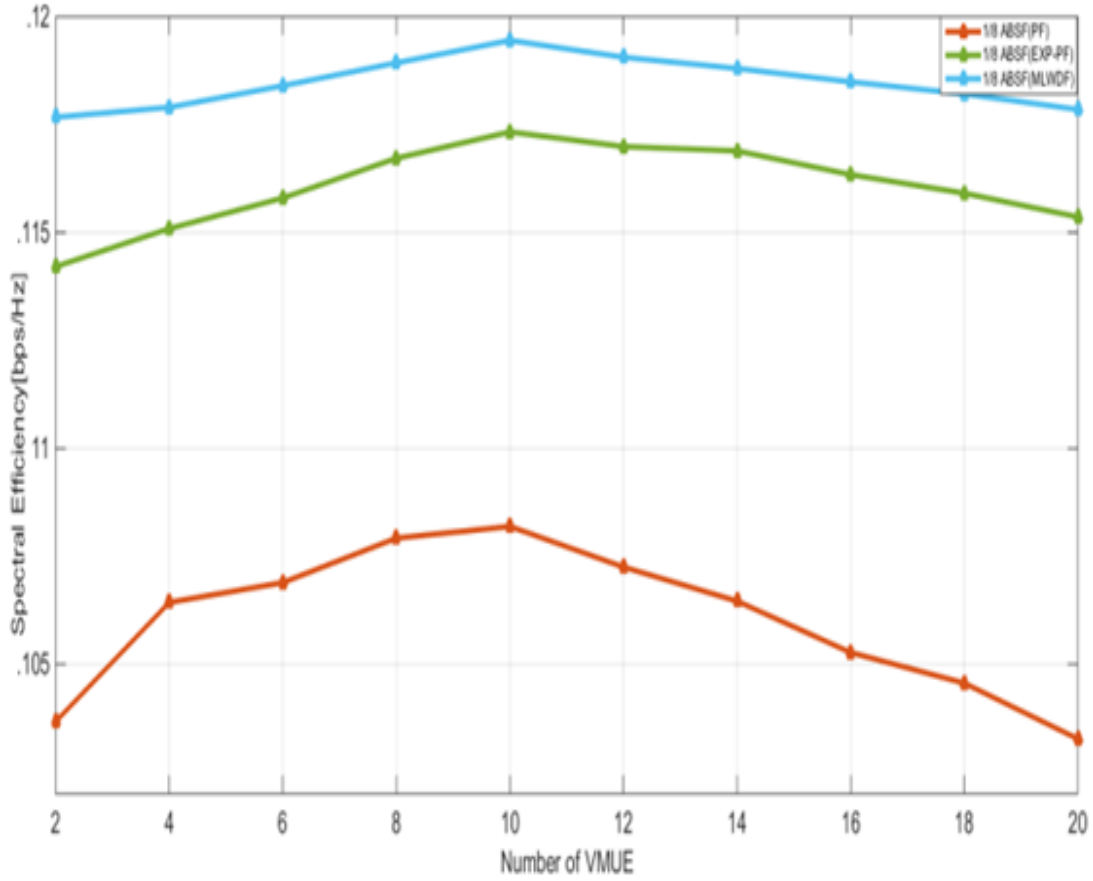

Figure 3.19: Spectrral efficiency comparison with different schedulers

Chapter 4

enhanced Inter-cell Interference Coordination (eICIC)-CRE

4.1 Cell Range Expansion and Mobility Management

In traditional cell selection schemes, UE selects the strongest macrocells as the target cell comparing the $RSRP$ from measurement report instead of Low Power Nodes(LPNs) ([64]) with shortest pathloss. This may cause coverage and traffic imbalance between macrocell and femtocells and lead to macrocell overloading [42]. On the other hand, maximizing the number of users served by LPNs will improve the network performance gain significantly [99]. The number of LPN users can be maximised by adding an offset to LPN $RSRP$ instead of increasing LPN transmit power. This technique to improve LPN coverage, known as Cell Range Expansion(CRE)was defined for LPNs in Release 8. CRE improves cell-edge throughput and overall network throughout.

In CRE, UE selects femtocells even though they are not the strongest cells as shown in Figure 4.1. If, the received $RSRP$ from the serving macrocell is stronger than that of the femtocell, the offset value for CRE less than threshold may lead to less number

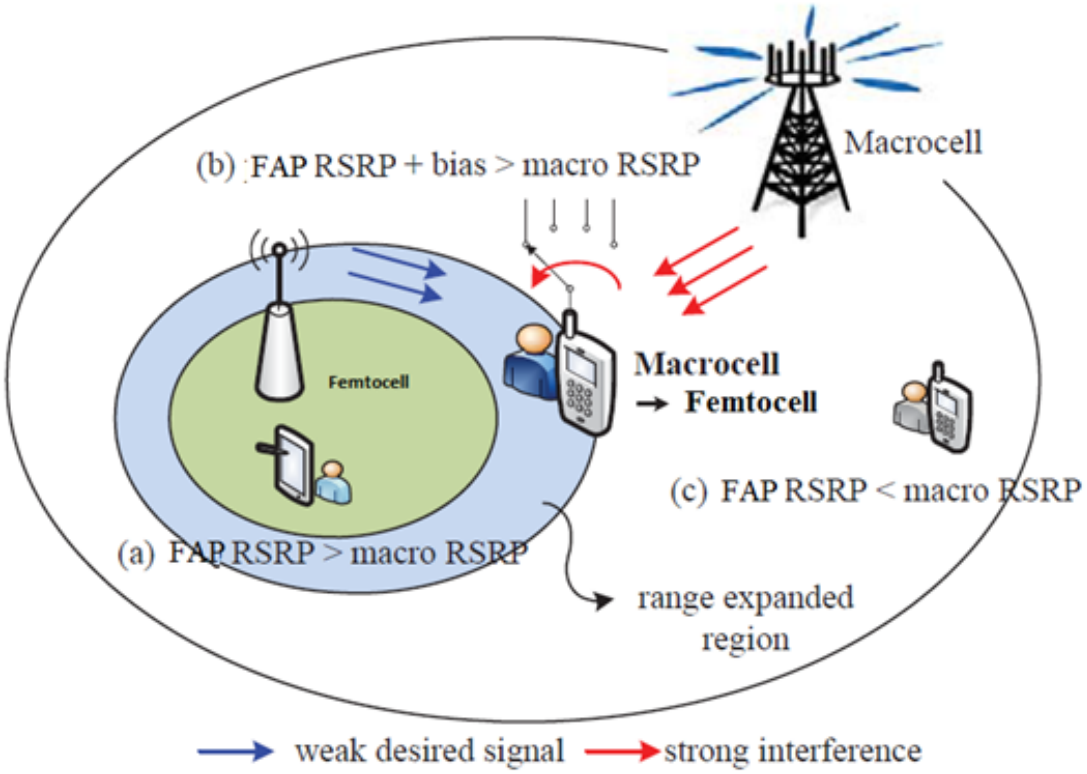

Figure 4.1: Femtocell cell range expansion [99]

of MUEs offloaded to femtocells. This in turn may cause resource underutilization of femtocells, congestion in eNBs and degraded performance of MUEs [97]. On the other hand, with large offset, more number of MUEs located far from FAP will be offloaded to femtocells and degrade throughput of FUEs in FAP range extended areas [97]. For these above reasons, achieving good performance while implementing CRE in femtocells, the optimal offset value has to be set.

4.2 Simulation Scenario with CRE and ABSF

Due to large differences in received powers, the probability of user selecting the FAP over eNB is low. Therefore, for user i on k^{th} subchannel in range expanded area to select femtocell over macrocell

can be represented as-

$$k^* = \arg\max_{k \epsilon m \cup F}(RSRP_{k,i} + bias_k) \tag{4.1}$$

where, m denotes macrocell and F denotes the set of femtocells in macrocell coverage area and $bias_k$ is the added offset value for range expanded femtocell. In this research work, bias 1, 2 and 2.5 dB were implemented in simulation scenario.

The received SINR of i^{th} user which is associated with macrocell m can be expressed as in Equation 4.2-

$$SINR_{i,k} = \frac{p^m_{i,k} h^m_{i,k}}{\sum_{n \neq m} p^n_{i,k} h^n_{i,k} + \sum_{x=1}^{F} r^x_{i,k} g^x_{i,k} \delta + N_p} \tag{4.2}$$

here, $p_{i,k}$ and $r_{i,k}$ are the transmit powers of serving eNB and adjacent femtocells on k^{th} sub-channel, h^m is the power gain from serving macrocell m to the user i. Here, denominator determines the sum of interferences from adjacent macros, femtocells and N_p is the noise power.

When user i selects femtocell f as serving cell, $SINR$ can be expressed as

$$SINR_{i,k} = \frac{r^f_{i,k} g^f_{i,k}}{\sum_{x \neq f} r^x_{i,k} g^x_{i,k} \delta + \sum_{n=1}^{m} p^n_{i,k} h^n_{i,k} + N_p} \tag{4.3}$$

where, g^f is the power gain from serving femtocell f to user i. Denominator denotes the sum of interferences from the neighbouring femtocells and macrocell. In both of the cases, δ is the scaling factor, which is 0 while triggering ABSF and 1 otherwise.

In this research work, CQI and $RSRP$ measurements were considered for coordination between eNB, VMUE and FAPs. The

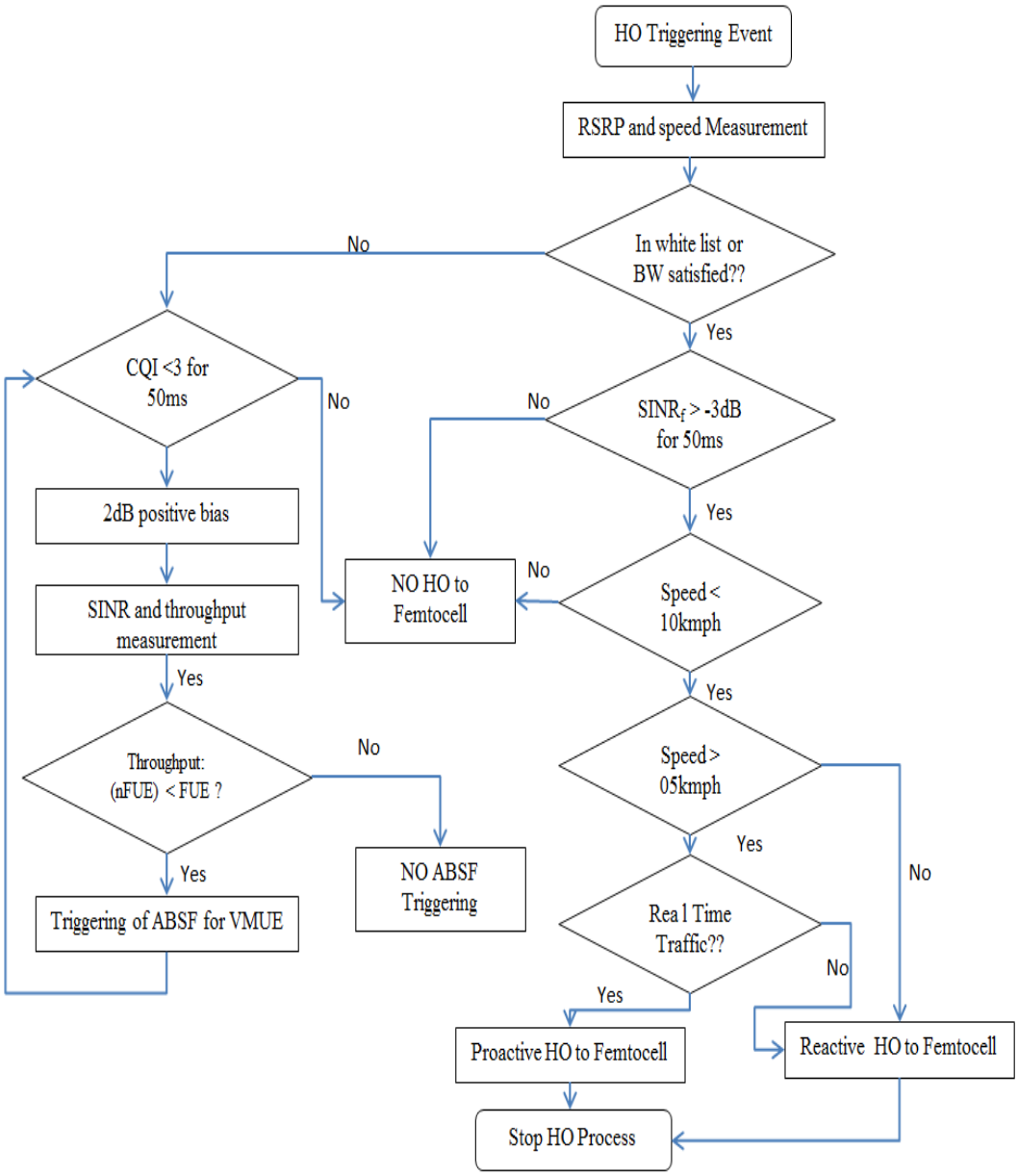

Figure 4.2: Modified handover algorithm with CRE and ABSF

nearby femtocell as depicted in Figure 4.1 is referred as aggressor FAP since it creates high interference both in downlink and uplink for nearby MUEs. To implement CRE in femtocells along with ABSF, a modification in the proposed algorithm in Chapter 3(3.1.1) is considered in this research work as shown in Figure 4.2. When, VMUEs are near to the interfering FAP, eNB injects the positive bias(CRE) to that aggressor FAP through backhaul link with a chosen ABSF pattern. A limited number (maximum of five

victim macro-cell users in this research) of VMUEs in this expanded range can be served by the FAP due to the limitation of femtocell capacity(1.2). Particular bias and ABSF pattern can be selected by exploiting the CQI feedback and $RSRP$ reports (VMUE tracking was described in 3.1.5).

4.3 Performance Analysis

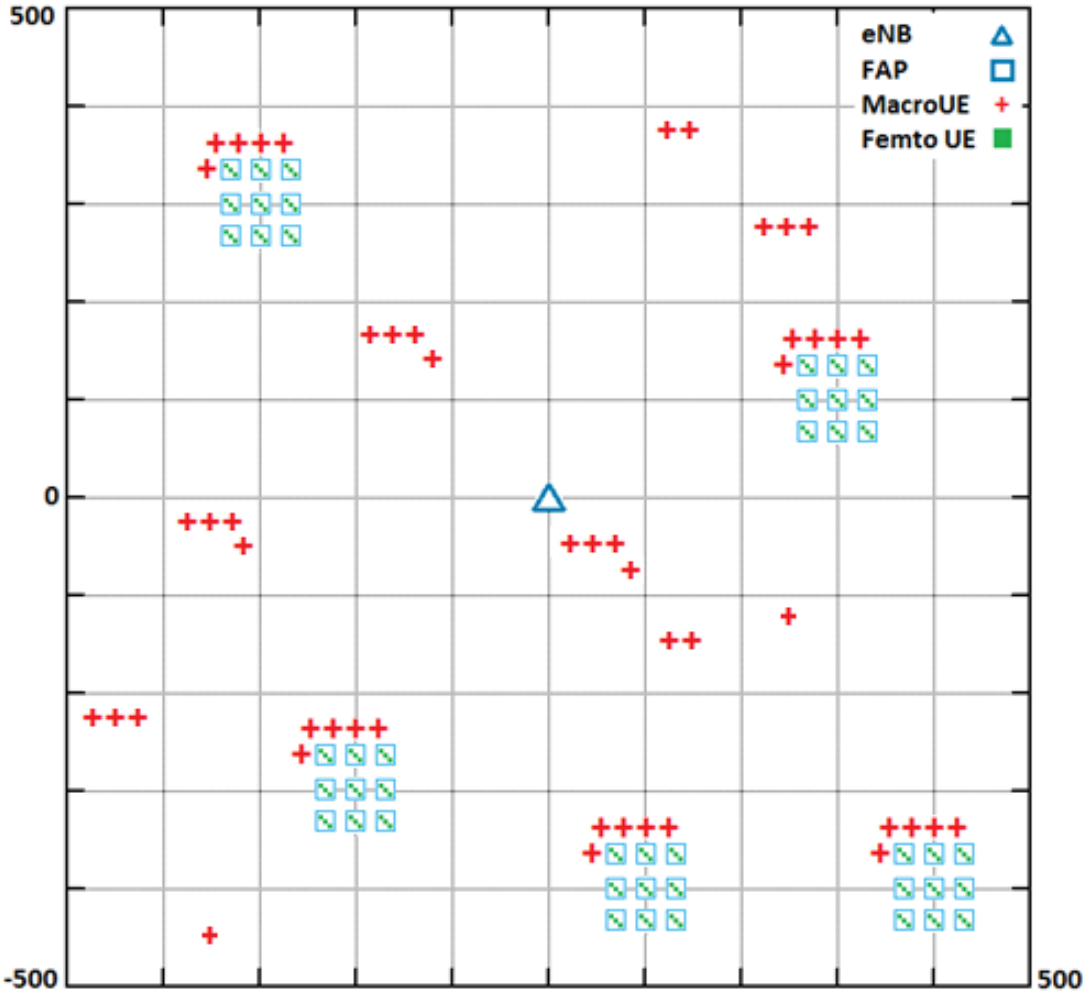

Figure 4.3: Single macrocell-multi femtocell scenario

Figure 4.3, shows the system model (updated from Figure 3.8, Chapter 3) where 24 MUEs, 25 VMUEs and 135 FUEs reside in macrocell coverage area of $500 \times 500 m^2$. It was assumed that all the users were distributed uniformly and running video application with

Table 4.1: Simulation Parameters

Parameter	Value
Operating BW	5 MHZ
eNB transmit power	43dBm
FAP transmit power	20dBm
Macrocell radious	500m
Building type	3×3 (m^2)
Apartment size	$100m^2$
Number of VMUE	25
Number of MUE	24
Users FUE	3 per FAP
Scheduler	PF
Bias value	1dB, 2dB, 2.5dB
Application	Video
ABSF Pattern	1/8, 2/8, 3/8(FDD)
Flow time	100sec

constant rate of R kbps. Cost-231 Hata model [98] was considered for urban path loss environment, both the shadow fading and path loss were considered fixed for each TTI. The simulation parameter is provided in Table 4.1.

The Cumulative Distribution Function(CDF) of downlink SINR in different ABSF modes given in Figure 4.4 shows the highest SINR for VMUEs can be obtained in 1/8 ABSF (considering bias value 2dB). From Figure 4.4, it is seen that, with 1/8 ABSF almost 25% of users are below -3dB(CQI value 3), which is the lowest among all the ABSF patterns. So, in the later simulations, ABSF 1/8 pattern was utilized as an reference.

In simulation scenario (Figure 4.3), the handover failure rate increases with increasing UE speed, which is shown in Figure 4.5. The handover failure is the highest when there is no range expansion and no ABSF applied. It can also be seen from the Figure 4.5 that, in all plotted eICIC scenarios, the handover failure rate becomes steady after a certain user speed (i.e., 10Kmph)for all the cases. This is because the applied handover algorithm in this research (Figure 4.2)

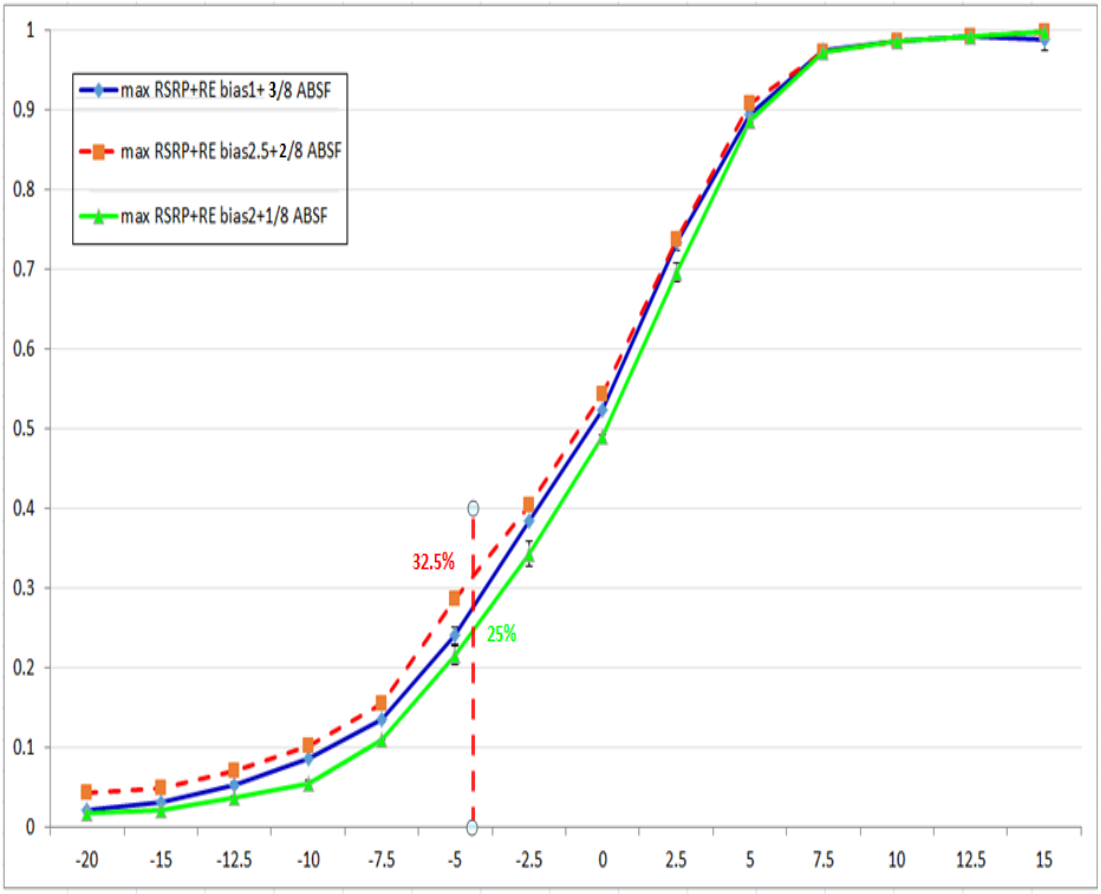

Figure 4.4: Comparison of CDF of SINR in different ABSF pattern

does not allow user's handover to femtocell when its speed is over 10kmph (2.3).

At user's regular walking speed of 3 kmph, the handover failure rate is almost **33%** when there is neither eICIC nor ABSF (**no RE+no eICIC**), **12.5%** when both CRE and ABSF are activated((**RE+eICIC**)) and **9%** when ABSF is activated for the victim MUEs but there is no CRE implemented ((**RE+no eICIC**)). The interesting fact to be noted here is that the handover failure rate is higher when CRE is implemented comapred tp when there is no CRE. This result is quite opposite to the range expansion behaviour of picocells [99]. One of the possible reasons could be an increase in co-tier interference from the adjacent femtocells. So, three experiments were made to analyze the impact of co-tier interference on femtocell performance: 1) changing bias(keeping apartment size

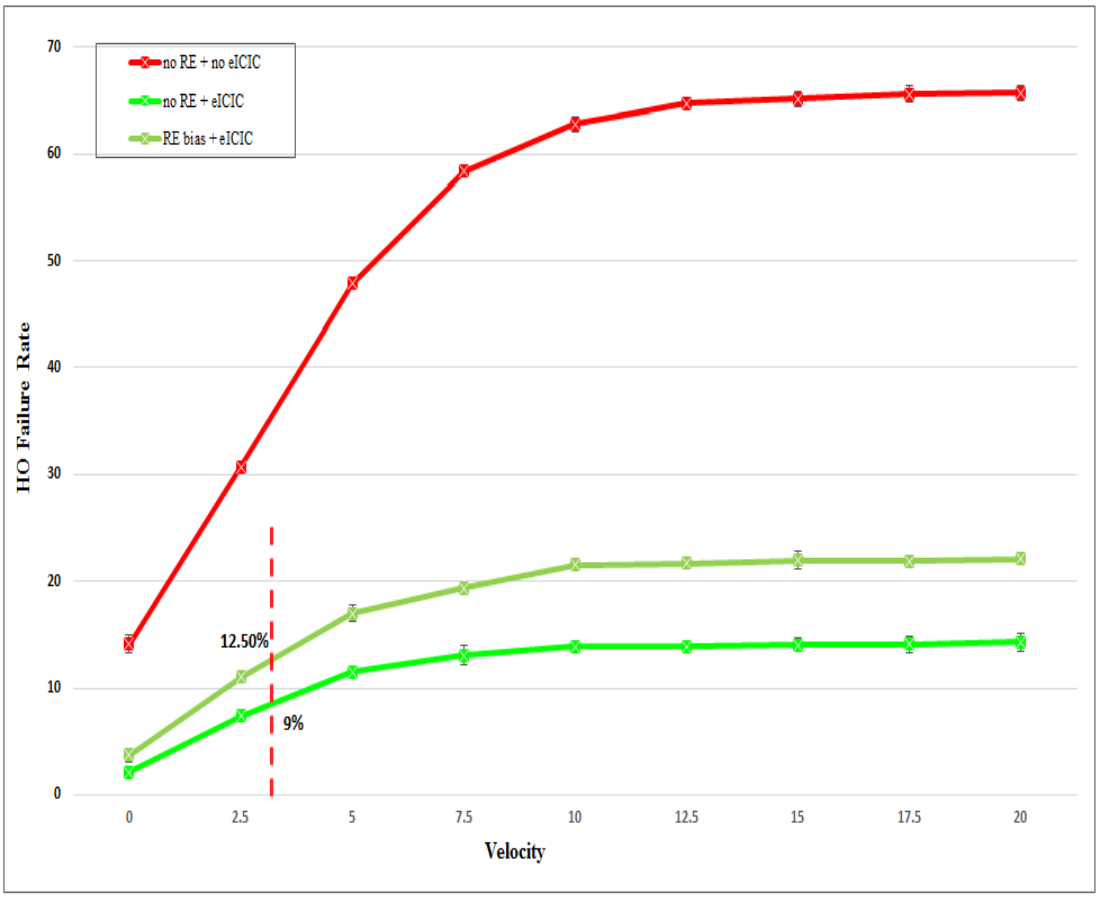

Figure 4.5: Handover Failure rate (%) with and without CRE

constant), 2) changing apartment size(keeping the bias constant), 3)validating the presence of co-tier interference.

4.3.1 Impact of Co-tier Interference on handover

From Figure 4.6, it can be seen that, when the bias is the highest (i.e.**2.5**), the $SINR$ is the lowest(almost **40%** of the users are below $-3dB$) and handover failure rate is maximum (4.7). So, intuitively it can be said that with *bias* 2.5, the FAP coverage area increased and FAP DL transmit power penetrated to other FAP coverage area. That in turn may lead to this poor $SINR$ and higher handover failure rate. From these figures it can also be seen that,

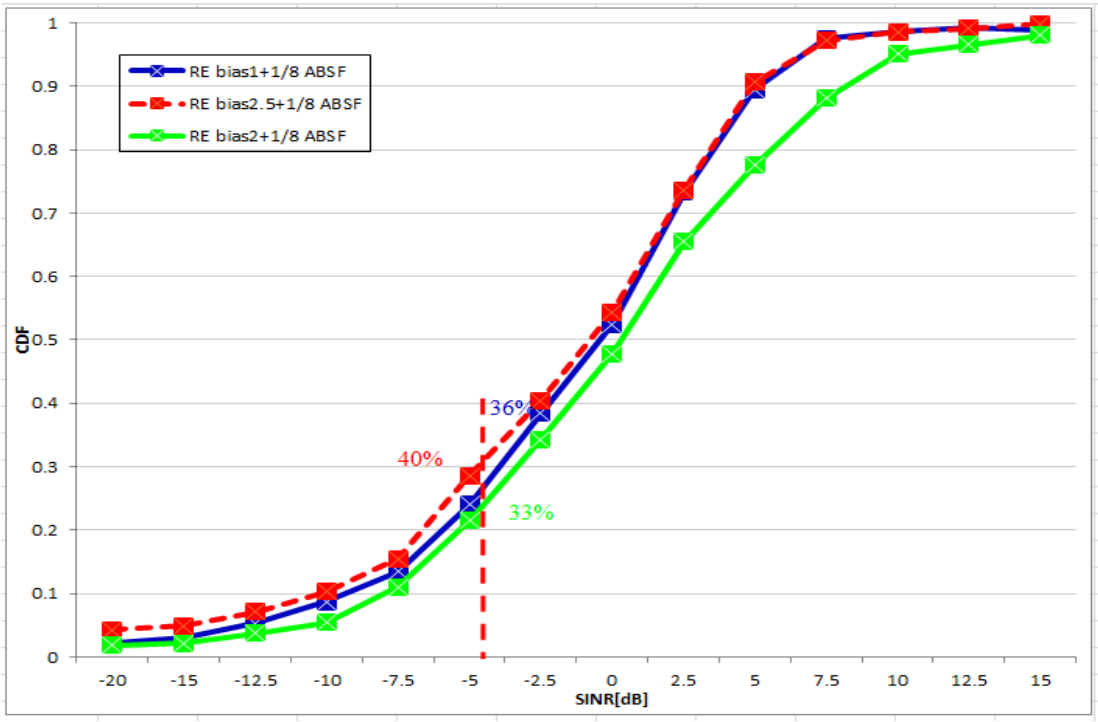

Figure 4.6: CDF of SINR with different bias

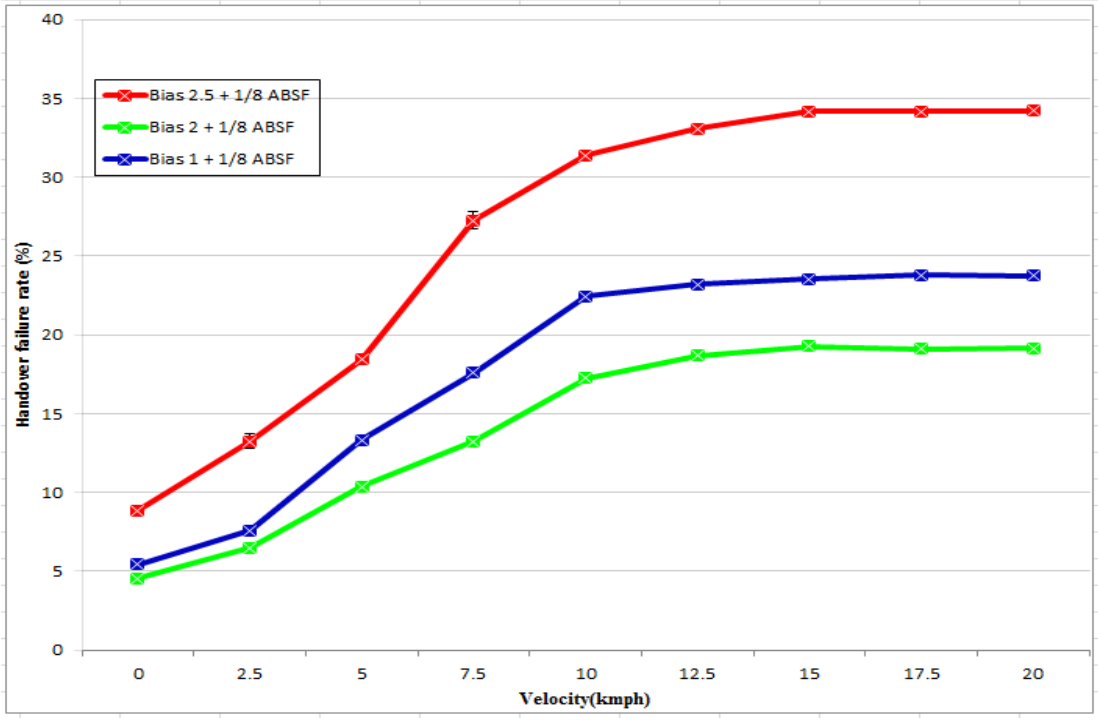

Figure 4.7: Handover failure rate in different bias

scenario with *bias*2 has the best performance. *Bias*1 has slightly poor performance than the bias 2 probably because of lower *RSS* experienced by the FUEs at the edge of the apartments.

Now, keeping the *bias* to 2 (since it has better achieved performance than *bias* 1 and *bias* 2.5), the apartment size is expanded and shrunk respectively by 25% of the actual apartment size. Simulation results in Figure 4.8 show that, when the area is shrun, SINR is the lowest and co-tier interference is maximum here because of the overlapping FAP coverage areas. Almost **50%** of the users are below $-3dB$ and handover failure rate is maximum too(shown in Figure 4.9). SINR is improved when area is expanded, which can alternatively be said that, the impact of co-tier interference is reduced.

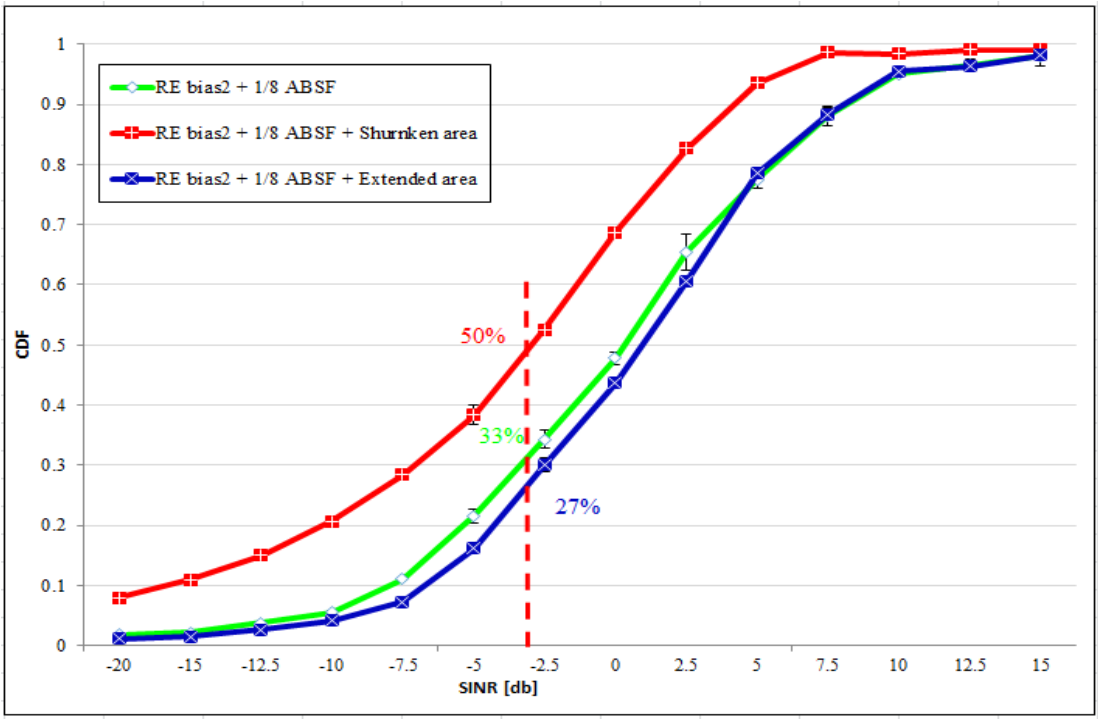

Figure 4.8: CDF of SINR with changing area

Above simulation results show the presence of significant co-tier interference when CRE is introduced in femtocell scenario. The presence of co-tier interference is also checked by building a scenario without macrocell users to omit the effect of cross-tier interference (Inter-FAP handover is described in A.2). The number of FAPs was increased gradually circling the reference FAP (located 300 meters east to the eNB in Figure 4.3)and FUEs are moving with pedestrian

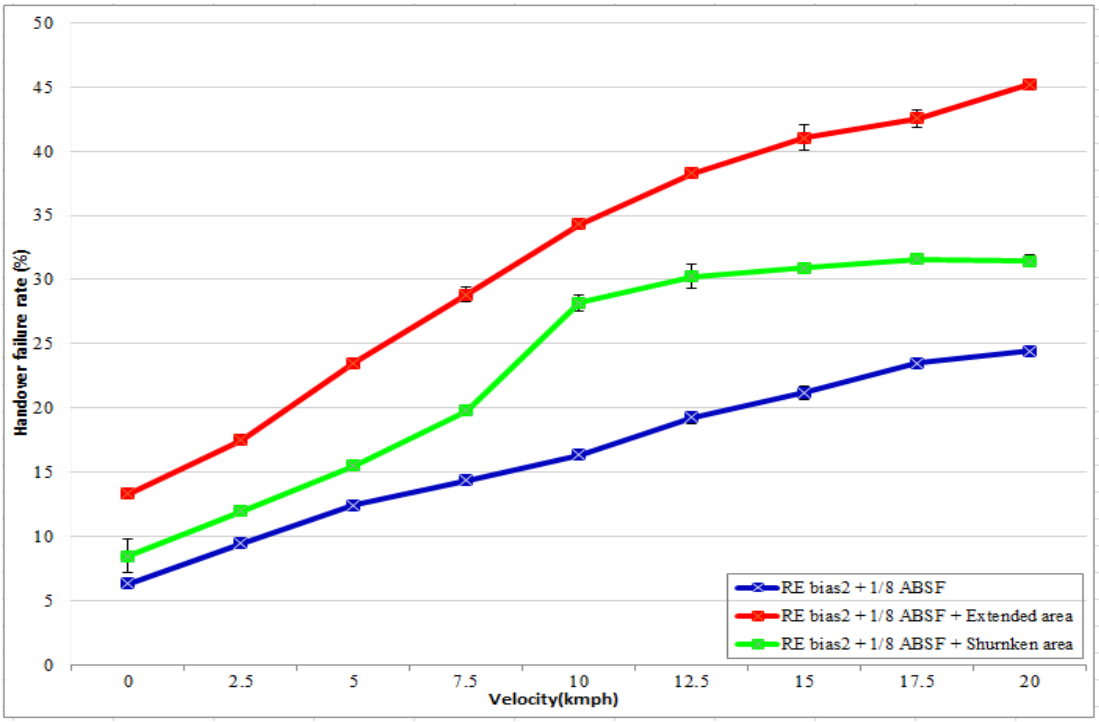

Figure 4.9: Handover failure rate with changing area

speed of 3kmph. Simulation results shown in Figure 4.10 depicts that, at bias 2, when there are 10 neighbouring FAPs, handover failure rate due to co-tier interference is **3.46%**. This percentage is almost same as the difference (**3.50%** of handover failure rates between(**noRE+eICIC** and **RE+eICIC**) shown in Figure 4.5.

With bias 2, the reference femtocell is not affected by co-tier interference when femtocells are deployed beyond 20 meters and handover failure rate remains almost same. In *bias* 1, the handover failure rate remains almost constant since low coverage (because of lower bias) femtocells deployed after 20 meters may have no affect on the reference femtocell. In bias 2.5, femtocells have the highest transmit power, penetration and the highest interference as well.

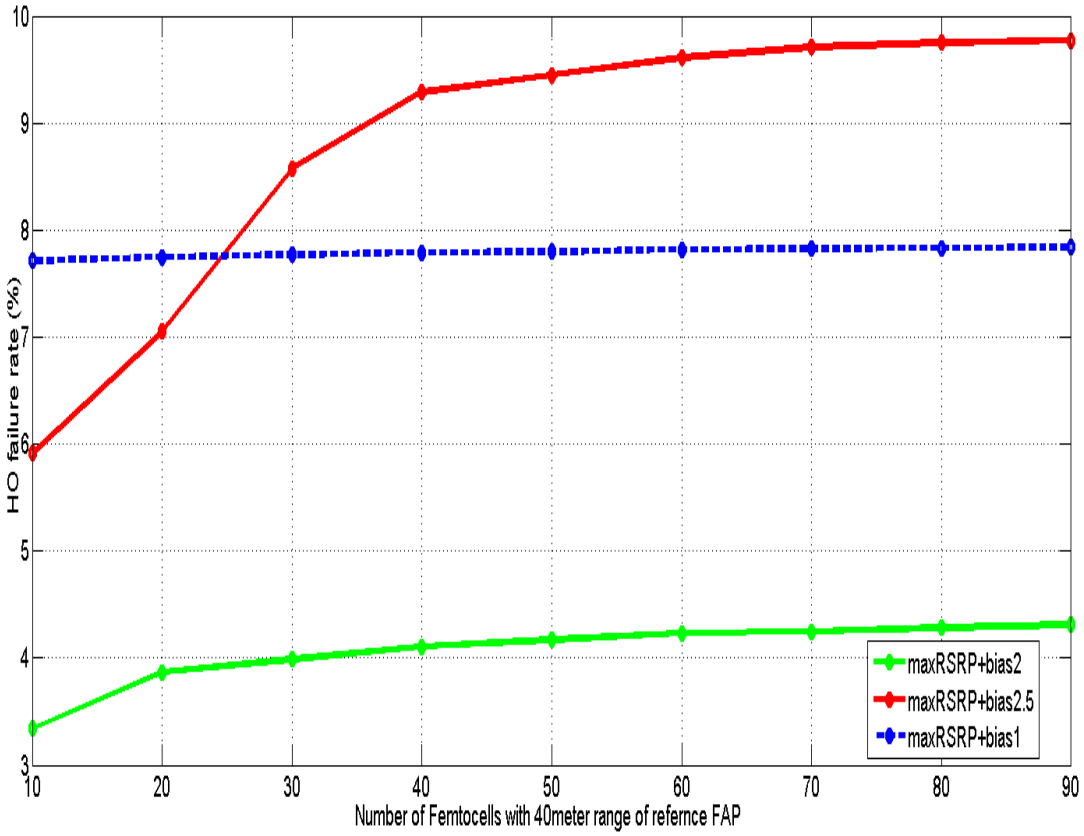

Figure 4.10: Inter FAP Handover failure rates with different CRE bias

4.4 Summary

In this chapter, a further modification in proposed speed based algorithm to adapt range expansion is discussed(Section 4.2). To the best of our knowledge, there is no research work which is incorporated CRE in femtocells and consider the network with higher interference when femtocells are deployed densely. Simulation results show (Section 4.3), the handover failure rate increases when CRE is incorporated with ABSF. The result is most unlikely since CRE for picocells improves the network and handover performance [78]. Thus, a number of simulations were performed in different single macrocell- multiple femtocells scenario to prove the degraded handover performance due to the presence of additional co-tier interference between femtocells (Section 4.3.1).

Chapter 5

Conclusions and Future Work

This thesis studied intercell interference, packet scheduling and handover algorithms in LTE Femtocell systems and a number of contributions are provided in this thesis to improve system performance in macrocell-femtocell scenarios. The final chapter summarises the research contributions of this thesis in Section 5.1 and then discusses directions for future research in Section 5.2.

5.1 Summary of Thesis Contributions

The contributions of this thesis are as follows:

- In order to study the effect of cross and co-tier interferences in the presence of femtocells in a macrocell scenario, a simulation framework was developed in this thesis and described in Chapter 2 and 3 and in Appendix A. Several interference management schemes such as femto-aware spectrum arrangement, FFR, and ABSF were studied in the simulation framework. A number of well-known handover techniques such as max RSRP based, user speed, experience interference(by UE) based were simulated to find a suitable algorithm for this research work.
- A comparative study on well known scheduling algorithms, PF, MLWDF and EXP/PF were described in Chapter 3. Interfer-

ence management through tracking of victim macrocell users and adaptation of several modifications in PF were discussed in Section 3.1.5. A significant improvement in network performance was obtained with the new algorithm and the results was shown in the simulation results.

- The major contribution of this thesis is a proposed modified speed based algorithm which adapted range expansion and studied interference performance when femtocells were deployed densely. Simulation results were given in Section 4.3 which showed that the handover failure rate increases when CRE is incorporated with ABSF.

5.2 Future Research Work

A number of important issues have been identified for future work and these issues are briefly discussed below.

- In the future, new eICIC approaches will be introduced to mitigate interference between macro and low power nodes such as pico, femto and relay nodes. These features will be added to LTE and LTE-A systems to enhance the system performance and this will create new challenges.

- 5G networks are expected to make use of small cells and Wi-Fi interworking to further improve the coverage, capacity, energy efficiency and cost aspects of 4G networks. The presence of IoT devices along with cellular users will further compound the eICIC problems and newer algorithms may have to be developed in future.

Appendix A

This Appendix provides a brief description of the simulator used in this research work. In addition to that, propagation model and Inter FAP handover algorithm are discussed. Thereafter, methods to use the simulation results are discussed.

Description of System Level Simulator

$LTE-Sim$ supports both single and multi-cell environments. Each network node of LTE-Sim environment is implemented through different classes (i.e eNB class, UE class, MME class). Several functionalities of LTE networks, including the models of e-UTRAN and EPC, DL and UL transmissions, QoS management, CQI reporting, AMC schemes, user mobility, handover procedures, and frequency reuse techniques are integrated in $LTE-sim$. The entire LTE network is composed of three network nodes, i.e., UE, eNB, and MME to form application to PHY layer including Radio Link Control (RLC), Radio Resource Control (RRC) and MAC entities. In addition to that, $LTE-Sim$ platform supports well known scheduling strategies like Proportional Fair (PF), Modified largest Weighted Delay First (MLWDF)and Exponential Proportional Fair(EXP/PF) [88]. In the application layer of $LTE-Sim$, there are traffic generators (trace-based, on-off, infinite buffer and constant bit rate)[88]. Packet transmission utilizes $ChannelRealization$ class to detect the channel condition. Channel condition varies considering four differ-

ent phenomena as suggested in [89], i.e., path-loss, penetration loss, shadowing and fast fading due to multipath propagation. The propagation loss model can be explained by equation A.1-

$$P_{RX,i,j} = (P_{TX,j} - M_{i,j} - L_i - T_i - S_{i,j}) \quad \text{(A.1)}$$

where, $P_{TX,j}$ and $P_{RX,i,j}$ are the eNB transmit power and received power of i^{th} user on j^{th} sub-channel. $M_{i,j}$, L_i, T_i, $S_{i,j}$ are the losses due to multipath, path-loss, penetration loss and shadowing. Fast fading was implemented following Jakes Model for Rayleigh Fading [90]. In this research, path-loss model for Macrocell- Urban and Suburban areas, shown in equation A.2 is implemented [88].

$$macrocellurbanpath - loss, L = 128 + \log_b(d) \quad \text{(A.2)}$$

In $LTE - Sim$, the path-loss calculation for macro users inside buildings considers additional attenuation factor due to the presence of external walls (default value of the external wall attenuation is 20dB [91]. Shadow fading was modelled using log-normal distribution with 0 mean and 8 dB of standard deviation.

Table A.1: Main components of $LTE - Sim$

Component	**Important Classes**	**Functionalities**
Simulator	- Schedule() - RunOneEvent() - Run()/ Stop()	- Creates a new event - Executes an event - Starts/ ends the simulation
FrameManager	- StartFrame() & StopFrame() - StartSubFrame() & StopSubFrame()	- Handles start and end of LTE frame
FlowsManager	- CreateApplication()	- Creates an application
NetworkManager	- CreateUserEquipment() - CreateCell() - UpdateUserPosition() - HandOverProcedure() - RunFrequencyReuse()	- Creates an User Equipment - Creates LTE cell - Update the user position - Handles the handover procedure - Implement frequency reuse technique

$LTE-Sim$ supports both cell re-selection and hard handover procedures. User mobility and direction is updated in each TTI to $NetworkMangerclass$. $Handovermanager$ is defined for each user and takes handover decisions. During handover, all the information from old eNB to target eNB is transferred and a new radio bearer is created between the new target eNB and user. Main classes of $LTE-Sim$ and their functionalities are shown in Table A.1. These features give it the flexibility and modularity to device a complete system for simulating LTE femtocells. Classes of LTE-Sim and their functionalities are show in Table. A.1.

A.1 Classification of Speed

Speed is the main factor that distinguishes walking from running. A persons age, height, weight and fitness and external factors such as terrain, surface and load play main role in maintaining the speed in different scenarios. As per [107] 5 Kmph is considered as average human walking speed.

A.2 Inter-FAP Handover Algorithm

When femtocells are installed densely inside macro cellular network, FUE receives signals from several neighbouring FAPs if the RSS of the serving FAP goes below threshold. This will make inter-FAP handover complex. Here, in this research inter-FAP handover mechanism proposed in [108] was followed.

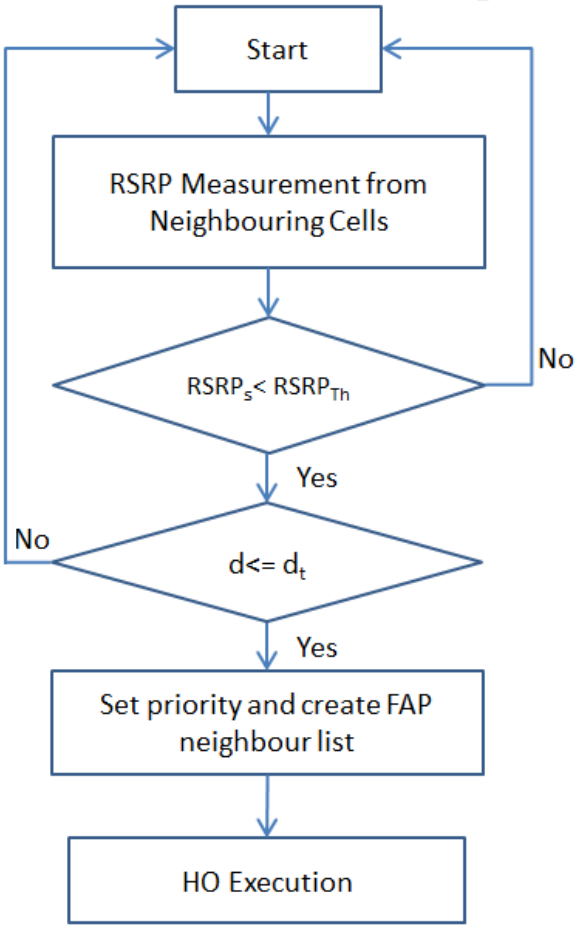

Figure A.1: Inter-FAP handover mechanism[108]

When, FUE moves away from the serving FAP, it forms a neighbour list based on measured $RSRP$ level. On the other hand,in CSG mode, each FAP has the white-list of accessing FUEs. So, unnecessary scanning of the large number of nearby femtocells can be avoided considering access list in addition to $RSRP$ measurement. Through X2 back-haul, serving FAP gets the access information and current load of the neighbouring FAPs. Then the serving FAP will contrast FUE'S ID (MS's ID) with the allowed CSG list and set priority to the prospective target FAP based on their $RSRP$ level and available bandwidth. This is show in Figure. A.1, when the serving $RSRP_s$ is less than threshold $RSRP_{Th}$, all the neighbouring FAPs within 20m(d_t) will be prioritized based on their access list and cur-

Table A.2: Simulation Parameters

Parameter	**Value**
Operating BW	5 MHZ
eNB transmit power	43dBm
FAP transmit power	20dBm
Macrocell radious	500m
Propagation loss for macrocell	$28 + \log_b(d)$
Path-loss for femtocell	$38.5 + 20\log_b(d) + 0.7d, d < 20m$ $15.3 + 37.6\log_b(d) + 0.7d, d \geq 20m$
Building type	3×3
Apartment size	$100m^2$
RSRPth	-75dBm
d_t	20m
Scheduler	PF
Application	Video
ABSF Pattern	1/8(FDD)

rent load for inter-FAP handover. [108]. Simulation parameters for inter-FAP handover is listed in Table A.2.

A.3 Validation of Simulation Results

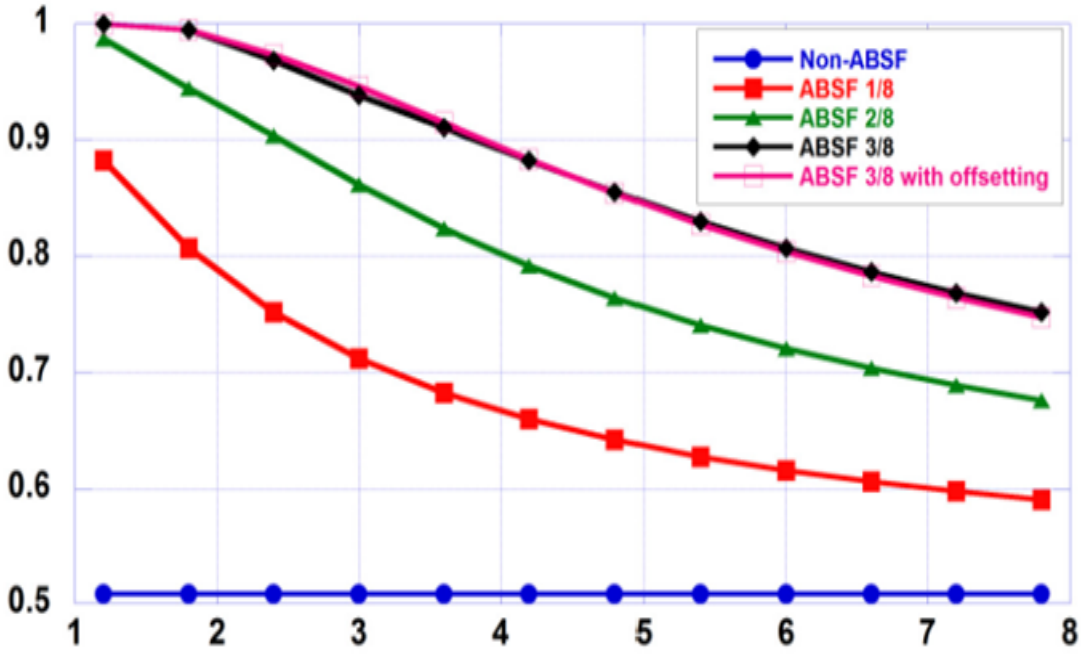

Figure A.2: Fairness Index [100]

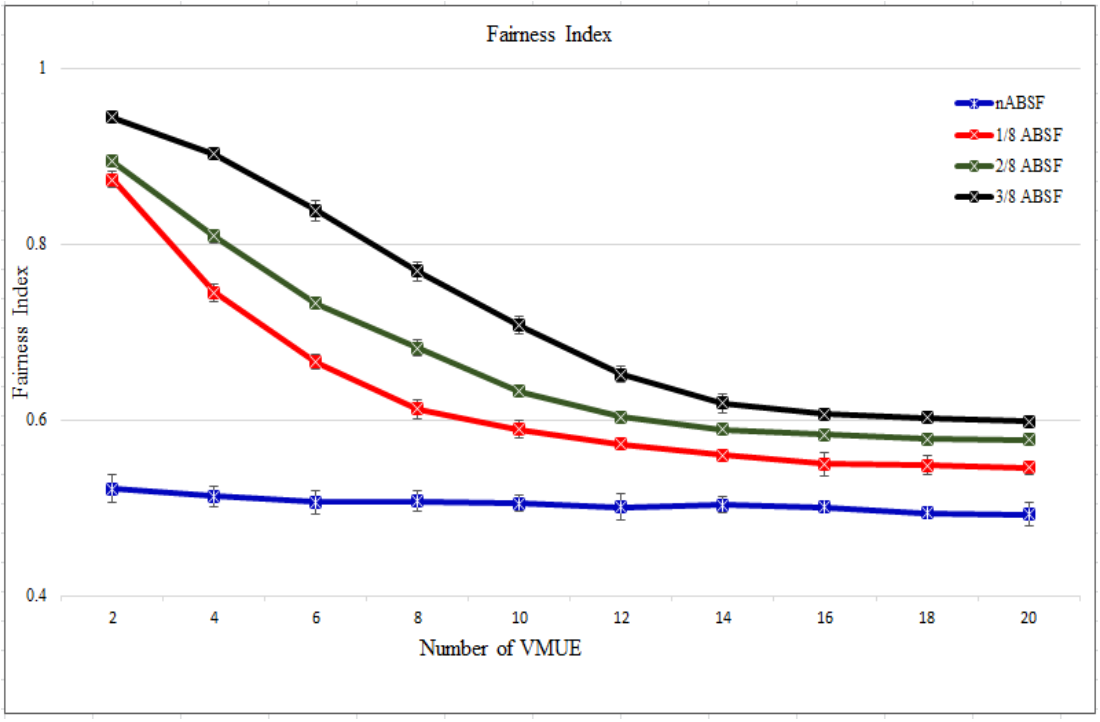

Figure A.3: Fairness Index

Validation of simulations results is necessary to ensure the correctness and reliability of obtained result. Simulation results obtained in this research work were compared with other research works [87], [100] keeping the same input/scenario and the simulator provided similar pattern. Figure A.2 and Figure A.3 shows the Jain's Fairness Index results in [100] and result obtained in this research work respectively. It can be seen comparing both results that, Fairness Index pattern is similar.

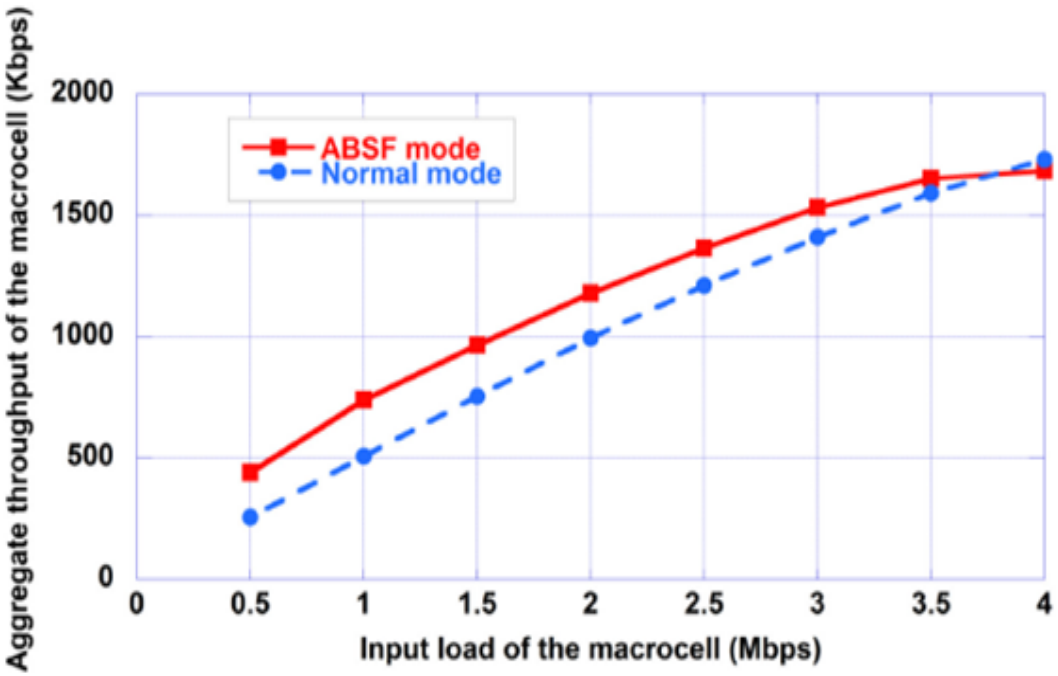

Figure A.4: Aggregated macrocell throughput [87]

Additionally keeping the same scenario, the aggregate obtained macrocell throughput(Figure A.5) also depicts the same pattern with the reference work Figure A.4.

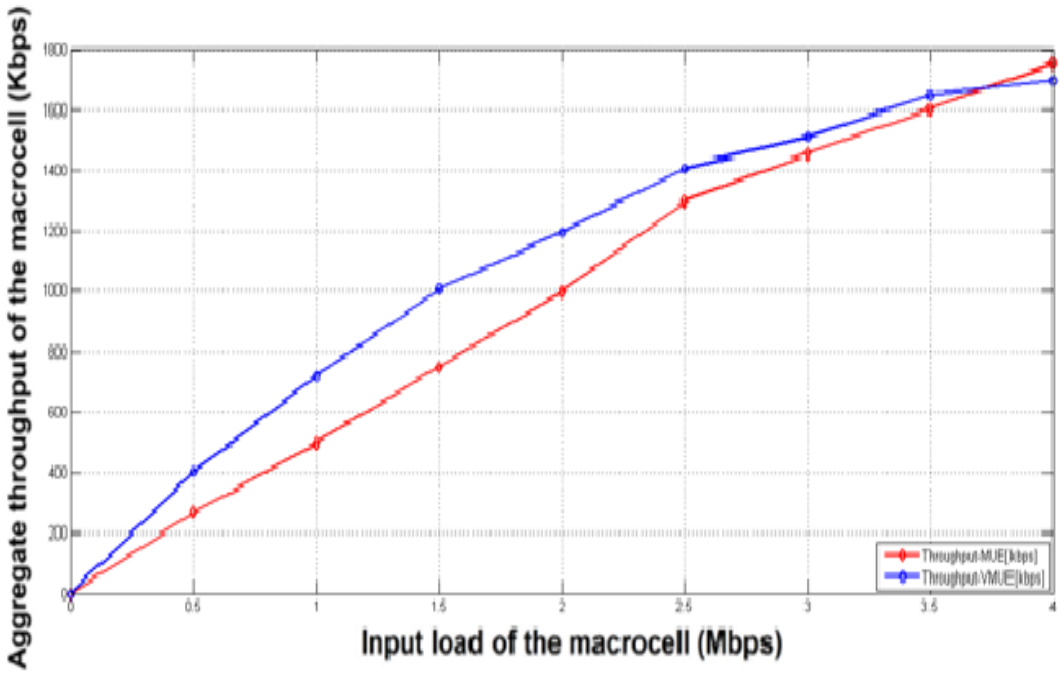

Figure A.5: Aggregated macrocell throughput

Bibliography

[1] https://en.wikipedia.org/wiki/Enhanced_Data_Rates_for_GSM_Evolution

[2] I.F. Akyildiz, D. M. G.Estevez., E.Ch.Reyes, The evolution to 4G cellular systems: LTE-Advanced,Physical Communication, pp. 217-244,December, 2010.

[3] https://en.wikipedia.org/wiki/CDMA2000

[4] Cox, C.,"An introduction to LTE: LTE, LTE-advanced, SAE and 4G mobile communications", John Wiley & Sons, 2012.

[5] Hamalainen, S., Sanneck, H., Sartori, C., "LTE self-organising networks (SON): network management automation for operational efficiency',. John Wiley & Sons, 2012.

[6] Alcatel-Lucent, 42890 4G Mobile Technologies, 2013.

[7] http://www.3glteinfo.com/lte-resources-free-system-posters

[8] https://en.wikipedia.org/wiki/LTE_(telecommunication)

[9] LTE and the Evolution to 4G Wireless: Design and Measurement Challenges, Second Edition, Edited by Moray Rumney. Copyright Agilent Technologies, Inc. 2013. Published by John Wiley and Sons, Ltd.

[10] ITU-R WP 5D 3rd Workshop on IMT-Advanced, 3GPP, 15 Oct 2009 .

[11] S.Sesia, I.Toufik, M.Baker. Lte - The Umts Long Term Evolution: From Theory to Practice,Wiley. 2011,pp. 1-648, ISBN:0470697164, 978047069716.

[12] F. Khan, LTE for 4G Mobile Broadband - overview of Inter-Cell Interference Coordination in LTE, United States of America by Cambridge University Press, 2009.

[13] M. Rinne, O. Tirkkonen, LTE, the radio technology path towards 4G,. Computer Communications, 33(10), October 2010, pp.1894-1906.

[14] M. S. Sharawi. RF Planning and Optimization for LTE Networks. In L. S. a. J. Shen (Ed.), Evolved Cellular Network Planning and Optimization for UMTS and LTE, CRC Press, pp. 399432, 2010, DOI: 10.1201/9781439806500-16.

[15] A. Krishnarajah and K. Sandrasegaran, "Lecture Notes: Mobile Communication Systems - Long Term Evolution," ed. University of Technology Sydney, 2008

[16] WCDMA for UMTS HSPA Evolution and LTE, Fourth Edition. Edited by Harri Holma and Antti Toskala 2007 John Wiley and Sons, Ltd. ISBN: 978-0-470-31933-8.

[17] https://en.wikipedia.org/wiki/Orthogonal_frequency-division_multiple_access)

[18] Myung, H. G., Lim, J., Goodman, D. J. "Peak-to-average power ratio of single carrier FDMA signals with pulse shaping". In IEEE 17th International Symposium on Personal, Indoor and Mobile Radio Communications, pp. 1-5, September, 2006.

[19] C. Gessner,"UMTS Long Term Evolution (LTE) Technology Introduction," Rohde and Schwarz Products, 2008.

[20] D.M.Sacristn, J. F.Monserrat, J.C.Peuelas, D.Calabuig, S.Garrigas and N.Cardona, On the way towards fourth-generation mobile: 3GPP LTE and LTE-advance, EURASIP Journal on Wireless Communications and Networking, 2009(4), March 2009, pp.1-10. doi: 10.1155/2009/354089.

[21] Agilent, "3GPP Long Term Evolution: System Overview, Product Development, and Test Challenges," ed, 2008.

[22] S.Kumar, Final Techniques for Efficient Spectrum Usage for Next Generation Mobile Communication Networks : An LTE and LTE-A Case Study, PhD Thesis, Aalborg University, Radio Access Technology Section, 2009. (8792328296, 9788792328298)

[23] M.Rumney, BSc, C. Eng, MIET "3GPP LTE: Introducing Single-Carrier FDMA".http://cp.literature.agilent.com/litweb/pdf/5989-7898EN.pdf, May 2010.

[24] D.M.Sacristn, J. F.Monserrat, J.C.Peuelas, D.Calabuig, S.Garrigas and N.Cardona, On the way towards fourth-generation mobile: 3GPP LTE and LTE-advance, EURASIP Journal on Wireless Communications and Networking, 2009(4), March 2009, pp.1-10. doi: 10.1155/2009/354089.

[25] http://blog.3g4g.co.uk/search/label/TD-LTE

[26] http://www.sharetechnote.com/html/FrameStructure_DL.html

[27] 3GPP TS 36.211, Evolved Universal Terrestrial Radio Access (E-UTRA): Physical Channels and Modulation, Dec. 2008.

[28] http://www.sharetechnote.com/html/Communication_OFDM.html

[29] http://www.sharetechnote.com/html/Handbook_LTE_MIB.html

[30] http://rfmw.em.keysight.com/wireless/helpfiles/89600b/webhelp/subsystems/lte/content/lte_sym_tbl_framesummary_pdcch.htm

[31] http://rfmw.em.keysight.com/wireless/helpfiles/89600b/webhelp/subsystems/lte/content/lte_sym_tbl_framesummary_pcfich.htm

[32] 3GPP TS 36.211: "Evolved Universal Terrestrial Radio Access (E-UTRA); Physical Channels andModulation". version 8.8.0 Release 8, 2009.

[33] H.Ekstrm, A.Furuskr, J.Karlsson, M.Meyer, S.Parkvall, J.Torsner and M.Wahlqvist. "Technical Solution for the 3G Long-Term Evolution," IEEE Communications Magazine, March 2006.

[34] http://lteuniversity.com/get_trained/expert_opinion1/b/nishithtripathi/archive/2010/07/27/lte-tdd-td-lte-how-much-different-from-lte-fdd.aspx

[35] http://danabayanaka.blogspot.com.au/

[36] D. Astely, E. , Dahlman, A. Furuskar, Y. Jading, M. Lindstrom, and S. Parkvall, LTE: the evolution of mobile broadband,IEEE Communications Magazine, 47(4), 2009, pp.44-51. doi: 10.1109/mcom.2009.4907406.

[37] F. Capozzi, G. Piro, L. Grieco, G. Boggia, P. Camarda, "On Accurate simulations of LTE femtocells using an open source simulator," in EURASIP Journal on Wireless Communication and Networking, 2012.

[38] http://www.en.wikipedia.org/wiki/Fixed_mobile_convergence/

[39] T. Zahir, K. Arshad, A. Nakata, K. Moessner,Interference Management in Femtocells, in Commun. Surveys and Tutorials, vol. 15, pp. 293-311, 2013.

[40] J. G. Andrews, H. Claussen, M. Dohler, S. Rangan, M. C. Reed, Femtocells: Past, Present, and Future, IEEE J. Sel. Areas Commun.,vol.30, no.3, pp.497-508, Apr. 2012.

[41] N. Saquib, E. Hossain, L. Long Bao, and K. Dong, "Interference management in OFDMA femtocell networks: issues and approaches," IEEE Trans. Wireless Commun., vol. 19, pp. 86-95, 2012.

[42] D. Lopez-Perez, I. Guvenc, G. de la Roche, M. Kountouris, T. Q. S. Quek, and Z. Jie, "Enhanced intercell interference coordination challenges in heterogeneous networks," IEEE Wireless Commun., vol. 18, pp. 22-30, 2011.

[43] Wu, Y., Zhang, D., Jiang, H., Wu, Y. A novel spectrum arrangement scheme for femto cell deployment in LTE macro cells. In Personal, Indoor and Mobile Radio Communications,IEEE 20th International Symposium,pp. 6-11, September, 2009.

[44] V. Chandrasekhar, G. Andrews, "Interference Management in Femtocells," IEEE COMMUNICATIONS SURVEYS AND TUTORIALS, vol. 1, pp. 293-311, 2014.

[45] A. Golaup, M. Mustapha, and L. B. Patanapongipibul, Femtocell access control strategy in umts and lte, IEEE Commun. Mag. , vol. 47, no. 9, pp. 117123, Sep. 2009

[46] H. Su, L. Kuang, and J. Lu, Interference avoidance in OFDMA based femtocell network, IEEE Youth Conference on Information, Computing and Telecommunication, pp. 126129, 20-21 Sept. 2009.

[47] H. Daehyoung, C. Seungwoong, and C. Jaeweon, Coverage and capacity analysis for the multi layer cdma macro/indoor pico-cells, IEEE International Conference on Communications, vol. 1, pp. 354 358, 1999.

[48] J. G. Andrews, Interference cancellation for cellular systems: A contemporary overview, IEEE Wireless Commun., vol. 2, no. 3, pp. 1929, April. 2005.

[49] M. F. Madkour, S. C. Gupta, and Y. P. E. Wang, Successive interference cancellation algorithms for downlink w-cdma communications, IEEE Trans. Wireless Commun., vol. 1, no. 1, pp. 169177, Jan 2002.

[50] F. Berggren and S. B. Slimane, Successive interference cancellation in multi-rate ds-cdma systems, 14th IEEE Proc. Personal, Indoor and Mobile Radio Communications, vol. 2, pp. 1752 1756, 7-10 Sept. 2003.

[51] S. P. Weber, J. Andrews, X. Yang, and G. de Veciana, Transmission capacity of wireless ad hoc networks with successive interference cancellation, IEEE Trans. Inf. Theory, vol. 53, no. 8, pp. 27992814, Aug. 2007.

[52] D. Divsalar and M. K. Simon, Improved cdma performance using parallel interference cancellation, IEEE Military Communications Conference, vol. 3, pp. 911917, 2-5 Oct. 1994.

[53] L. G. F. Trichard, J. S. Evans, and I. B. Collings, Large system analysis of linear parallel interference cancellation, IEEE International Conference on Communications, vol. 1, pp. 2630, 11-14 Jun. 2001.

[54] P. Patel and J. Holtzman, Analysis of a simple successive interference cancellation scheme in a ds/cdma system, IEEE J. Sel. Areas Commun., vol. 12, no. 5, pp. 796807, Jun. 1994.

[55] F. Wijk, G. Janssen, and R. Prasad, Groupwise successive interference cancellation in a ds/cdma system, Sixth IEEE International Symposium on Personal, Indoor and Mobile Radio Communications, Wireless: Merging onto the Information Superhighway, pp. 742746, 27-29 Sep 1995.

[56] M. Ghosh, Co-channel interference cancellation for hdtv receivers, IEEE International Conference on Acoustics, Speech, and Signal Processing, vol. 5, pp. 26752678, 1999.

[57] R. S. Karlsson, Radio resource sharing and capacity of some multiple access methods in hierarchical cell structures, in Vehicular Technology Conference, vol. 5, pp. 28252829, Sep. 1999.

[58] M. Fan, M. Yavuz, S. Nanda, Y. Tokgoz, and F. Meshkati, Interference management in femto cell deployment, in 3GPP2 Femto Workshop, Oct. 2007.

[59] W. Yi, Z. Dongmei, J. Hai, and W. Ye, A Novel Spectrum Arrangement Scheme for Femtocell Deployment in LTE Macrocells, Proc. IEEE 20th Symposium on Personal, Indoor and Mobile Radio Communications, pp. 611, 13-16 Sept. 2009.

[60] L. Zhang, L. Yang, and T. Yang, Cognitive Interference Management for LTE-A Femtocells with Distributed Carrier Selection, Proc. IEEE 72nd Vehicular Technology Conference Fall (VTC 2010-Fall), pp. 15, 6-9 Sept. 2010.

[61] T. Kim and T. Lee, Throughput Enhancement of Macro and Femto Networks by Frequency Reuse and Pilot Sensing, Proc. IEEE International Performance, Computing and Communications Conference (IPCCC), pp. 390394, Dec. 2008.

[62] L. Poongup, L. Taeyoung, J. Jangkeun, and S. Jitae, Interference Management in LTE Femtocell Systems Using Fractional

Frequency Reuse, Proc. 12th International Conference on Advanced Communication Technology, vol. 2, pp. 10471051, 7-10 Feb. 2010.

[63] R. Juang, P. Ting, H. Lin, and D. Lin, Interference Management of Femtocell in Macro-cellular Networks, Proc. Wireless Telecommunications Symposium (WTS10), pp.14, 21-23 April, 2010.

[64] D. Xenakis, N. Passas, L. Merakos, C. Verikoukis, Mobility Management for Femtocells in LTE-Advanced: Key Aspects and Survey of Handover Decision Algorithms, IEEE Commun. Surveys and Tutorials, Vol. 16, 2014.

[65] http://5gmobile.fel.cvut.cz/activities/

[66] J. Moon, D. Cho, Efficient handoff algorithm for inbound mobility in hierarchical macro/femto cell networks, IEEE Commun. Mag. Letters, vol.13, no.10, pp.755-757, Oct. 2009.

[67] J. Moon, D. Cho, Novel Handoff Decision Algorithm in Hierarchical Macro/Femto-Cell Networks, IEEE Wireless Commun. and Netw. Conf. (WCNC) 2010, pp.1-6, Apr. 2010.

[68] P. Xu, X. Fang, R. He, Z. Xiang, An efficient handoff algorithm based on received signal strength and wireless transmission loss in hierarchical cell networks, Telecom. Sys. J., Elsevier, pp. 1-9, Sept. 2011.

[69] Lpez-Prez, D., Valcarce, A., Ladnyi, ., de la Roche, G., Zhang, J. (2010). Intracell handover for interference and handover mitigation in OFDMA two-tier macrocell-femtocell networks. EURASIP Journal on Wireless Communications and Networking, 2010.

[70] A. Ulvan, M. Ulvan, and R. Bestak, The Enhancement of Handover Strategy by Mobility Prediction in Broadband Wirel. Ac-

cess, Netw. and Electronic Commerce Research Conf. (NAEC) 2009, TX: American Telecom. Sys. Mgmt. Assoc. Inc., pp. 266-276, 2009. ISBN 978-0-9820958-2-9.

[71] H. Zhang, X. Wen, B. Wang, W. Zheng, Y. Sun, A Novel Handover Mechanism Between Femtocell and Macrocell for LTE Based Networks, IEEE 2nd Internat. Conf. on Comm. Softw. and Nets. 2010 (ICCSN), pp.228-231, Feb. 2010.

[72] G. Yang, X. Wang, X. Chen, Handover control for LTE femtocell networks, 2011 IEEE Internat. Conf. on Electronics, Comm. And Control (ICECC), vol., no., pp.2670-2673, Sept. 2011.

[73] D. Xenakis, N. Passas, C. Verikoukis, An energy-centric handover decision algorithm for the integrated LTE macrocell-femtocell network, Comp. Comm., Elsevier, 2012

[74] 3GPP, Radio Resource Control (RRC); Protocol specification, TS 36.331 V10.5.0, Mar. 2012.

[75] R. S. Karlsson, Radio resource sharing and capacity of some multipleaccess methods in hierarchical cell structures,in Vehicular Tech. Conf., vol. 5, pp. 28252829, Sep. 1999.

[76] Siemens, R1-060135, Interference Mitigation by Partial FrequencyReuse, 3GPP RAN WG1-42, London, UK, January, 2006.

[77] http://www.raymaps.com/index.php/soft-frequency-reuse/

[78] Kitagawa, K., Komine, T., Yamamoto, T., & Konishi, S., "Performance evaluation of handover in LTE-advanced systems with pico cell range expansion", 23rd International Symposium on Personal Indoor and Mobile Radio Communications (PIMRC),IEEE,pp. 1071-1076, September, 2012. IEEE.

[79] http://www.queryhome.com/43010/rsrp-and-rsrq-measurement-in-lte

[80] Chen, X., Yi, H., Luo, H., Yu, H. and Wang, H., "A novel CQI calculation scheme in LTE, LTE-A systems", International Conference on Wireless Communications and Signal Processing (WCSP), IEEE, (pp. 1-5),l November 2011.

[81] 3GPP TS 36.213 V8.8.0 (Sep. 2009) 3rd Generation Partnership Project; Technical Specification Group Radio Access Network; Evolved Universal Terrestrial Radio Access (E-UTRA); Physical layer procedures.

[82] http://lteuniversity.com/get_trained/expert_opinion1/b/hongyanlei/archive/2009/08/06/cqi-reporting-in-lte.aspx#comments

[83] http://www.sharetechnote.com/html/Handbook_LTE_CQI_PMI_RI_ReportingConfiguation.html#Wideband_Subband

[84] R.Ghaffar and R.Knopp, "Fractional frequency reuse and interference suppression for OFDMA networks," in Proc. 8th International Modelling and Optimization in Mobile, Ad Hoc and Wireless, June 2010, pp. 273 277.

[85] V. Chandrasekhar, J. G. Andrews, T. Muharemovic, Z. Shen, and A. Gatherer, Power control in two-tier femtocellnetworks, IEEE Trans. Wireless Commun., vol. 8, no. 8, pp. 43164328, Aug. 2009.

[86] R4-104932, Way Forward on Candidate TDM Patterns for Evaluation of eICIC Intra-Frequency Requirements, 3GPP Std., Jacksonville, USA, Nov. 2010.

[87] Kamel, M. I.,Elsayed, K. M., "Performance evaluation of a coordinated time-domain eICIC framework based on ABSF in

heterogeneous LTE-advanced networks", In Global Communications Conference (GLOBECOM), IEEE, pp. 5326-5331, December, 2012.

[88] G Piro, L Grieco, G Boggia, F Capozzi, P Camarda,Simulating LTE cellular systems: an open-source framework, in Vehicular Technology, IEEE Trans. vol. 60, pp. 498-513, 2011.

[89] 3GPP TR 25.814, Physical layer aspect for evolved Universal Terrestrial Radio Access (UTRA) (Release 7), 2006.

[90] W. C. Jackes, Microwave Mobile Communications New York. Wiley, 1975.

[91] 3GPP, R4-092042, Simulation assumptions and parameters for FDD HeNB RF requirements, 3GPP TSG RAN WG4 Meeting 51, 2009.

[92] Winner, WINNER II Channel Models Deliverable,www.ist-winner.org/WINNER2-Deliverables/D1.1.2v1.2.pdf, D1.1.2 V1.2, 2007.

[93] H. Mahmoud, I .Guvenc, A comparative study of different deployment modes for femtocell networks, in IEEE Int. Symposium on Personal, Indoor and Mobile Radio Commun. , Palo Alto, USA, pp. 15, 2009.

[94] H. Al-Jaradat, K. Sandrasegaran, On the Performance of PF, MLWDF and EXP/PF algorithms in LTE, International Journal of Computers and Technology, Vol. 8, No. 1, pp. 698-706, June 2013.

[95] M. Andrews, K. Kumaran, K. Ramanan, A. Stolyar, P. Whiting, and R. Vijayakumar, "Providing Quality of Service over a Shared Wireless Link," IEEE Communications Magazine, vol. 39, pp. 150-154, 2001.

[96] J.-H. Rhee, J. M. Holtzman, and D. K. Kim, "Scheduling of Real/Nonreal Time Services: Adaptive EXP/PF Algorithm," in the 57th IEEE Semiannual Vehicular Technology Conference, 2003, vol. 1, pp. 462-466.

[97] I.Guvenc, M.R.Jeong, I.Demirdogen, B.Kecicioglu and F.Watanabe, Range Expansion and Intercell Interference Coordination (ICIC) for Picocell Networks, Proceeding of 20th International Conference on Computer Communications and Networks (ICCCN), August.2011, pp.1-6.

[98] Priya, T. S, "Optimised COST-231 Hata models for WiMAX path loss prediction in suburban and open urban environments," in Modern Applied Science,p75, 2010.

[99] Oh, J., and Han, Y, "Cell selection for range expansion with almost blank subframe in heterogeneous networks", In Personal Indoor and Mobile Radio Communications (PIMRC), 2012 IEEE 23rd International Symposium on (pp. 653-657). IEEE, September, 2012.

[100] Kamel, M. I.,Elsayed, K. M. ABSF offsetting and optimal resource partitioning for eICIC in LTE-Advanced: Proposal and analysis using a Nash bargaining approach. In IEEE International Conference on Communications (ICC), 2013 (pp. 6240-6244), June, 2013.

[101] D. Xenakis, N. Passas, and C. Verikoukis, A Novel Handover Decision Policy for Reducing Power Transmissions in the two-tier LTE network, 2012 IEEE Internat. Comm. Conf. (ICC), pp.1352-1356, June 2012.

[102] An Introduction to LTE: LTE, LTE-Advanced, SAE and 4G Mobile Communications, First Edition, Copyright John Wiley and Sons Ltd., Inc. 2012. Published by John Wiley and Sons, Ltd, ISBN: 9781119970385.

[103] R. Jain, D. Chiu, and W. Hawe, A quantitative measure of fairness and discrimination for resource allocation in shared computer systems, Digital Equip. Corp., Littleton, MA, DEC Rep., DEC-TR-301, Sep. 1984.

[104] 3GPP TR 25.820, 3G Home NodeB Study Item Technical Report (Release 8), Sept. 2008.

[105] Ghanem, K., Alradwan, H., Motermawy, A., Ahmad, A, "Reducing ping-pong handover effects in intra EUTRA networks". In IEEE Communication Systems, Networks and Digital Signal Processing (CSNDSP), July,2012 8th International Symposium on (pp. 1-5).

[106] Ulvan, A., Bestak, R., Ulvan, M.," The study of handover procedure in LTE-based femtocell network". In Wireless and Mobile Networking Conference (WMNC), IEEE, Third Joint IFIP (pp. 1-6), October, 2010.

[107] https://en.wikipedia.org/wiki/Walking

[108] Zhuang, Y., Zhao, S., Zhu, X," A new handover mechanism for femtocell-to-femtocell". In International Conference on Wireless Communications & Signal Processing (WCSP),IEEE,(pp. 1-4), October, 2012.